AMIRA International

June 2001

CONFIDENTIAL

MEETING 3

Proterozoic Sediment-hosted Copper Deposits

P544

CODES SRC

AMIRA INTERNATIONAL ACN 004448266
LEVEL 9, 128 EXHIBITION STREET, MELBOURNE, VIC 3000 AUSTRALIA
TEL: (61) 3 9679 9999, FAX: (61) 3 9679 9900. WEB: WWW.AMIRA.COM.AU

Proterozoic sediment-hosted copper deposits

AMIRA/ARC project P544

Meeting 3, Kitwe
June 2001

CODES SRC
Centre for Ore Deposit Research

UNIVERSITY
OF TASMANIA

Produced by the
Centre for Ore Deposit Research
School of Earth Sciences
University of Tasmania
GPO Box 252-79
Hobart, Tasmania
Australia 7001

An ARC Special Research Centre at the University of Tasmania

www.geol.utas.edu.au/codes

June 2001

another Pongratz & Hlaing Production 2001

Contents

ARC/AMIRA P544

Proterozoic sediment-hosted copper deposits

- Aims to compare and contrast Proterozoic sediment-hosted copper deposits in Australia and Zambia
  - Study Areas: Zambian Copperbelt, South Australian Neoproterozoic sequences, Paterson Orogen in WA
- The level of basic information and description is low in Zambia (much better in South Australia; limited by lack of outcrop in WA)
- Much previous Zambian work has been model driven

Techniques

Zambia

- **Critical assessment of existing models**
- **Basic descriptive work in key areas and at important deposits**
- **Develop a new/revised stratigraphic and structural/ metamorphic framework for the Copperbelt rocks**
- **Document the chemical and isotopic signatures of various hydrothermal (including Cu) and metamorphic processes that have affected Katangan rocks**

Techniques

South Australia

- **'basin analysis' building on existing high quality geological and geophysical databases**
  - **focus on key areas or stratigraphic levels**
  - **structural transects**
- **lithogeochemical and Pb isotope studies of Stuart Shelf Cu deposits**
- **fluid flow and fluid chemical modelling**

Western Australia

- **regional compilation & new potential field interpretation**

Initial Zambian Framework

Lithostratigraphy / structure

- **"sedimentology" / "stratigraphy"**
- **metasomatism / alteration**
- **metamorphism**
- **structure**

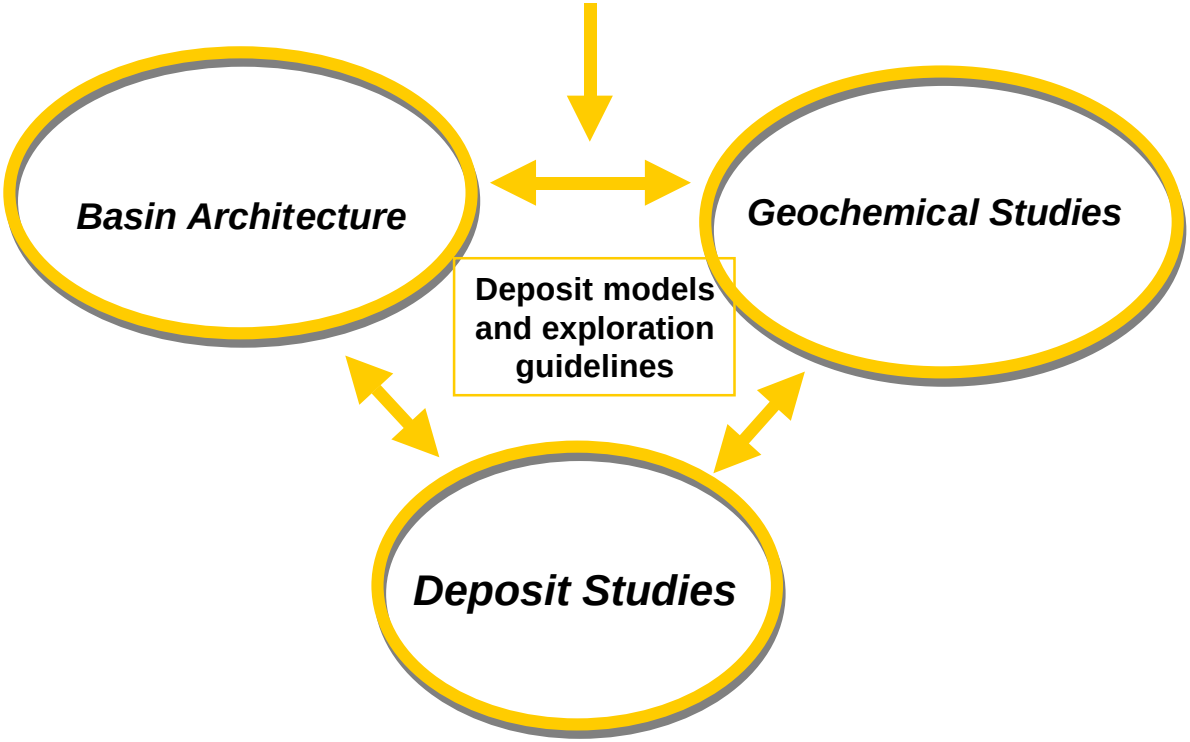

Current Zambian Framework

Copperbelt stratigraphy/ basin architecture

- regional - Kafue Anticline (DB, MH)
- Chambishi Basin
  - basement topography (DS, SB)
- Chambishi Basin
  - growth faults (SB, DS, PMcG)

Orebody geometry/geology

- Nkana (DS, HC, MC)
- Mufulira (NP, PMcG, SB)
- Konkola (RS, PMcG, SB)
- Chambishi (MH + ?)
- Chibuluma (?)

Copperbelt deformation history

- thrust at top of Mwashia (DB, MH)
- structural history of Katangan cf Muva & Lufubu (DS)

Katangan chemistry, isotopes & mineralogy

- orebody specific studies (MC, NP, PMcG)
- stratigraphic studies (DB, PMcG, DS, SB)
- alteration (DB, MH, PMcG, DS, MC, NP)

Zambia: key questions

- **What is basin vs what is basement?**
- **In the Roan, what is sedimentary vs structural (vs alteration vs metamorphic) in origin?**
- **What do the mineral assemblages tell us about alteration, metamorphism and mineralisation?**
- **What types of fluids have existed in the basin at different times in its history?**
- **What traps copper?**

Sponsors Meeting, Kitwe June 2001

- **Sponsor requested field meeting in Zambia within 12 months of project start-up**
- **AMIRA agreed to collaborate with AMF with regard to field trip organisation and scheduling**
- **The field trip coincides with the start of 2001 field season for both CSM & CODES**
- **Hence, limited new results for this meeting**
- **A further two hours have been set aside on Saturday afternoon for research planning with sponsors**

Sponsors Meeting, Kitwe June 2001

Meeting Format

- **The geology of DDH NN47, Chambishi Basin (SB,DS)**
- **Zambian Copperbelt stratigraphy (DB,MH)**
- **Deposit study PhD proposals: Nkana, Mufulira**
- **Applications of SHRIMP dating to sedimentary rocks (Galvin Dawson - UWA)**
- **Zambian forward program**

Meeting Format (cont)

- South Australian progress report and forward program (DS, PMcG)
- Paterson Orogen forward program (PMcG, RS)

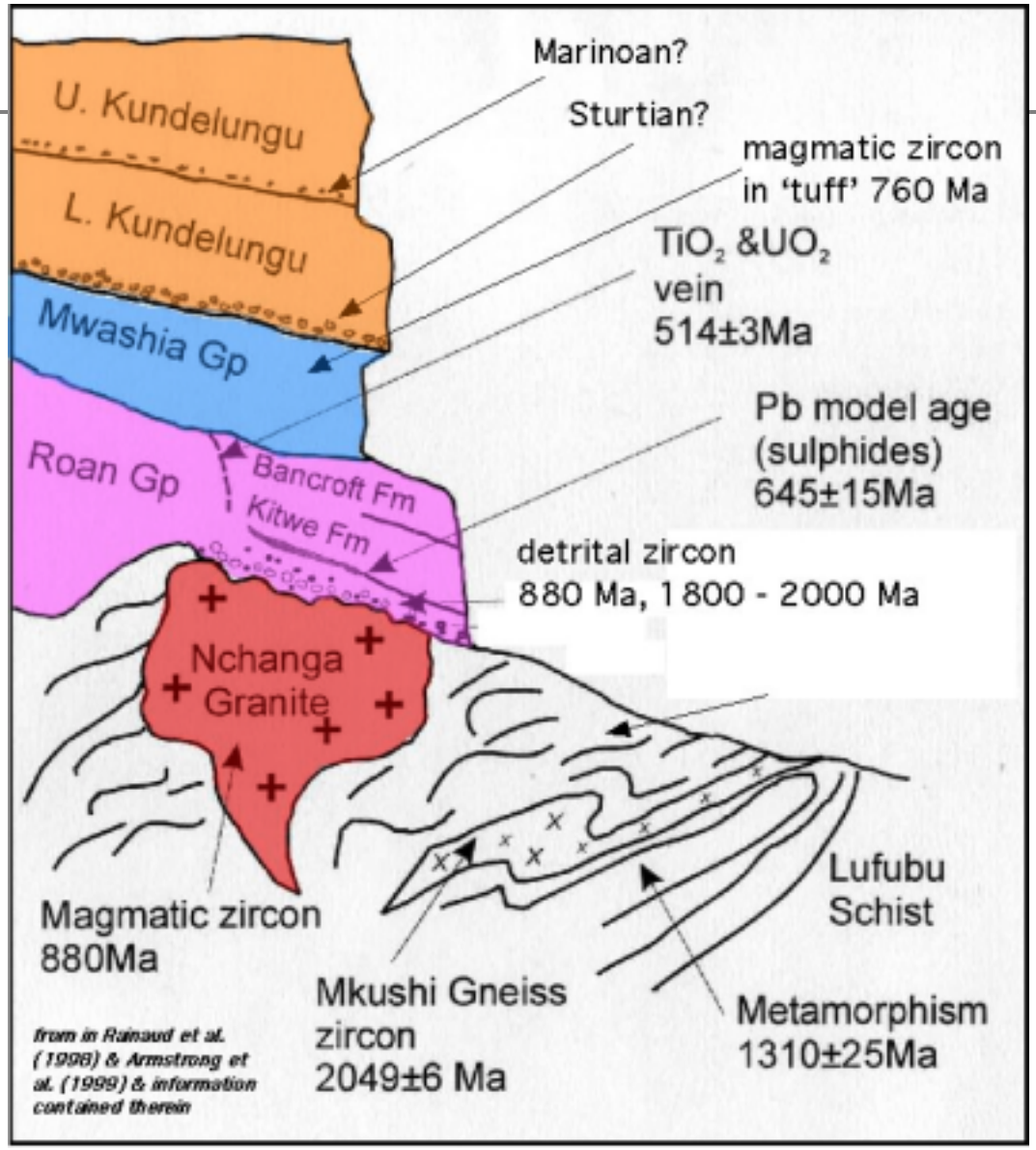
Marinoan?
Sturtian?
U. Kundelungu
L. Kundelungu
Mwashia Gp
Roan Gp
Bancroft Fm
Kitwe Fm
magmatic zircon
in 'tuff' 760 Ma
TiO2 &UO2
vein
514±3Ma
Pb model age
(sulphides)
645±15Ma
detrital zircon
880 Ma, 1800 - 2000 Ma
Nchanga
Granite
Magmatic zircon
880Ma
Mkushi Gneiss
zircon
2049±6 Ma
Lufubu
Schist
Metamorphism
1310±25Ma
from in Rainaud et al.
(1998) & Armstrong et
al. (1999) & information
contained therein

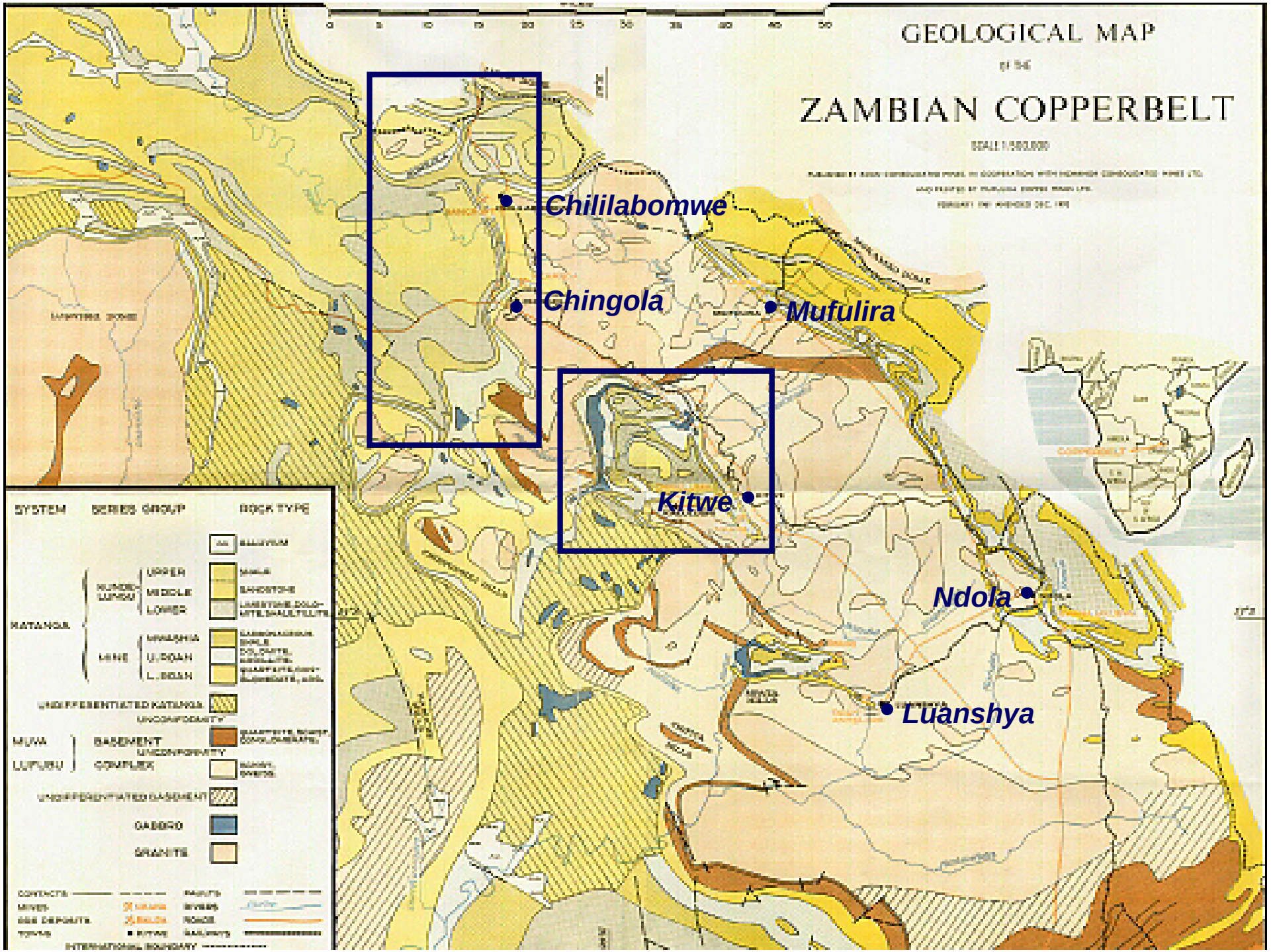
GEOLOGICAL MAP
ZAMBIAN COPPERBELT
Chililabombwe
Chingola
Mufulira
Kitwe
Ndola
Luanshya
SYSTEM
SERIES GROUP
ROCK TYPE
ALLUVIUM
KATANGA
UPPER
MIDDLE
LOWER
MINE
MWASHIA
U. ROAN
L. ROAN
UNDIFFERENTIATED KATANGA
UNCONFORMITY
MUVA
LUFUBU
BASEMENT COMPLEX
UNCONFORMITY
UNDIFFERENTIATED BASEMENT
GABBRO
GRANITE

Geology of DDH NN 47, Chambishi Basin

Stuart Bull and David Selley
Centre for Ore Deposit Research, University of Tasmania

Summary

The basal half of DDH NN 47 that was re logged for this study was interpreted to represent Roan cover over Lufubu Schist basement. Detailed petrographic examination indicates some justification for; a lower Roan interval dominated by coarse-grained arkosic protolith (~ 548 to 625 m); and an upper Roan interval dominated by fine-grained protolith of the same provenance (320 to 501 m); separated by an interval dominated by carbonate/anhydrite and carbonate-biotite schist (501 to 548 m).

However, the carbonate-biotite-quartz schist interval at the base of the hole (624 m to eoh) previously interpreted as basement (Lufubu Schist) is not basement in a metamorphic sense, since biotite is stable throughout the overlying intersection.

The lithofacies interpreted as Roan cover were difficult to interpret during the initial sedimentological logging because the primary sedimentary textures are always partially to completely overprinted by poly-crystalline quartz, anhydrite, albite and mica (sericite/muscovite/chlorite/biotite). In some cases this process appears to be essentially isochemical metamorphic recrystallisation, but in others it may be metasomatic alteration of the arkosic sedimentary protolith to new carbonate- and mica-dominated assemblages.

At least four discrete phases of mineral growth overprint original detrital textures. Grain-scale and to a lesser extent mesoscopic textural relationships indicate that these metasomatic/metamorphic mineral assemblages formed during a progressive fold and thrust event. Fluid infiltration was largely structurally controlled by shear zones, bedding-parallel veins and localised domains of dilatancy within steepened fore-limbs of large-scale folds. In this context, the minor copper mineralisation in NN 47 is associated with structurally-focussed alteration/metasomatism, as Cu is not present in the arkosic protolith. A hypothetical working model for the structural and metasomatic evolution of the package intersected by NN47 is shown in Figure 75. Fundamental aspects of this model are: (1) concentration of fluid flow along major thrusts; (2) pervasive alteration within lower coarse-grained portions of the stratigraphy associated with structurally-induced permeability; (3) "jacking-up" of fine-grained portions of the stratigraphy (ie. "ore shale facies") in response to initial layer-parallel shortening, leading to layer-parallel permeability (e.g., veins); (4) refolding of layer-parallel veins and "flooding" of dilatant forelimbs.

Preliminary results from a zircon dating study from both NN47 and NE112 indicate that alteration (including Cu-sulfide precipitation) is most likely to be Ordovician in age. This finding is broadly consistent with previous chronological studies of alteration and Cu-mineralisation within high grade deposits outside the Copper Belt.

Introduction

At the last P544 meeting (Perth, December 2000), our initial work in Zambia was presented in terms of the key questions identified by the research team that need to be answered in order to understand the Cu system. In this context, this report will address the questions:

- What is basin vs what is basement?
- In the Katangan, what is sedimentary vs structural (vs metamorphic vs alteration) in origin?

DDH NN 47 was chosen for our initial studies because it has been used previously as a typical example of the copperbelt stratigraphy. It was collared ~ 2 km west of the edge of the Chambishi Basin 500 m NW of the Mufulira Rd (Fig. 1). Previous interpretations (Fig. 2) are that the hole was collared in upper Roan (0-~520 m), transected the lower Roan (~520-625 m), including intervals of ore shale, and terminated in basement (625- 643 m) comprising both granite and Lufubu Schist.

The basal part of DDH NN 47 was re logged and sampled during our field visit to Zambia in October / November 2000. This intersection nicely illustrates the difficulties both in interpreting the protolith and alteration / metamorphic history of individual lithological intervals, and in determining the overall stratigraphy in the Chambishi Basin region. The approach taken in the field was to log the hole in terms of its constituent lithofacies and structural domains (Fig. 3). As presented at the Perth meeting, the distribution of the lithofacies corresponds broadly with the previous stratigraphic interpretation in the following manner:

Carbonate-biotite schist is dominant at, but certainly not restricted to, the base of the hole, where it was previously interpreted as Lufubu Schist basement. A 1 m thick coarse-grained quartz–feldspar-biotite interval overlying this basal schist has been interpreted as granitic basement.

The interval interpreted as lower Roan consists, in order of decreasing abundance; of sandy / gravelly quartz and feldspar facies; massive to stratified albite quartz facies; massive to laminated carbonate–anhydrite ± biotite facies; ore shale facies.

The interval interpreted as upper Roan is dominated by fine sandstone and siltstone facies but also incorporates significant intervals of massive to laminated carbonate- anhydrite ± biotite facies and carbonate-biotite schist.

The samples taken from both DDH NN 47 and DDH NE 112 have now been examined using the following techniques:

- Petrographic and structural analysis of polished thin sections.
- Preliminary microprobe analysis of key mineral phases.
- Preliminary zircon geochronology by laser ablation ICPMS

The results and their interpretation form the bulk of this report.

Petrography of NN 47 lithofacies

Sandy/gravelly textured quartz and feldspar facies

Description

This lithofacies occurs in the lower part of the logged intersection (between 550 and 620 m; Fig. 3) and consists of massive to stratified, pale to dark grey sandy and gravelly textured quartz and feldspar (Figs 4 and 5). In thin section it has a locally bimodal framework of granules (< 4mm) of feldspar and poly-crystalline quartz dispersed within a medium- to coarse-grained (<1mm) fabric of mono-crystalline quartz and feldspar (Fig. 6). The fine-grained matrix appears to be a quartz and feldspar aggregate that is locally overprinted by carbonate, anhydrite, sericite or fine-grained biotite. The mono-crystalline quartz consists of sub-angular to rounded < 1 mm grains (Figs 6 and 7) but individual grains with undulose extinction up to 2 mm in size are locally present. Feldspar occurs as rounded (<4mm) grains and is mostly variably serecitised microcline (Fig. 7) but some plagioclase is also present. Poly-crystalline quartz is the most cryptic framework grain type present. It often appears to be rounded composite detrital grains of 0.1-0.3 mm crystals (Figs 6 and 7). However, in other areas it appears to overgrow the pre-existing fabric (e.g. microcline grains; Fig. 8), and in more altered samples, the same texture can also occur as patchy irregular shaped domains (Fig. 9). Minor metasedimentary (Fig. 10) and cherty (Fig. 11) lithic fragments (<3mm) and zircon (0.2 mm) are also present.

Interpretation

In thin section it is clear that the sandy/gravelly protolith to this facies was a coarse-grained arkose dominated by quartz and k-feldspar (Figs 6 and 7). However, this facies was difficult to interpret in had specimen when logging the core because its primary sedimentary texture is invariably overprinted to some degree by quartz, anhydrite, plagioclase (albite), sericite, biotite and carbonate. This is illustrated in the series of figures from 12 through 16 as follows:

Figure 12 sandstone framework of mono-crystalline quartz and feldspar with the matrix and to some extent the framework overprinted by carbonate, sericite/biotite (fine brown material) and anhydrite.

Figures 13 and 14 same as above with poly-crystalline quartz also overprinting both the matrix and the framework grains.

Figure 15 same as above with almost all relict protolith texture now gone.

Figure 16 same as above but dominated in this case by poly-crystalline quartz (note heavily sericitised microclines interpreted as relict detrital grains).

It is not clear from this series of samples whether the partial to complete overprinting of original detrital textures represents essentially isochemical metamorphic recrystallisation or partial to wholesale alteration/metasomatism. The poly-crystalline quartz is particularly hard to interpret, but on textural grounds (e.g. the overprinting relationship in Fig. 8) it would appear that even the rounded and apparently detrital grains may have a replacement/recyrstallisation origin (see also "ore shale" section below).

Massive to stratified quartz albite facies

Description

This lithofacies occurs in the same lower interval as the previous one (Fig. 3) and consists of white/cream/grey units that may be massive or have a sandy texture defined by the pale feldspars (Fig. 17). In thin section this facies consists of relatively even-grained (< 2 mm) aggregates of quartz and plagioclase (albite?; Fig. 18) with associated anhydrite and carbonate (Fig. 19).

Interpretation

The diagnostic texture of this facies is clearly analogous to the overprinting recrystallisation/alteration fabric described above, except that in this case albite is a major phase. Once again, due to the destruction of primary textures it is difficult to say whether the process is largely isochemical or involves alteration/metasomatism of the protolith.

"Granite"

Description

This lithofacies is only present as one 2 metre thick interval at the base of the section previously interpreted as lower Roan (622 to 624 m). It comprises a pebble sized aggregate (<10mm) of poly-crystalline quartz, feldspar and carbonate (Fig. 20). Poly-crystalline quartz occurs as clots and elongate domains of 0.2-0.4 mm quartz grains (Fig. 21). Some inter-grown plagioclase (albite?) at contacts with sericitised large feldspars (Fig. 22). Feldspar is heavily sericitised (with biotite and minor anhydrite) and albitised but was probably originally both microcline and plagioclase.

Interpretation

Once again the distinctive poly-crystalline quartz texture links this lithology with the other overprinting recrystallisation/alteration phases. The only evidence of the protolith in this case are the heavily replaced feldspars, but there is insufficient texture preserved to make a well constrained interpretation. They may have been a coarse-grained detrital component if the original rock was clastic, or may indicate that it was a coarse-grained felsic intrusive (granite boulder?). The fact that the plagioclase (albite?) occurs in the poly-crystalline quartz along contacts with micro-clines that are breaking down (Fig. 22) suggests that the some control by the protolith on the overprinting assemblage in this case.

Fine sandstone and siltstone facies

Description

Fine-grained green/grey sandstone/siltstone (Fig. 23). Where primary textures are preserved (Fig. 24), characteristic thin bedding/lamination is defined by massive and normal graded, fine-grained sandstone to siltstone layers. Well-preserved ripple cross-lamination is also locally present. In detail, the coarser layers consist of quartz, feldspar, opaque fragments and scattered zircons in a fine-grained matrix of sericite/muscovite/chlorite/biotite and quartz. This laminated fabric is progressively disrupted where cross-cutting fluid escape structures become dominant (Figs 25 and 26), and is ultimately destroyed by this fluidisation process (Figs 27 and 28).

Interpretation

The preservation of unambiguous sedimentary structures (e.g. lamination and ripples) make the protolith of this facies, that dominates the part of the hole interpreted as upper Roan (Fig. 3), the easiest to constrain. It was a clearly a fine-grained clastic package, which although it probably represents lower-energy sedimentary environments than the underlying coarser-grained package (~ lower Roan), has an identical arkosic provenance and has been subjected to the same phases of overprinting recrystallisation/alteration. Conflicting facing indicators are present, but it appears from normal grading of sandy laminae that mud crack-like features (Fig. 25) are actually upward propagating fluid escape structures.

"Ore shale" facies

Description

The ore shale consists of several thin (m-scale) units of alternating sub-cm to sub-mm brown-white parallel laminae that occur in the interval interpreted as lower Roan (Fig. 3). They contain numerous indicators of deformation such as shearing, folding and quartz augen (Figs 29 and 30). In thin section, the laminae are defined by coarser-grained aggregates of quartz and sericitised microcline (< 0.2 mm), muscovite and biotite (Figs 31 and 32). The matrix consists of a fine-grained felted aggregate of quartz, muscovite and biotite or may be carbonate-dominated. Isolated clots of poly-crystalline quartz are scattered throughout (Fig. 31) but are mainly concentrated into coarser-grained laminae (Fig. 33) where they are associated with albite, carbonate and chalcopyrite (Fig. 34a and b).

Interpretation

Although generally more deformed, micaceous and recrystallised, the finer-grained (~ less recrystallised) parts of the ore shale (Figs 31 and 32) indicate that the protolith was a thin-bedded, fine-grained sediment similar to the fine sandstone and siltstone facies that dominates the upper Roan. As is the case in the coarser-grained facies, the poly-crystalline quartz and albite is interpreted as an overprinting alteration phase. It is clear from their distribution in this facies, where they are often isolated within the fine-grained matrix(Fig. 31), that the rounded patches of poly-crystalline quartz that could be interpreted as detrital grains in the coarser facies are actually recrystallisation/alteration features. The manner in which the recrystallisation/alteration is utilising the sedimentary laminae, as indicated by the association with detrital microclines (Fig. 33), indicates they were fluid conduits. If the recrystallisation/alteration was syndiagenetic this would be because they retained primary porosity and permeability longest, or if it occurred later in the deformation history, it would be because they were areas of focussed strain and hence increased secondary porosity and permeability. This is a critical question with regard to the mineralisation, as the chalcopyrite was clearly introduced during this recrystallisation and/or alteration/metasomatic process in this locality (Fig. 34a and b).

Carbonate-biotite-quartz schist facies

Description

A thick interval of carbonate-biotite-quartz schist at the base of the hole has been interpreted as basement Lufubu Schist (Figs 3 and 35), however this lithofacies

is also an important constituent of the overlying package interpreted as Roan cover (Figs 3 and 36). The basal intersection (Lufubu Schist; Fig. 37) comprises felted foliated biotite and chlorite (<50% and 10% respectively) defining foliation, with clots/stringers of quartz (< 1 mm) and calcite (40% combined) with gradational margins. Scattered patches of distinctive brown (Fe-rich?) biotite are associated with clusters of epidote crystals (Fig. 38).

The carbonate-biotite-quartz schist intervals higher in the stratigraphy (Fig. 39a and b) consist of an interlocking framework of varying proportions of biotite, carbonate (0.5 mm, mostly dolomite), lesser quartz (< 2 mm) and minor zircon. Varying proportions of clots/stringers of coarse-grained (2 mm) anhydrite crosscut the biotite fabric.

Interpretation

The biotite that is characteristic of this facies illustrates that the metamorphic grade throughout the logged intersection, is at least greenschist facies. The high fluorine content of the biotite, and its patchy brown and green zoned appearance (Fig. 39c) suggest it represents the lower end of the temperature range of biotite stability (~ 300° C). This is supported by the lack of associated high temperature metamorphic phases (eg. garnet, cordierite etc.), and the lack of contact skarn assemblages (eg. tremolite, diopside etc.) at quartz carbonate contacts (eg. Fig. 40). The fact that biotite occurs throughout the intersection, indicates that although the basal interval of this facies previously interpreted as Lufubu Schist basement differs from other biotite schists higher in the sequence in some respects (eg. it has a higher proportion of biotite and is calcite rather than dolomite dominated), it is not basement in the sense that it is higher in metamorphic grade.

Texturally, all of the schists are clearly totally recrystallised to metamorphic/metasomatic textures so it is difficult to interpret their protolith. Figure 40 shows the contact between the sandy/gravelly textured quartz and feldspar facies and an interval of carbonate-biotite-quartz schist at a depth of 615 m within the interval interpreted as lower Roan. A thin section across this boundary shows a gradational contact from a quartz microcline sandstone overprinted by poly-crystalline quartz (Fig. 40); to a zone where this texture is overprinted by carbonate, albite and biotite (Fig. 41); to a carbonate-biotite schist with only isolated remnants of the quartz fabric and the zircon is preserved (Fig. 42).

This transition may represent recrystallisation of a gradational contact between arkosic and carbonate sedimentary protolith. Alternately it may represent wholesale alteration/metasomatism of the arkosic protolith such that all but isolated remnants of the quartz fabric have been replaced by carbonate and biotite.

Massive to laminated carbonate- anhydrite ± biotite facies

This lithofacies consists of massive to stratified, medium- to coarse-grained white–cream–pale green–purple coloured carbonate and quartz with cross-cutting blebs and stringers of anhydrite (Fig. 44). In thin section it comprises an equant mosaic of carbonate and coarser-grained anhydrite (Fig. 45) with variable proportions of domainal poly-crystalline quartz (Fig. 46). Biotite is also present in some samples.

Interpretation

A 30 m thick interval of this facies (Fig. 3) separates a lower zone where the protolith appears to have been dominantly coarse-grained arkoses (~ lower Roan) from an overlying zone where the protolith appears to have been dominantly fine-grained arkoses (~ upper Roan). This facies is similar to the carbonate-biotite-quartz schist except that it is coarser and more recrystallised and has less bitotie and therefore no well-developed foliation. It is equally difficult to interpret in terms of its protolith and could represent either metamorphically recrystallised sedimentary carbonate, or the end product of extreme carbonate and anhydrite metasomatism of original clastic sedimentary rocks. The lack of resistant phases such as zircon, that are abundant where both coarse- and fine-grained sedimentary textures are preserved in the intervals interpreted as lower and upper Roan

respectively, may indicate that in this case the protolith was a sedimentary carbonate.

Structural Geometry

Although drill core is unoriented, insight to macroscopic structural geometry can be gained by measuring angles between core axis and various phases of mesoscopic fabric development. The relationship between primary layering (interpreted as a ghost bedding fabric) and the main phase of cleavage development as shown in Figure 47a, reveals a systematic fold and thrust geometry. Major shear zones, interpreted as relatively shallowly-dipping thrusts, bound the Roan stratigraphy at the top and base, with a number of subsidiary structures identified throughout the interval. The basal thrust separates originally coarse grained Lower Roan strata in the hangingwall from biotite-schist in the footwall, the latter potentially also representing highly altered Neoproterozoic strata (see previous section).

Macroscopic folds range from one to forty metres in amplitude and have distinctive asymmetric profiles defined by shallowly dipping upper limbs and subvertical to just overturned forelimbs. This geometry, as interpreted from bedding to core-axis angles, is supported by pervasively developed asymmetric mesoscopic folds (Fig. 47b). Macroscopic folds commonly root into thrusts suggesting a genetic relationship between two structural elements: folds probably generated above ramps in the thrust architecture or alternatively as fault-propagation folds in front of blind thrusts. The dominant penetrative cleavage, S1 in most domains, but locally S2, is axial planar to these folds, however complications occur in shear zones and locally within forelimbs, where two or in rare cases three cleavage phases are recorded. Partitioning of multiple cleavages into high strain zones is considered to reflect localised refolding or rotation of early formed cleavages away from the bulk flattening plane during a progressive thrusting and folding event. This interpretation of multiple cleavage development during a single event is supported by the observation that within a given sample, each cleavage phase is defined by the same mineral assemblage (see below). In other words, environmental conditions during each phase of cleavage remained constant.

The fold and thrust geometry, including scale of structures developed, is highly reminiscent of the N-directed thrust package exposed in the wall of the Chambishi open pit (Fig. 47c). It would be reasonable to assume therefore, that the structural geometry in NN47 records a similar phase of N-directed thrusting.

A pre-cleavage phase(s) of deformation is implied by fluidization-liquefaction textures within the upper Roan stratigraphy. These textures include clastic dykes and domains of homogenization. It was reported at the December 2000 meeting that the dykes displayed a systematic relationship to folding and cleavage development: clastic dykes invariably occupy the cores of asymmetric folds and are aligned into a sericite/biotite-defined axial planar cleavage (Fig. 48a). It was argued at the time that the spatial and geometric relationship between the dykes and folds may indicate a phase of shortening prior to lithification (ie. a mid-Neoproterozoic orogenic phase). However, recent dating of detrital zircons indicate a Phanerozoic resetting age, which is inferred to provide a good approximation of the age of cleavage development (see below). Clearly Roan strata would have been well-lithified by the Phanerozoic, leaving two possible explanations for the association of clastic dykes and folds: 1) clastic dykes formed whilst the sediments were unlithified, but remained within the extensional field of strain during subsequent layer-parallel shortening and provided sites for fold nucleation; 2) the clastic dykes are not a pre-lithification phenomenon and represent some form of metamorphic fluid over-pressuring during Phanerozoic orogenesis. Although the latter explanation is not totally discounted at this stage, textural evidence in the form of thorough sandstone disaggregation without grain breakage, would make it unlikely. In either case, evidence of fluidization is a conspicuous, regionally developed feature within the upper Roan (i.e. "shale-with-grit" facies), indicating that a widespread fluid over-pressuring event affected this level of the stratigraphy at some stage.

Small-scale pre-cleavage folds were observed immediately above the "ore shale" and within Upper Roan strata at 380m. Profiles are tight, inclined to recumbent, and generally record an opposing sense of vergence to the main folding event (Fig. 48b). The one sample collected for microstructural analysis contained no evidence of an axial planar fabric and as such, could be argued to have formed whilst sediments were unlithified (possibly recording an early thin-skinned extensional or compressive event). On the other hand, they may record the major S-verging fold and thrust phase identified during preliminary mapping at Nkana SOB. Further work is required to establish the significance of these folds.

Alteration–Metamorphism

This section presents initial results from a paragenetic study of post-depositional mineral assemblages. In additional to determining a relative chronology of alteration/metamorphic phases, emphasis was placed on linking the various styles and phases of mineral growth with structural fabrics. An attempt was also made to constrain the absolute age of one of the mineralogical phases (namely the growth of biotite) using U-Pb age systematics in zircons.

Preliminary results indicate that most if not all of the alteration phases span the development of the main cleavage. Furthermore, the distribution of various mineral assemblages appears in cases to be domainal and structurally controlled in the form of veins, secondary permeability induced by distributed grain breakage, enhanced dilation or permeability associated with shear zones and/or fold geometry. Veins and grain-scale fracture zones commonly show evidence of multistage reactivation, with several phases of alteration. These initial results point towards an alteration history (which includes precipitation of Cu-sulfides), which relates to discrete phases of fluid infiltration that were synchronous with deformation.

Four distinct mineral assemblages have been identified: (1) polycrystalline quartz + albite ± microcline ± anhydrite ± carbonate; (2) sericite + muscovite ± quartz; (3) carbonate + biotite ± anhydrite ± Cu-sulfides; (4) chlorite + rutile. Textural characteristics of these phases have been discussed in some detail in the previous section. The following description concentrates on interpretation of their relative temporal relationships and structural control.

Assemblage 1: quartz + albite ± microcline ± anhydrite ± carbonate

Assemblage 1 is best preserved within relatively undeformed, coarse-grained metasediments towards the base of the hole, where new mineral growth occurs initially along detrital grain boundaries (intergranular "pore" space), grading towards a completely recrystallised texture in which pre-existing detrital fabrics are annihilated (Figs 49 & 50). The apparent relationship between *assemblage 1* and originally coarse-grained facies is best shown in the "ore shale", where mineral growth is largely restricted to thin silt or fine sandstone layers (crytoctsytalline quartz or feldspar spheroids are developed locally within the finer grained portions). Polycrystalline quartz is the main mineral phase at the least altered end of the spectrum, with feldspar ± anhydrite becoming important components as detrital textures are progressively destroyed. Rare veins, generally oriented sub-parallel to original layering, contain either fibrous or randomly oriented interlocking crystal aggregates. In the most extreme case of recrystallisation associated with this phase of alteration, twinned albite represents the principal vein component (Fig. 50b). The lack of mica in these domains is conspicuous.

Temporal Relationships

Although overprinting relationships consistently indicate "early" generation relative to later micaceous alteration assemblages, its timing relative to the development of structural fabrics is poorly constrained. Furthermore, although polycrystalline quartz and albite appear to have grown in equilibrium in most samples, we are not certain that they represent a single alteration event (largely due to the problems of discriminating between single and multiple phases of polycrystalline quartz growth on a textural basis).

As the alteration assemblage is largely inter-

granular and confined to originally coarse-grained lithotypes, it could be argued that fluids were introduced relatively early in the burial history, prior to significant compaction and permeability/porosity loss. Indeed, it is difficult to argue on textural grounds alone that the simplest polycrytsalline quartz assemblage did not form in this manner. In a small number of cases however, evidence exists in favour of at least one phase of cryptocrystalline quartz or feldspar having been synchronous with cleavage development and grain breakage. Figure 51 shows evidence of localised sandstone disaggregation interpreted to reflect cataclasis or grain breakage during limited layer-parallel shear. Domains of inferred cataclasis are shown by progressive reduction in grainsize, disaggregation of poly-crystalline quartz-"cemented" detrital textures and formation of angular "shard-like" grains (Fig. 52a & b). Fractured grains are enclosed within a recrystall-ised, cryptocrystalline groundmass (presumably comprising quartz and/or feldspar) and crudely aligned into a bedding sub-normal cleavage (S1). Fibrous tails at the termination of elongate grains (arrows in Fig. 52b) and layer-parallel fibre veins (Fig. 53a: with internal fibres tracking the cleavage) indicate that recrystallization accompanied layer-normal shortening and cleavage development.

Assemblage 2: Sericite + muscovite ± quartz

Sericite and muscovite growth occurs at all levels of the hole, with overprinting of *assemblage 1* minerals best evident within disrupted lower sandstones and coarse-grained intervals within the "ore shale" facies. It produces a honey-grey colour in hand specimen, which progressively replaces and isolates bleached patches of pre-existing *assemblage 1* alteration (Fig. 54 a-c). In thin section, muscovite occurs as elongate grains, commonly aligned sub-parallel to primary layering, particularly within lower levels of the hole. They superficially resemble detrital grains, however, clear overprinting relationships with polycrystalline and cryptocrystalline quartz and/or albite militates against such an interpretation (Fig. 55a). Furthermore, anomalously long grains very commonly have fibrous quartz beards (Fig. 55b). These quartz beards are entirely restricted to the margins of muscovite flakes and importantly are not developed around more rigid quartz or feldspar grains as would be expected if they represented fibrous overgrowths developed in pressure shadow regions during layer-parallel shortening. The muscovite grains themselves are undeformed, and are interpreted to have formed as cores to quartz-mica micro-veinlets which opened in response to layer sub-perpendicular stretch.

Temporal Relationships

Within domains interpreted to have been affected by distributed cataclasis, the sericite-muscovite abundance increases disproportionately with grainsize. Figure 56 shows a relict "pod" of *assemblage 1* altered sandstone enclosed by a finer grained, open framework texture of quartz, feldspar and anhydrite grains set within a sericitic groundmass. Detail of this transition from *assemblage 1* to *assemblage 2* within increasing disruption of original detrital fabrics is shown in Figure 57a-c. As the margin of the relict pod is approached, sericite is initially distributed along fine fracture seams which effectively follow detrital grain boundaries (Fig. 57a, b). With further reduction in grainsize (Fig. 57c), a crude grain-shape fabric is defined by coarser grained growth of muscovite and alignment of fragmented detrital grains. These textural relationships are interpreted to indicate that alteration was synchronous with, and focussed along domains of cataclastically-induced grain-size reduction.

Similar examples of sericite-muscovite growth within domains of cataclasis are shown in Figures 58-60. In each example, micas overprint domains of *assemblage 1* cataclasis and/or veining, with layer-parallel alignment of muscovite and rotated quartz fragments. In Figure 58, layer-parallel micas overprint S1 defined by an *assemblage 1* grain shape fabric, however in Figure 59, the same micaceous fabric is subtly crenulated by S1. The implication of these complex overprinting relationships is that cataclasis and both *assemblage 1* and *assemblage 2* mineral growth (including layer-parallel muscovite growth) span the development of the S1 cleavage. A similar textural relationship involving growth of white mica both

parallel to layering and the S1 cleavage was observed in the "ore shale" facies (Fig. 61).

Fluid focussing by D1 structures can also be argued by the apparent concentration of sericite within F1 fold hinges breached by clastic dykes and fracture seams within "fluidized" strata from the upper part of the logged section. The composite micrograph in Figure 62 demonstrates a progressive increase of S1-parallel streaky sericite towards the core of a fluidization dyke. This spatial association of sericite and breached F1 fold hinges is potentially explained by fluid infiltration along secondary permeability induced by during the folding event. Alternatively, it could be argued that K-rich mineral assemblages were concentrated within clastic dykes prior to F1 folding.

Assemblage 3: Carbonate + biotite - phlogopite ± anhydrite ± chalcopyrite

Biotite and to a lesser extent carbonate growth is almost ubiquitous in NN47. Although all biotite growth is included within this assemblage, there is considerable variation in its composition from very pale phlogopite to dark green-brown Fe-rich end members.

The mineral assemblage ranges from disseminations in both fine and coarse grained lithofacies to broad domains of structurally-controlled flooding in which all pre-existing detrital and alteration textures are destroyed. The domainal nature of *assemblage 3* is perhaps more obvious than prior alteration at the macroscopic scale, as there is a crude relationship between greater intensity of carbonate + biotite ± anhydrite alteration and both increasing "bedding" dip and major shear zones.

Where disseminated or weakly developed, *assemblage 3* biotite and carbonate occurs throughout the matrix of fragmented sandstones, fine siltstones or shaley facies, within thin layer-parallel veins containing either fibrous or randomly oriented infills, and in narrow deformation seams (Figs. 63 & 64). Dilation or reactivation of *assemblage 1* quartz + feldspar layer-parallel "veins" or recrystallized zones is common, within which carbonate, biotite and locally anhydrite appears to have grown in textural equilibrium with chalcopyrite (Fig. 65). In general, the distribution of *assemblage 3* at the grain-scale conforms most closely with that of *assemblage 2*, particularly within disaggregated sandstone domains, where fine grained biotite progressively replaces muscovite (Fig. 67). Within the "granite" facies near the base of the hole, biotite occurs as clots positioned in pressure shadow regions about the terminations of relict quartz and feldspar porphyroclasts flattened into the S1 cleavage.

In a number of cases, there is an apparent spatial association of biotite with concentrations of zircon grains in fine-grained domains (Fig. 68). This association was originally interpreted to indicate a phase of hydrothermal zircon growth that was potentially coeval with biotite growth. Examination of zircon morphology however, indicated complex internal zoning (uncharacteristic of hydrothermal zircons) and rounded to subrounded or abraded habits, suggestive of sedimentary reworking. A detrital origin for these zircons was further supported by U-Pb age dating, which indicated Palaeoproterozoic ages partially 'reset' by a 500-450 Ma thermal event (see next section).

Concentration of detrital zircons within a noticeably finer grained interval of a relatively coarse sandstone, as shown in Figure 68, is inconsistent with the mechanics of sedimentation. The concentration process is thus considered to be post-depositional, in which detrital zircons represent the resistate phase during some form of volume loss. Chemical dissolution of more labile constituents including quartz and feldspar or mechanical breakdown of weak grains via cataclasis, in either case leaving a zircon-enriched residuum, would seem the most likely processes. The heavily fractured nature of some of these zircon grains (Fig. 69: note not that sample shown in Fig. 68) would tend to suggest that cataclasis played an important role in grain-size reduction. Thus, as with *assemblage 2*, it can be argued that grain-scale concentration of biotite occurred within domains of cataclasis, which in turn can be interpreted to indicate that localised, structurally induced permeability provided the means of fluid infiltration.

Domains of *assemblage 3* "flooding" conform to **carbonate-biotite-quartz schist facies** and **carbonate-anhydrite-biotite facies** of the earlier "lithofacies" section of this report. To group this complex facies association into a single alteration assemblage is perhaps overly simplistic, however its has been difficult to discriminate between on them on temporal grounds and they are commonly spatially associated. As noted in the "lithofacies" section, the level of recrystallisation makes the protolith difficult to resolve. An apparent lack of detrital zircons is anomalous in terms of the overall stratigraphy however, and may indicate a sedimentary carbonate or fine grained siliciclastic origin. On the other hand, as mentioned earlier the distribution of flooding zones appears in part structurally controlled, with pale carbonate + anhydrite + biotite flooding in particular displaying crude vein-like forms and commonly occupying the steepened forelimbs of macroscopic folds (Fig. 70 & 71).

Temporal Relationships

As with the previous assemblages, biotite and carbonate growth appears to span cleavage development, although locally temporal relationships are complicated and conflicting. Within domains in which structural fabrics are relatively simple and relate to only one phase of folding or cleavage development, mineral growth is generally syn- to late S1. In such cases, biotite and carbonate can be strongly aligned into the cleavage, forming bedding-parallel veins whose internal fibres track the trace of the external cleavage, or alternatively occur as fairly randomly oriented, stubby grains which overprint a pre-existing muscovite-defined S1 cleavage. By contrast, in more complex domains, such as zones of high shear strain or refolding of early fabrics, strongly aligned biotite invariably defines each cleavage (Fig. 72). There is little variation in the composition or morphology of each phase of biotite growth within a given sample (as determined from their optical characteristics), suggesting that successive episodes of cleavage development formed under similar environmental conditions.

Assemblage 4: Chlorite + Fe-Ti oxide

Within high strain domains, such as the thrusted upper contact of the Roan package and the biotite-carbonate-quartz schist at the base of the hole, biotite shows progressive degradation to chlorite and rutile (Fig. 73). This phase of alteration is interpreted to represent localised retrogression of *assemblage 3* minerals within and adjacent to major shear zones towards the end of the main thrusting event.

Zircon Dating Study

A pilot U-Pb zircon dating study (using laser ablation ICPMS) was undertaken on samples from NN47 and NE112 (collared east of Nchanga) in an attempt to resolve problems concerning the discrimination of "basement" from highly strained and/or altered portions of the Katangan stratigraphy. As reported in at the December 2000 meeting (and reiterated in previous sections of this report), units interpreted in a number of company logs as Lufubu Schist or "granitic gneiss" do not display greater degrees of metamorphism or additional phases of deformation than those logged as Katangan sequence. We concluded that either peak metamorphism was not achieved until after deposition of the Katangan sequence, or structurally lower units were incorrectly logged as "basement" but in fact represented highly strained Neoproterozoic rocks. The importance of confidently discriminating between "basement" and "basin" becomes very apparent in terms of reconstructing original basin geometries (for instance, critically reviewing onlap relationships of lower Katangan rocks onto "basement" highs).

It was envisaged that basement units, including the Muva Quartzite and Lufulbu Schist could be distinguished from Katangan in terms of their respective zircon populations: ie. a component of detrital 880 Ma zircons eroded from the Nchanga Red Granite phase would be restricted to the Katangan rocks.

A second, and equally as compelling reason for the study was that initial petrographic studies indicated that some of the zircons within the Katangan rocks may have formed during

hydrothermal alteration phases. Although the majority of zircons have 'typical' detrital morphologies (ie. rounded habits, anhedral forms with truncated zonation on grain faces) and are strongly partitioned into coarse-grained facies, a significant proportion have euhedral habits and occur irregularly clustered within (syn-kinematic) biotite-rich domains, anomalously fine-grained portions of the sample, shear zones or fractures. It was considered that if these "anomalous" grains had grown during a syn-kinematic hydrothermal or metamorphic event, U-Pb systematics could be used to constrain the age of this event(s).

Results

SEM back-scatter imaging was used to enhance zircon morphology. Grain habits range from beautifully rounded to euhedral, with various degrees of fracturing. In general, unequivocal detrital grains, with texturally mature rounded morphologies are more common within units originally logged as Katangan. Units logged as "basement" (granite or granitic gneiss) have a greater abundance of euhedral zircons, with well developed internal zoning, consistent with a magmatic origin and little or no sedimentary reworking. This relationship does not hold for all cases however, with sub-rounded habits occurring within "granitic gneiss" at the base of NE112, suggesting that this highly strained (locally mylonitic) was derived from a sedimentary rather than plutonic protolith.

Internal textures are complex: up to three phases of zircon growth evident in some grains, with xenotime overgrowths becoming particularly common within the upper Roan stratigraphy in NN 47. In general, original cores are well zoned (suggestive of a magmatic origin), whereas overgrowths are more homogenous. At least two phases of zircon growth predate sedimentary reworking, whereas the final phase of growth arguably post-dates redeposition. The latter possesses a distinctive "mottled" texture, which occurs as overgrowths on rounded grain margins, internal fractures, or in extreme cases apparently 'replaces' the entire grain. In general, the component of "mottled" zircon increases proportionally with grain fracture.

A $^{206}Pb/^{238}U$ vs $^{207}Pb/^{235}U$ concordia plot is shown in Figure 73. Immediately apparent, is the overall paucity of 880 Ma grains derived from the Nchanga Red Granite phase. Only three of fifty three quality U-Pb ages are likely to record reworking of this plutonic phase, indicating that its detrital contribution is either very localised or considerably less significant than generally thought. One of these grains came from Lower Roan strata in NE112, whereas the other two came from the "granite" facies towards the base of NN47. It could be argued that the 837 ± 57 Ma and 914 ± 66 Ma grains in the "granite" facies indicate that this unit is in fact a thin sliver of Nchanga Red Granite phase, however they represent just two of twenty three analyses in this unit, the remainder returning Meso- to Palaeoproterozoic ages (see samples 622.6 and 624.7). Unless it can be shown that the Nchanga Red Granite phase comprises an anomalously high component of inherited zircons (>90%), it would seem more reasonable to interpret this unit as a Neoproterozoic metasediment, with detrital contribution mainly from Palaeoproterozoic (and possibly Mesoproterozoic) basement source rocks.

The overall lack of contribution from an Nchanga Red Granite type source creates a problem in terms of discriminating "basement" from "basin". Breakdown of data according to the stratigraphy interpreted in company logs (Fig. 73) shows gross similarities between zircon age spectra (with the exception of 617.4 from NN47), regardless of their structural position.

Although the spread of age data is broad, it defines a fairly simple discordia trend which links Palaeoproterozoic and earliest Phanerozoic concordant end members (Fig. 73). Furthermore, a crude systematic relationship can be shown between grain morphology and age. In general, individual grains reveal progressively younger ages as zircon growth becomes more complicated. This is to be expected, as the laser effectively homogenises the grain, providing an average of all stages of zircon growth. Euhedral to well-rounded, but noticeably unfractured grains with up to two phases of zircon growth (but lacking the

final "mottled" phase) consistently return Palaeoproterozoic ages: roughly 2100 – 1670 Ma (ignoring errors). This spread of ages is tentatively interpreted to represent various ratios of contribution from an initial 2000-2100 Ma magmatic source and a probable high grade metamorphic overgrowth during the late Palaeoproterozoic. This finding is inconsistent with the original petrographically-based interpretation that strongly clustered, euhedral grains record a phase of hydrothermal growth. As argued in the previous section, we now believe the 'clustering' of detrital grains to be in part, at least, the result of post-depositional grain-scale deformation.

On the other hand, grains which are both fractured and contain a component of the "mottled" zircon phase, have ages which are consistently younger than those associated with relatively undeformed and well-polished examples. Moreover, we make the observation that as the "mottled" phase increases in abundance, the age becomes younger. Our provisional interpretation of this relationship is that the "mottled" zircon phase records the younger end member of the age spectrum. The interpretation is provisional, as unfortunately due to time constraints, we were prevented from obtaining SEM back-scatter images of the youngest zircons from 617.4 (NN 47: Fig 73 & 74). This sample has a discordant range of ages from earliest Mesoproterozoic/latest Palaeoproterozoic to Ordovician, with a calculated weighted mean of the four youngest concordant ages of 477 ± 16 Ma.

Sample 617.4 is also anomalous in terms of its microstructural and alteration textures. It represents the most intensely recrystallised of all the samples collected for petrographic study, with pervasive albite and subsequent phlogopite "flooding" (*assemblages 1 & 3* respectively). This apparent spatial association of "reset ages" with a domain of anomalously intense alteration raises the possibility of a genetic and hence temporal relationship between zircon recrystallisation and metamorphism/hydrothermal activity (although it is unclear as to whether zircon recrytallisation relates to albitic or phlogopitic alteration). As we consider the various alteration phases to span cleavage development, the 477 ± 16 Ma age also provides our best estimate for the main fold and thrust event recorded in NN47.

We stress that these results and interpretations are preliminary as the textural characteristics of the youngest zircons and their genetic relationship to alteration/deformation are yet to be fully resolved. However, supporting this interpretations is the 513-496 Ma age of albitization reported at Musoshi (Hitzman and Broughton; preliminary report).

Geology of DDH NN 47, Chambishi Basin

Stuart Bull & David Selley

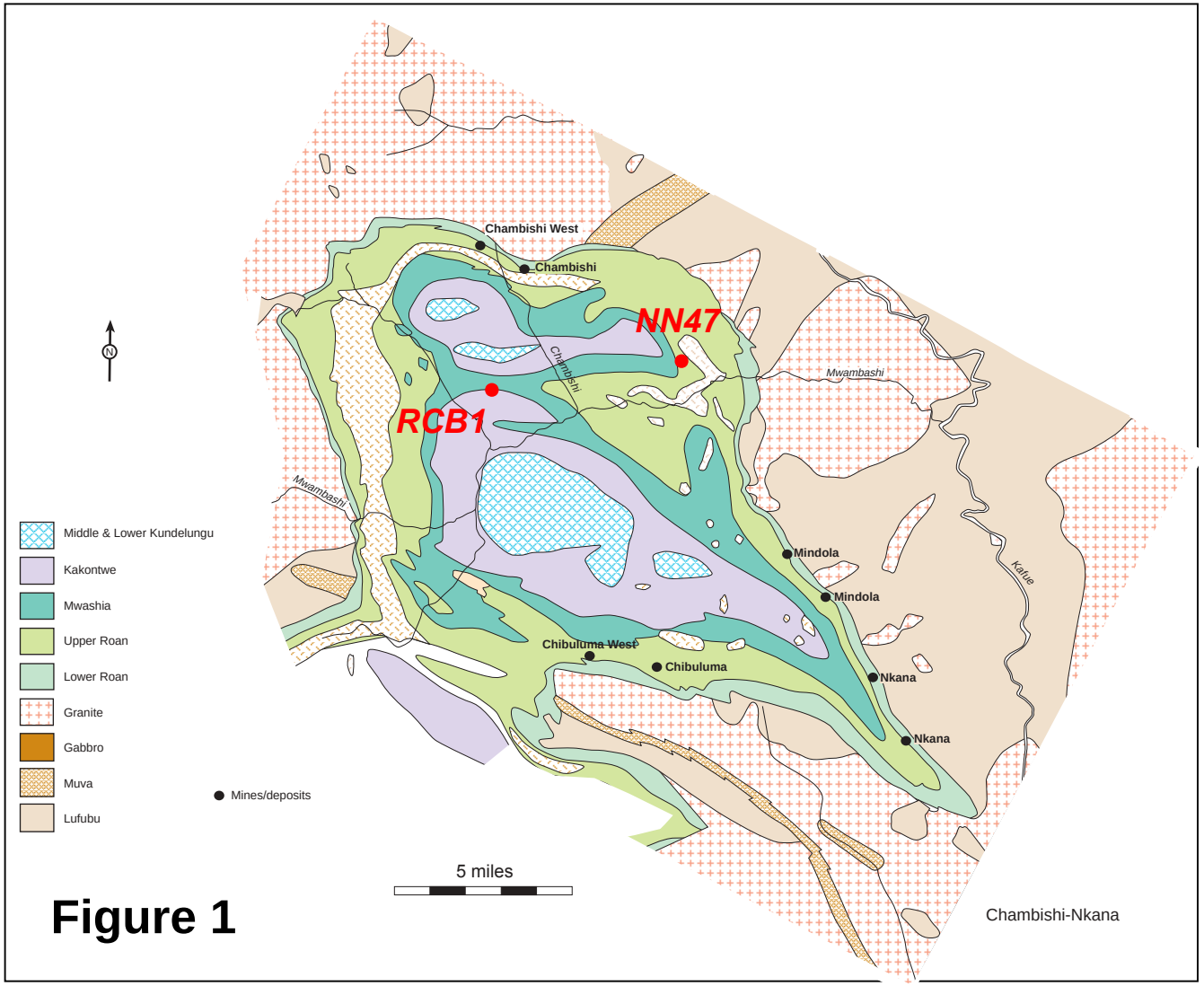

Figure 1

In the Roan, what is sedimentary vs structural (vs alteration vs metamorphism)?

Collared in the upper Roan and terminated in Basement Complex (granite/Lufubu Schist)

With respect to the features you see in the Katangan rocks, two end member views

- most are primary sedimentary features
- most are alteration and structural fabrics

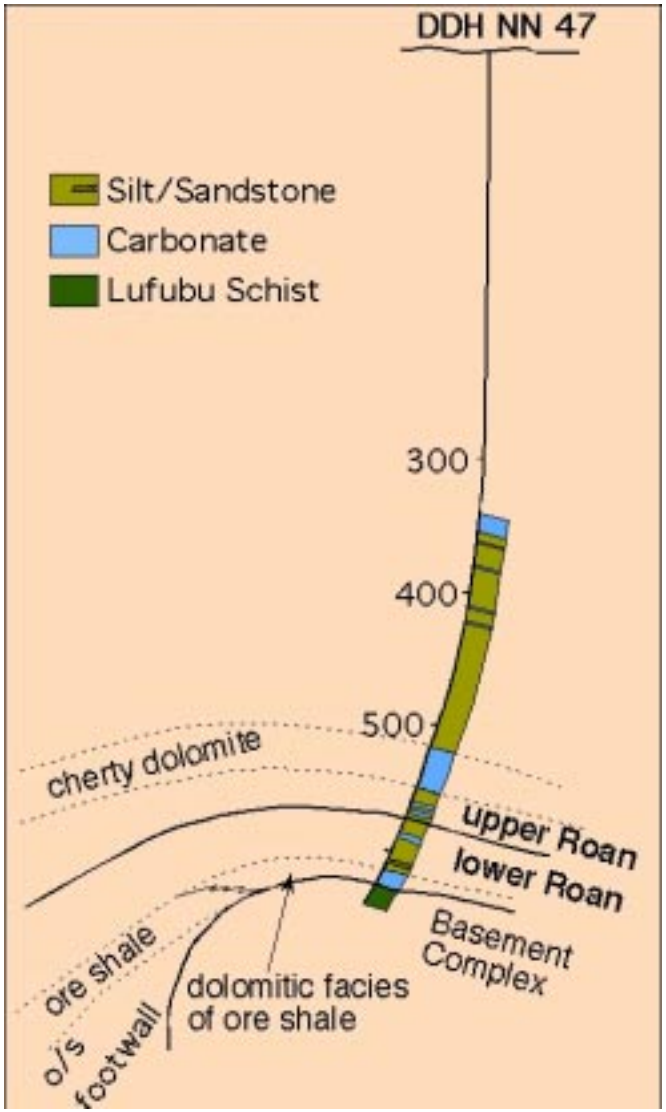

Figure 2

In the Roan, what is sedimentary vs structural (vs alteration vs metamorphism)?

Difficult rocks! Roan sediments are fluidised, altered/metasomatised, recrystallised/metamorphosed and deformed

Hard to understand:

- What we are looking at
- Reconciling previous interpretations

Logged the hole in terms of 6 lithofacies

Have now been studied petrographically

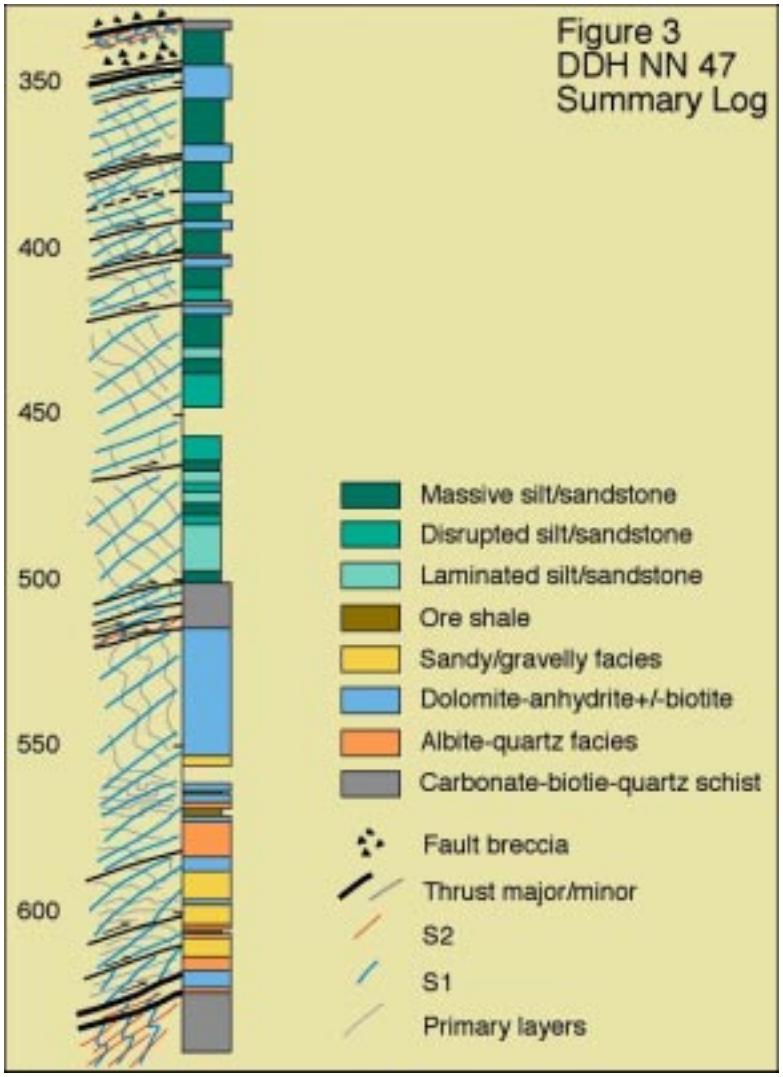

Figure 3

Sandy/gravelly textured facies

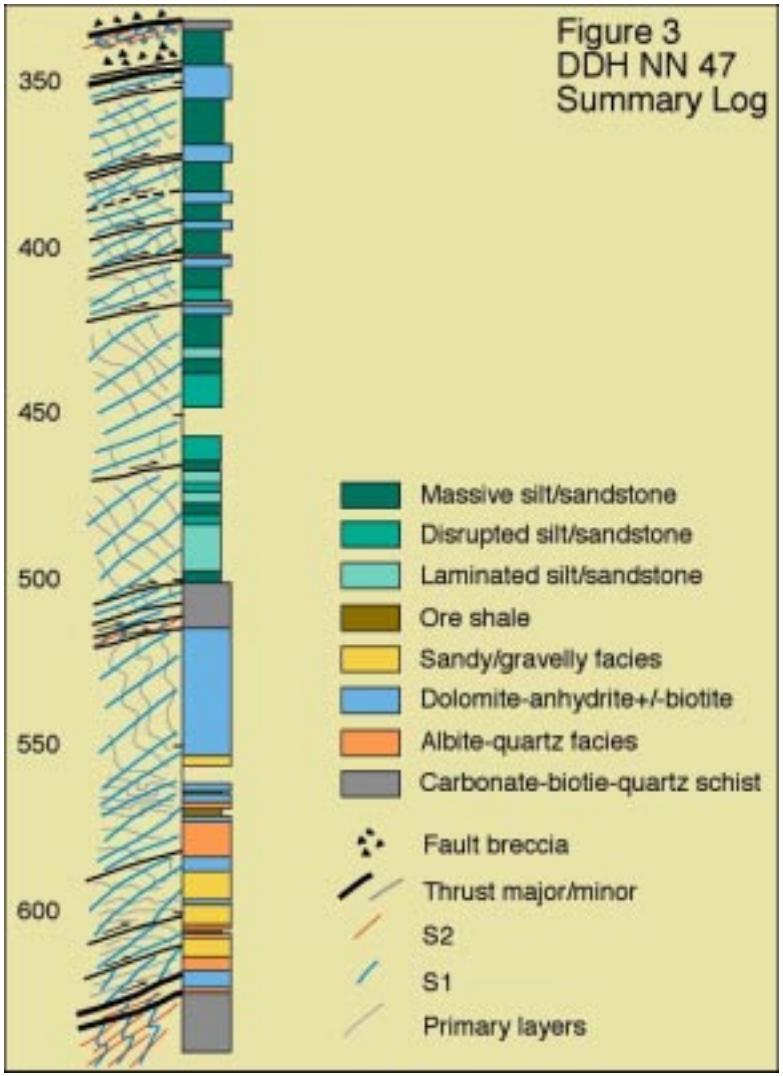

Sandy/gravelly textured facies

Hand specimen description

- Massive/stratified (foliated?)
- Grey/green - cream - pink coloured
- Sandy/gravelly texture defined by dispersed colourless and blue quartz and feldspar grains

Figure 5

Sandy/gravelly textured facies

Thin section description

Framework;

- 1-4 mm crystals of mono crystalline quartz, feldspar (mostly microcline)
- And poly-crystalline quartz?
- Lesser lithic fragments (cherty and metasedimentary), plagioclase & zircon

Matrix;

- Fine-grained aggregate of feldspar & quartz overprinted by biotite, carbonate & anhydrite

6a

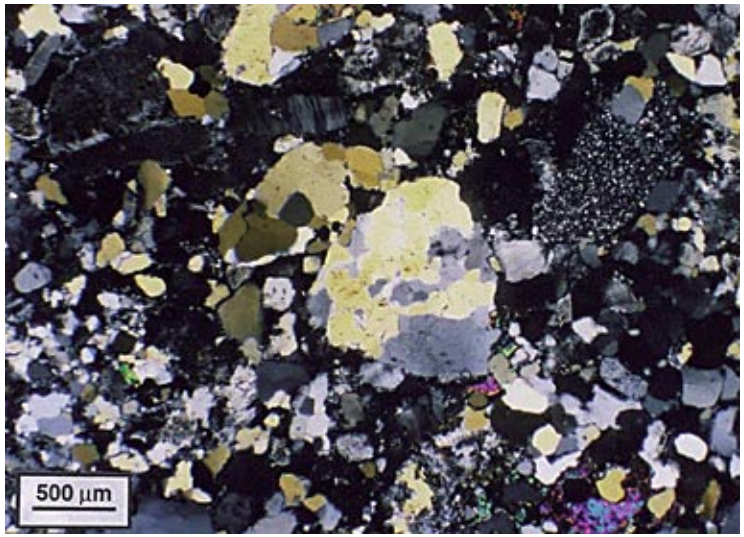

6b

Sandy/gravelly textured facies

7a

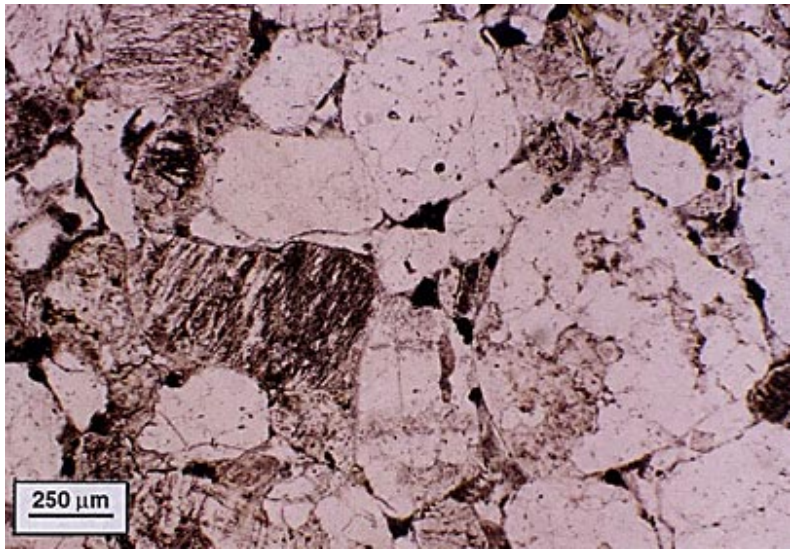

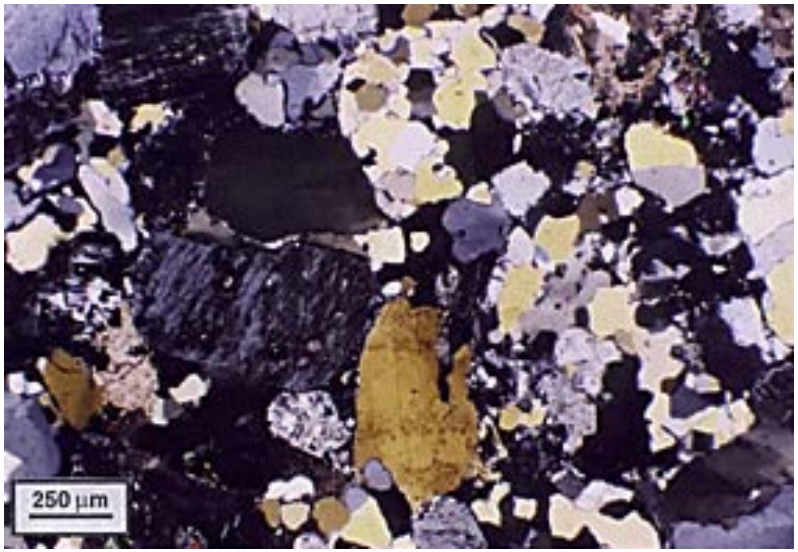

7b

8

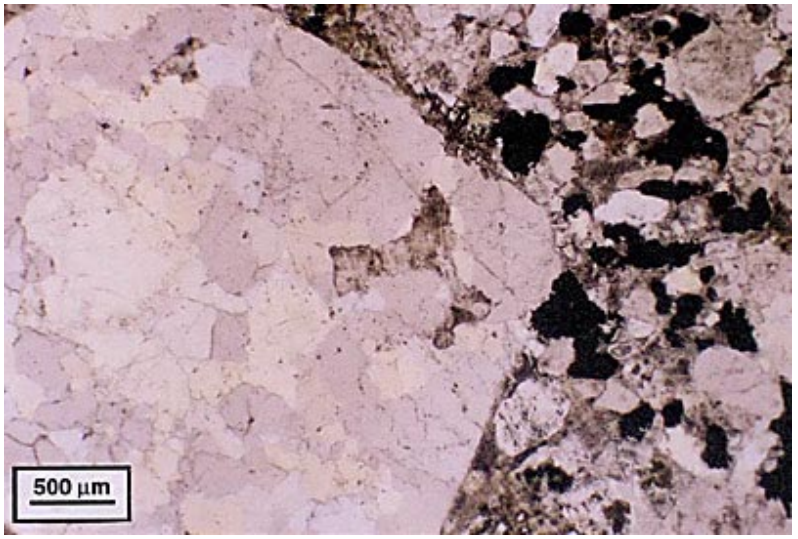

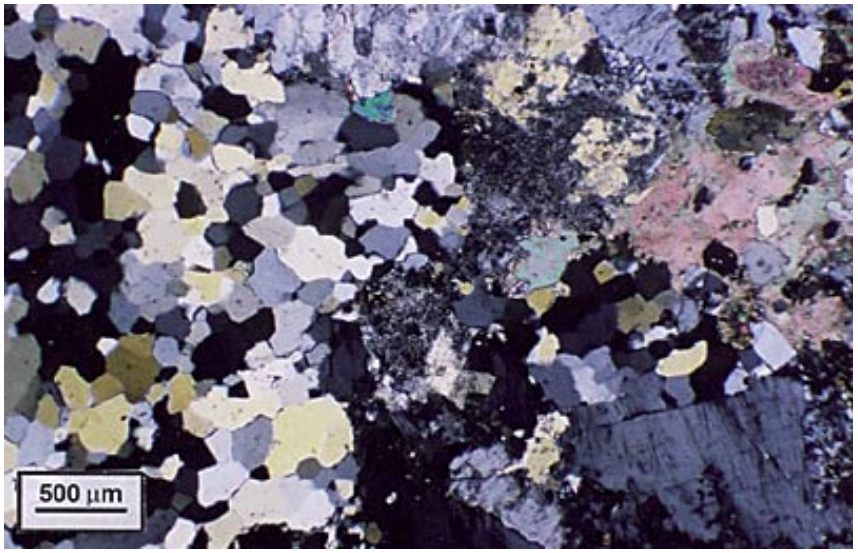

9

Sandy/gravelly textured facies

10

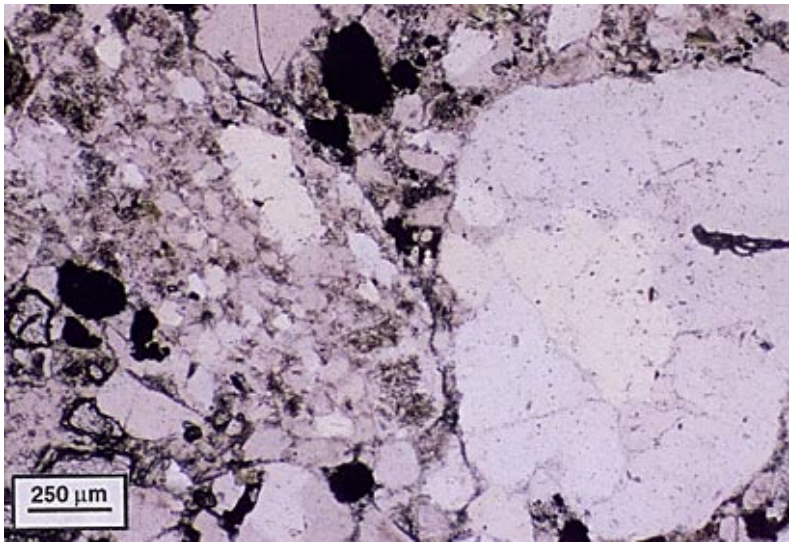

11

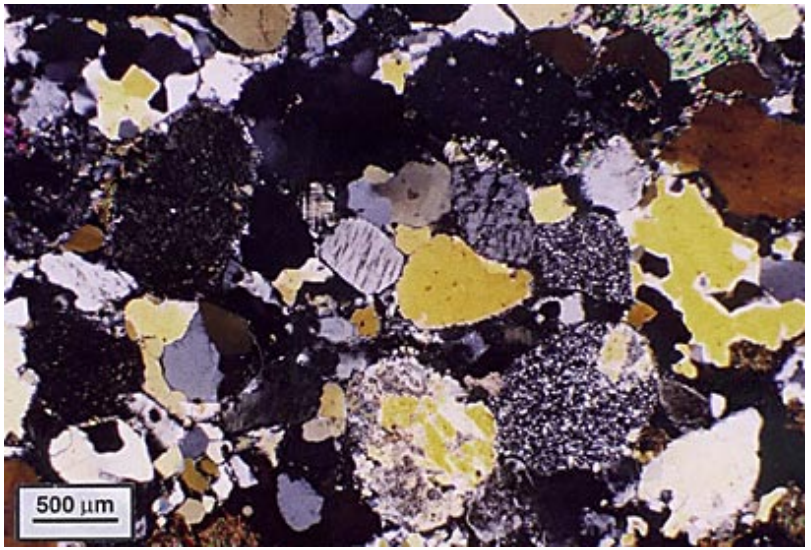

12a

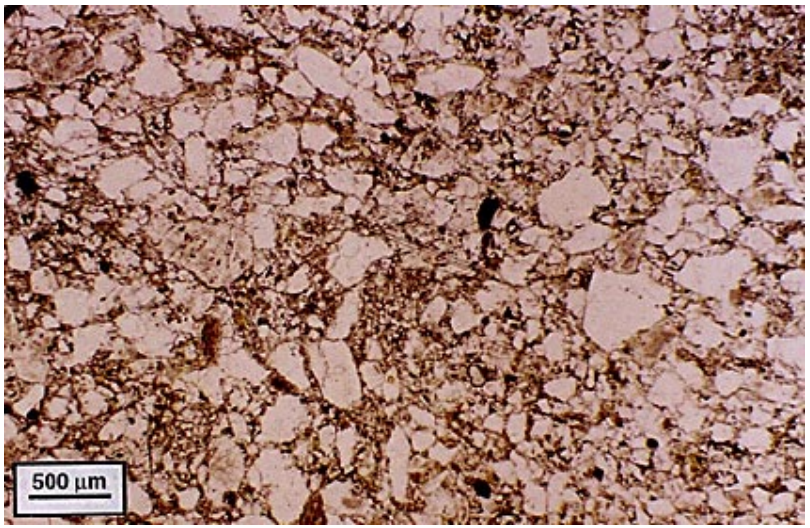

12b

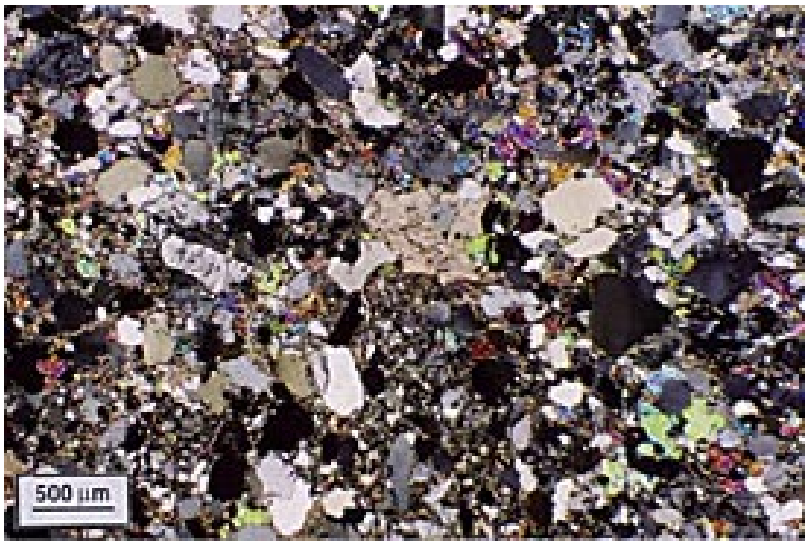

Sandy/gravelly textured facies

Why were these rocks so hard to interpret?

Progressive overprinting of protolith clastic textures by poly-crystalline quartz, carbonate, plagioclase (albite?), micas (sericite/muscovite, chlorite, biotite) & anhydrite

Unclear whether this process represents metamorphic recrystallisation (essentially isochemical) or progressive alteration/metasomatism?

Figure 5

Sandy/gravelly textured facies

13

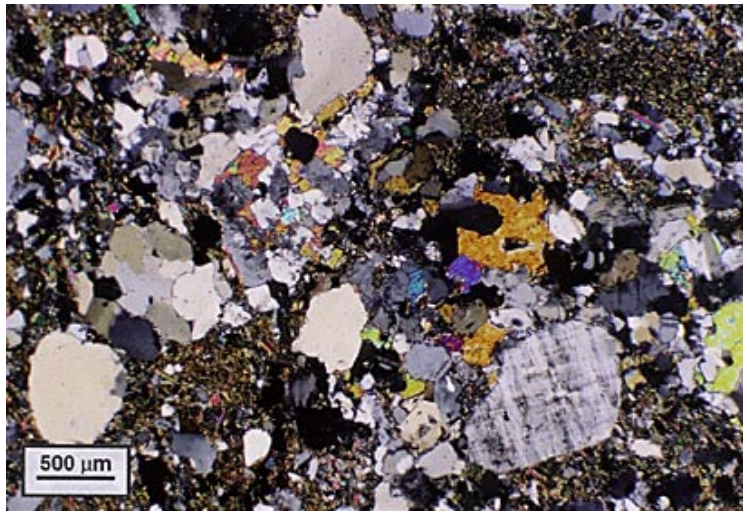

14

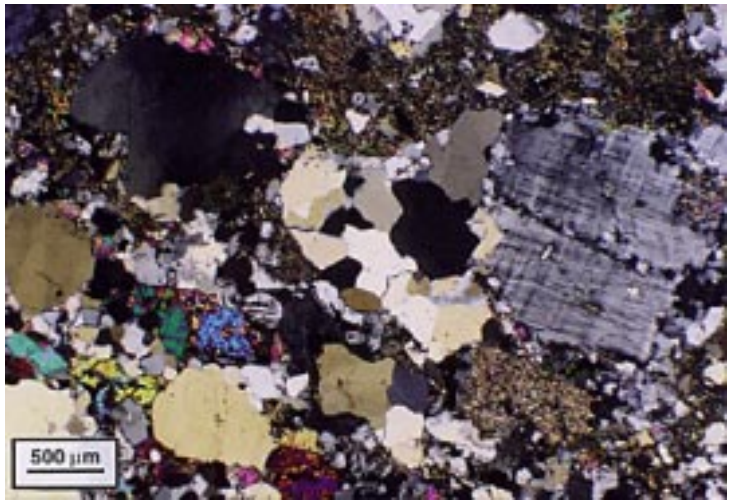

15

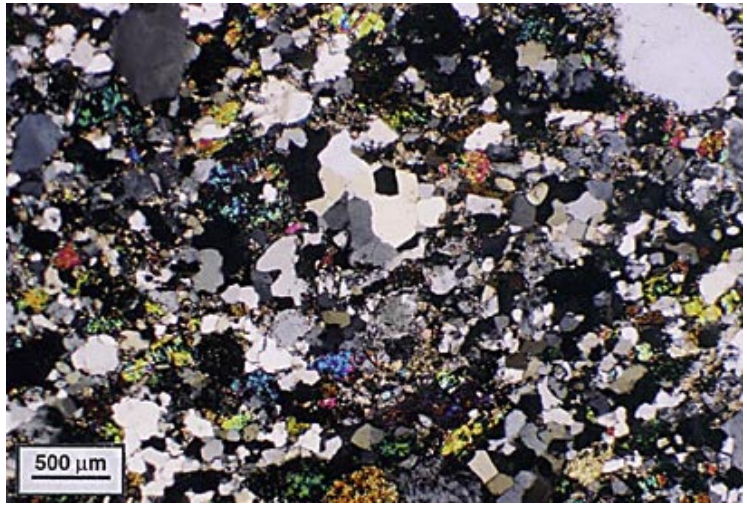

16

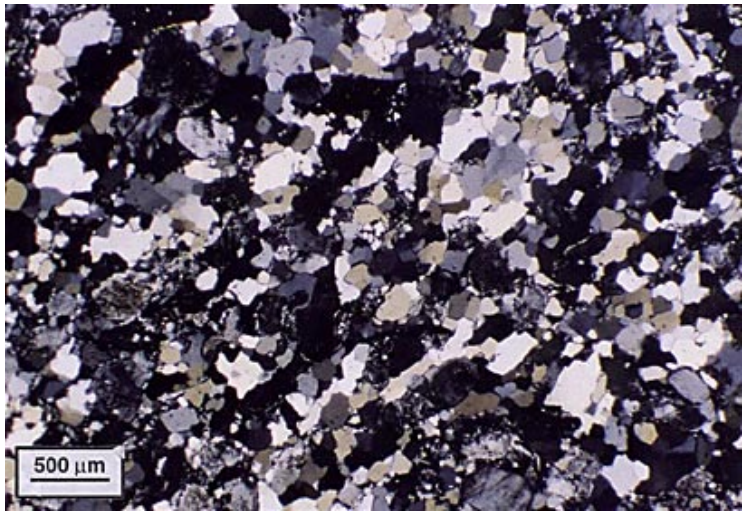

Quartz albite facies

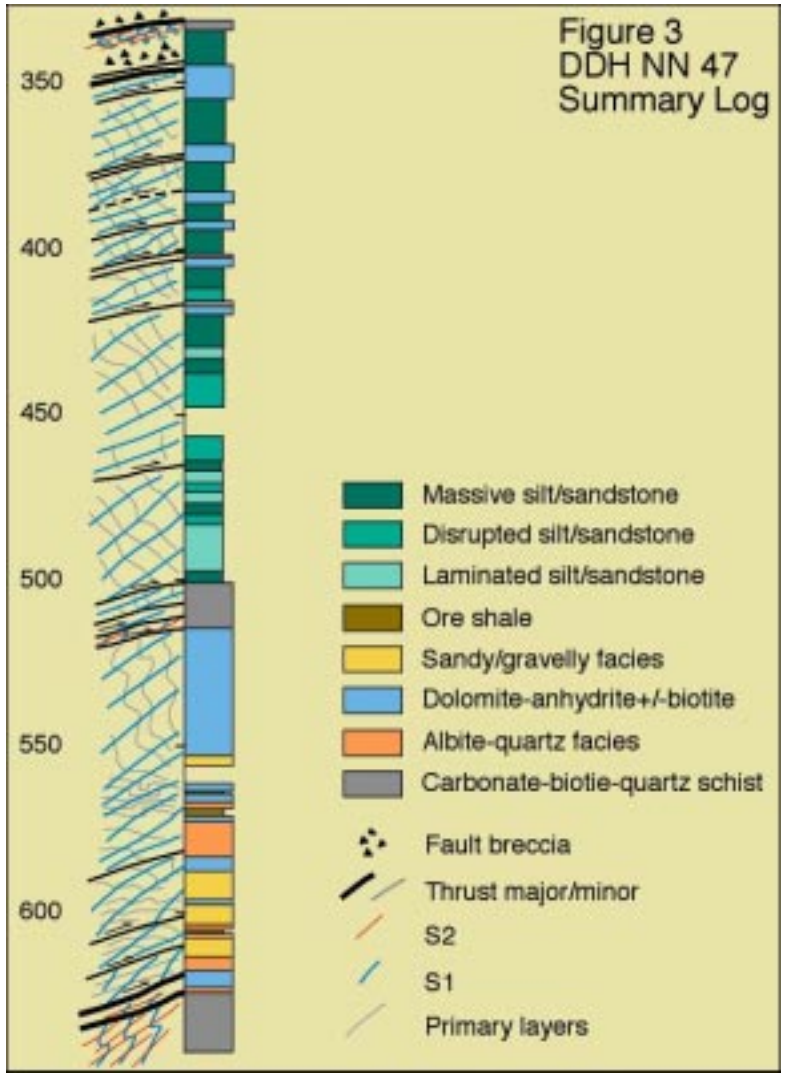

Quartz albite facies

Quartz albite rocks are an end member of one of these overprinting/alteration phases

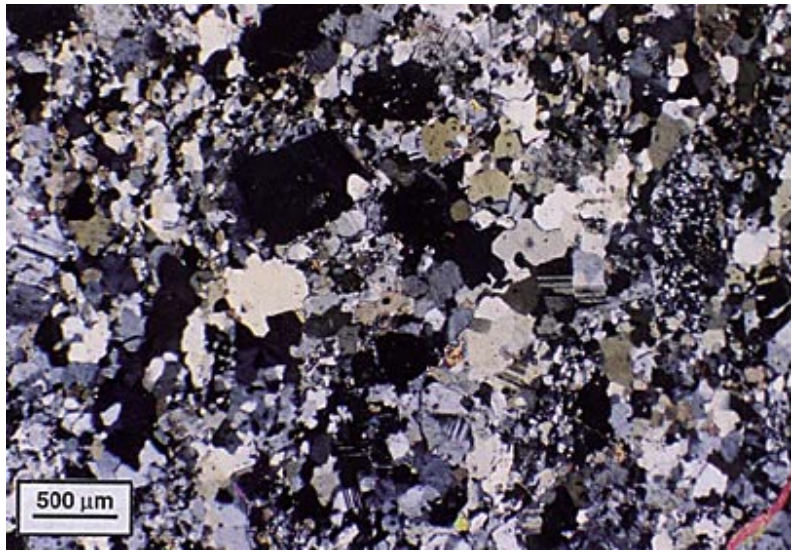

18

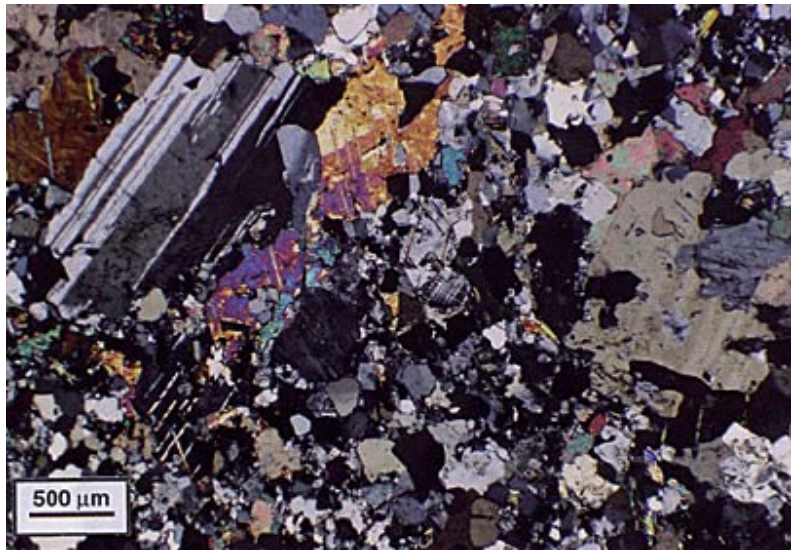

19

“Granite”


Figure 20

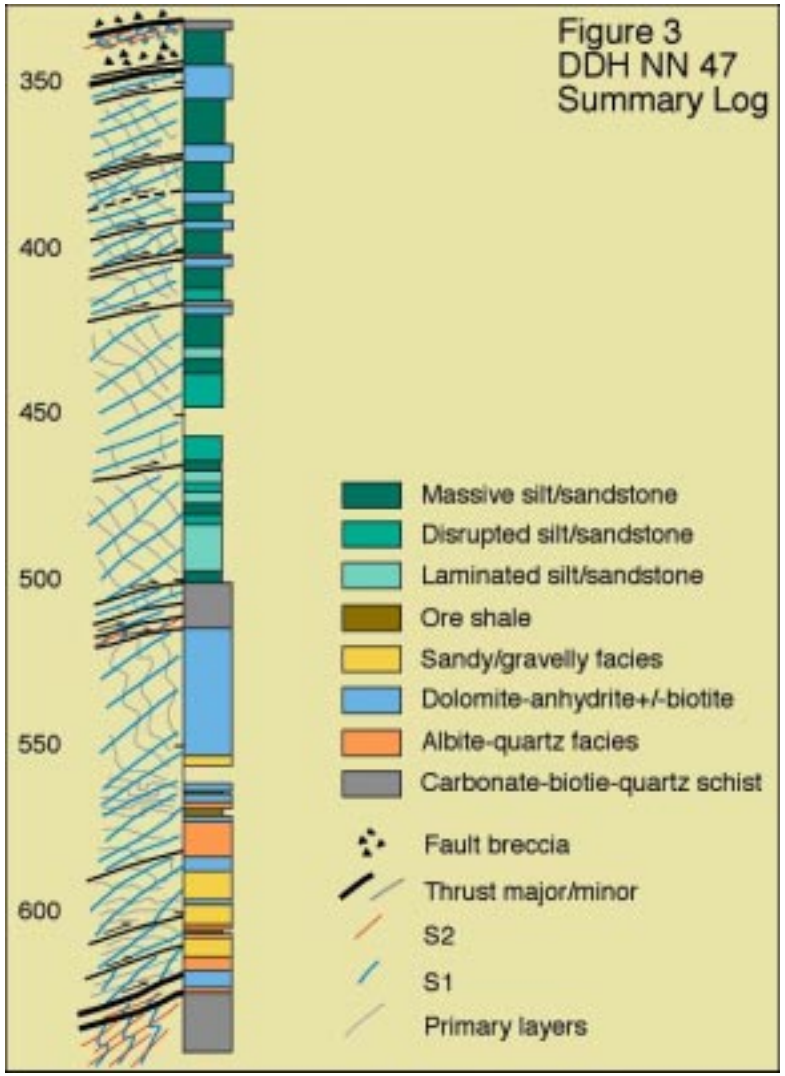
Figure 3
DDH NN 47
Summary Log
350
400
450
500
550
600
Massive silt/sandstone
Disrupted silt/sandstone
Laminated silt/sandstone
Ore shale
Sandy/gravelly facies
Dolomite-anhydrite+/-biotite
Albite-quartz facies
Carbonate-biotie-quartz schist
Fault breccia
Thrust major/minor
S2
S1
Primary layers

“Granite”

Mosaic of poly-crystalline quartz, feldspar, biotite and carbonate

End member of one of the recrystallisation/alteration phases

Nb plagioclase (albite) occurs as rims around degraded microclines suggesting some control by protolith on overprinting assemblage

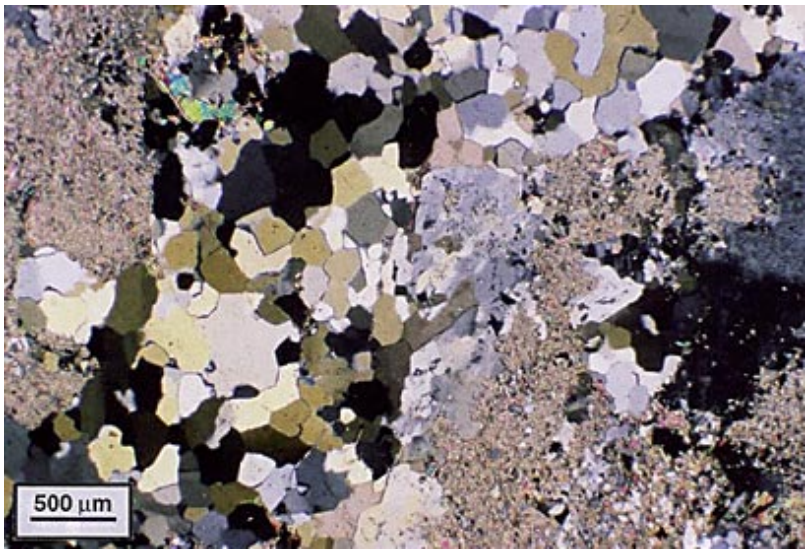

21

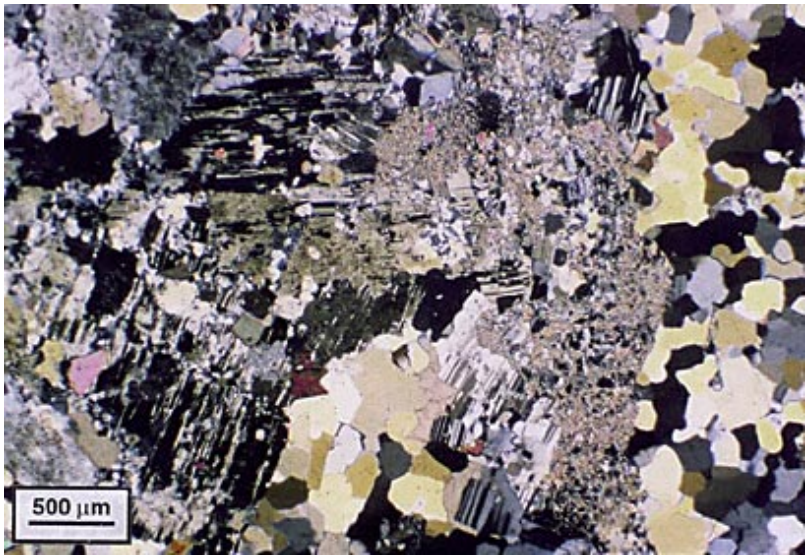

22

Fine sand & siltstone facies

Figure 23

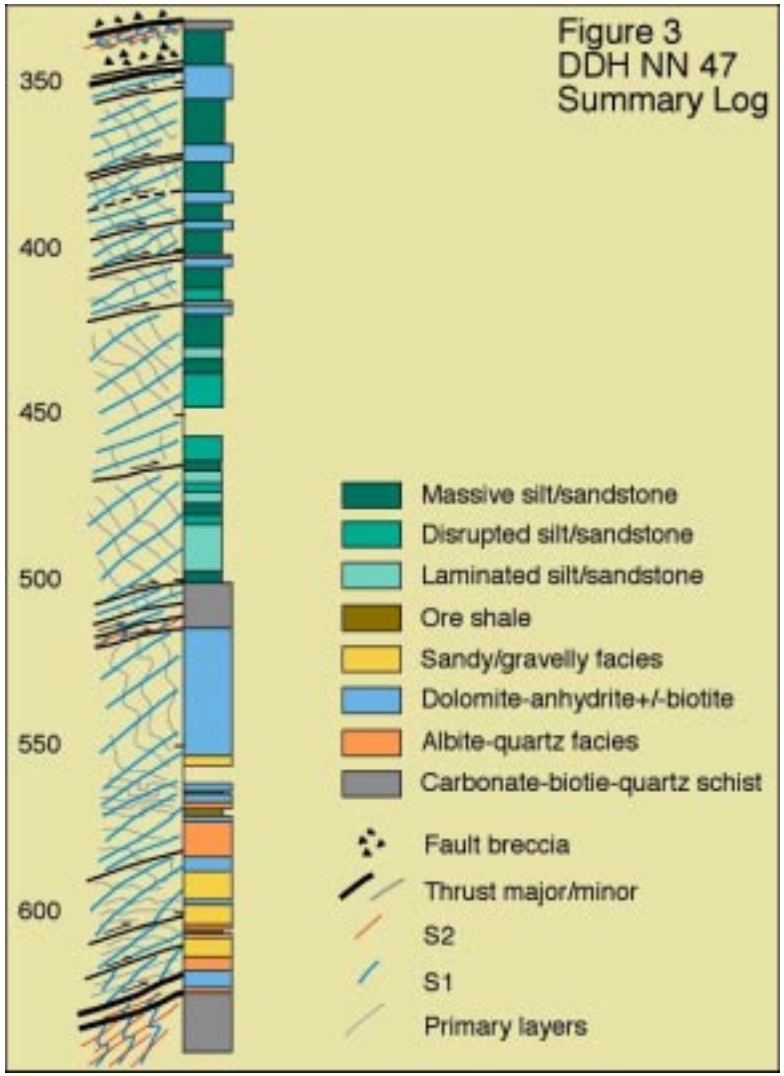

Fine sand & siltstone facies

Hand specimen description

- Grey/green coloured (chloritic) metasediments
- Fine-sandstone/siltstone texture defined by colourless and blue quartz and feldspar grains
- Where primary sedimentary structures are preserved is thinly-bedded/laminated (locally rippled)
- Generally disrupted to entirely homogenised (early fluidisation or later deformation?)

Figure 23

Fine sand & siltstone facies

Thin section description

Framework;

- Laminae are massive to normally graded fine-grained sandstone of mono-crystalline quartz & microcline

Matrix;

- Silt-sized aggregate of feldspar, quartz & micas locally overprinted by carbonate &/or anhydrite

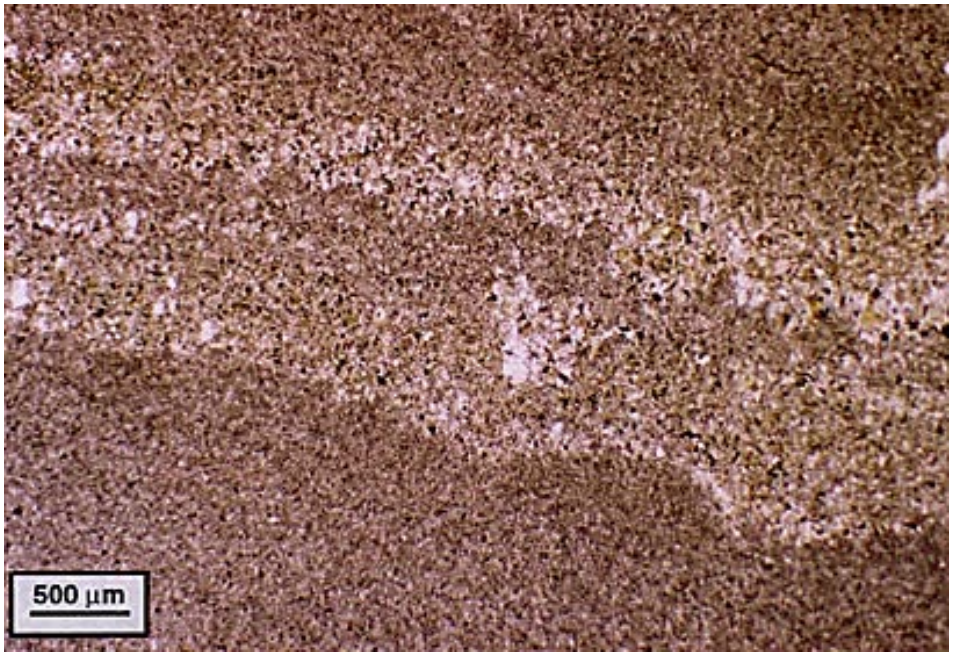

Fine sand & siltstone facies

25

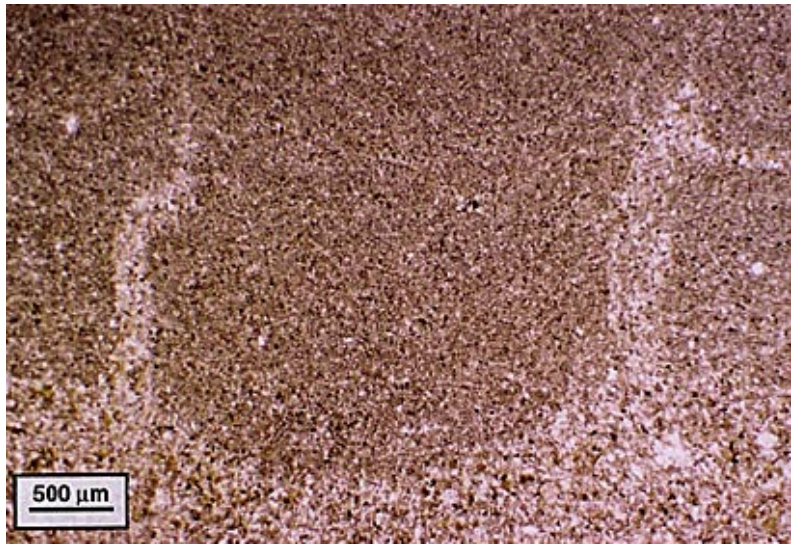

26

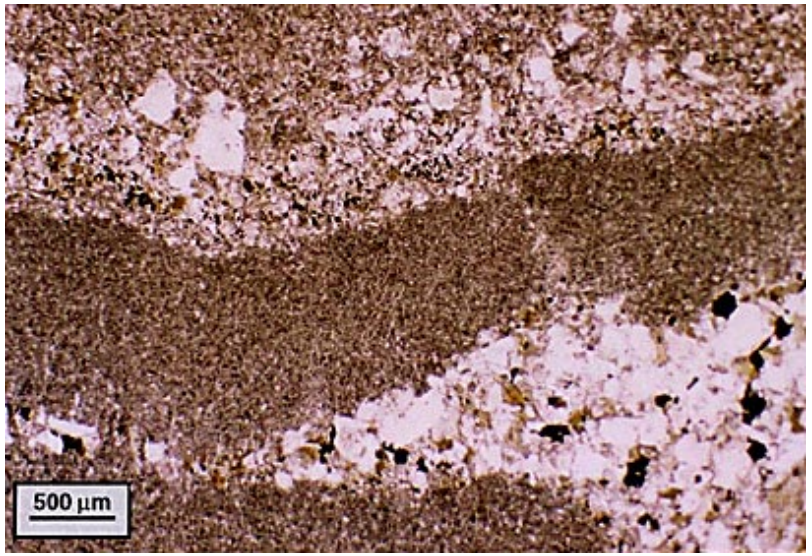

27

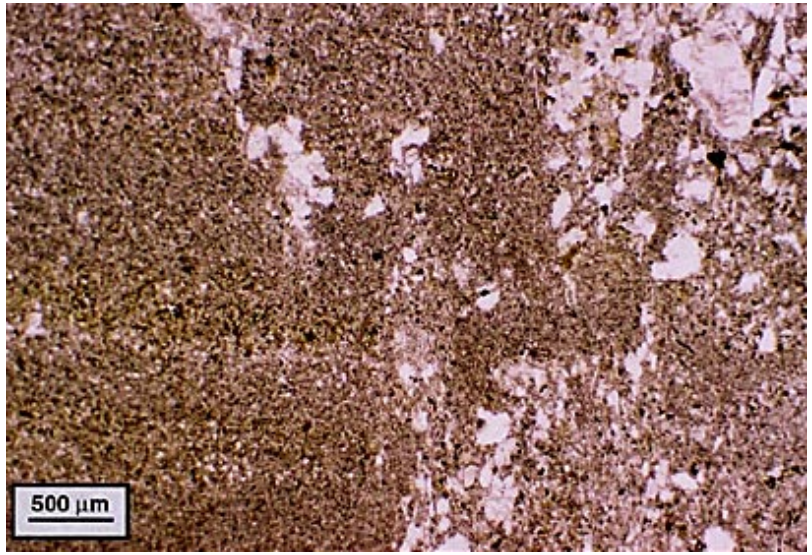

28

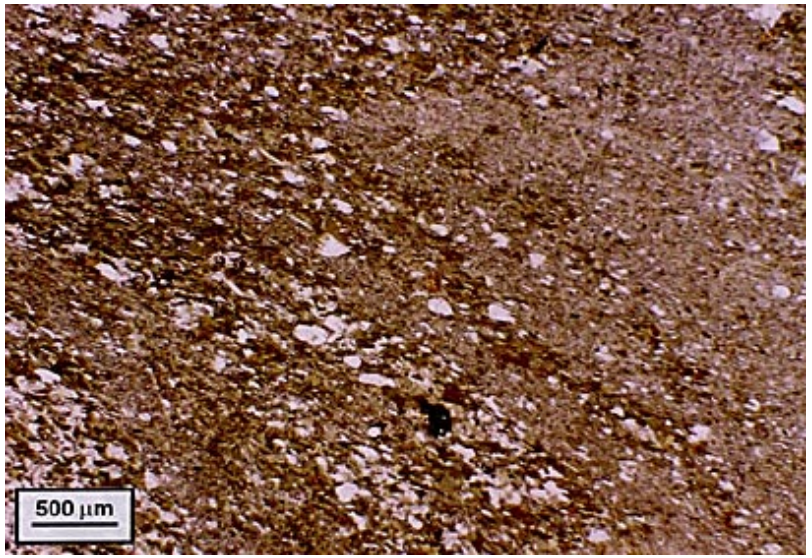

Ore shale


Figure 29

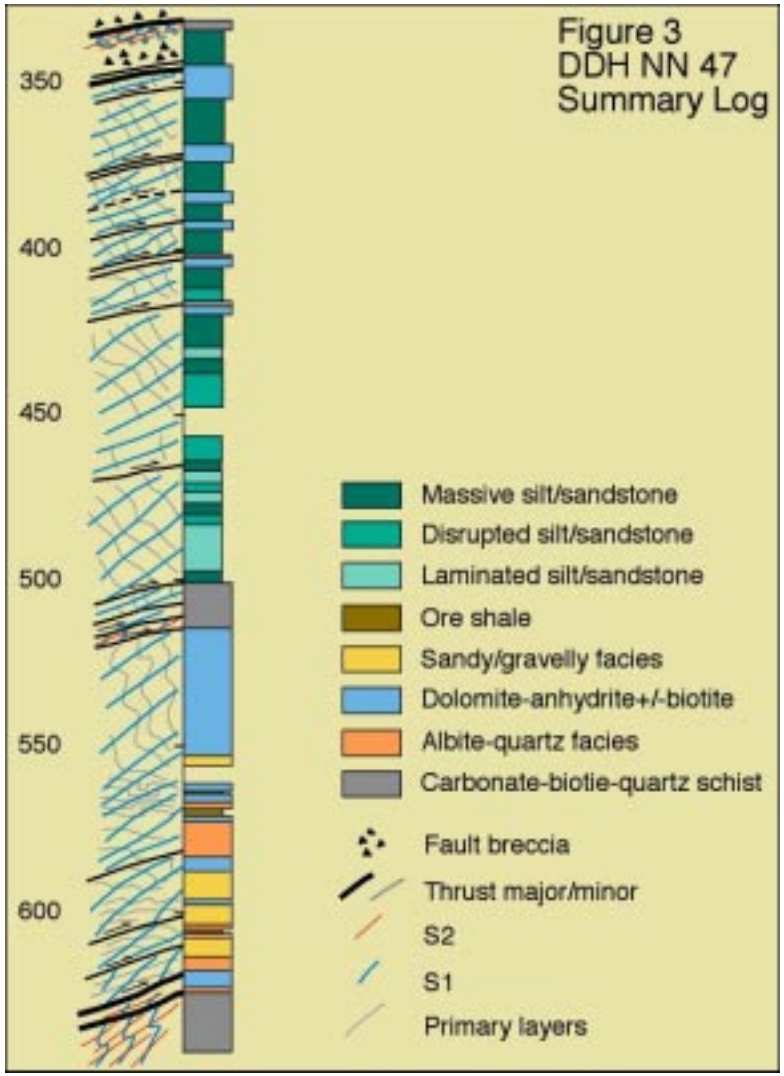
Figure 3
DDH NN 47
Summary Log
350
400
450
500
550
600
Massive silt/sandstone
Disrupted silt/sandstone
Laminated silt/sandstone
Ore shale
Sandy/gravelly facies
Dolomite-anhydrite+/-biotite
Albite-quartz facies
Carbonate-biotie-quartz schist
Fault breccia
Thrust major/minor
S2
S1
Primary layers

Ore shale

Hand specimen description

- Thin lamination defined by (5 - < 1 mm) grey/green vs cream bands

- Numerous deformation features from sheared & folded laminae to quartz augen

Figure 30

Ore shale

Thin section description

Framework;

- Laminae are sheared intervals of mono xi quartz & microcline
- Locally overprinted by poly crystalline quartz blebs

Matrix;

- Fine-grained aggregate of quartz, feldspar & mica locally overprinted by carbonate & anhydrite

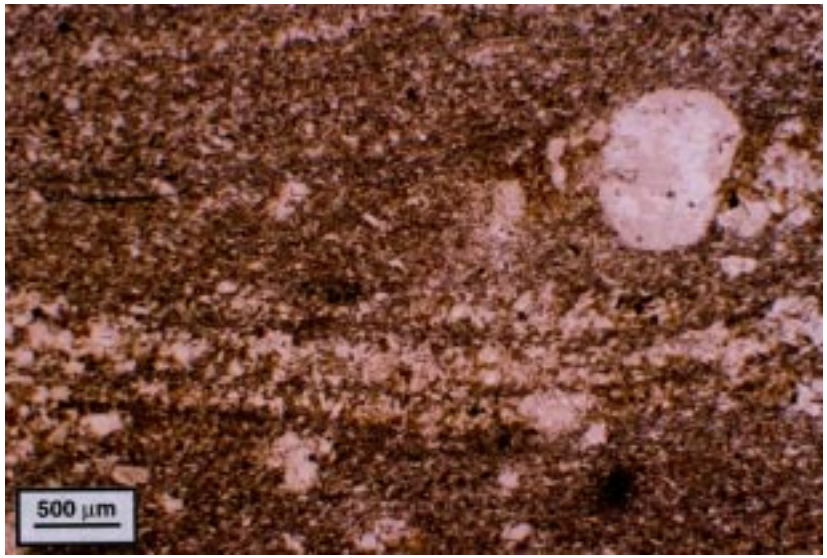

31

32

Ore shale

Original lamination appears to have had a sedimentary origin but has been the focus for poly-crystalline quartz and albite alteration

The Cu is in textural equilibrium with this assemblage in the NN47 sample set

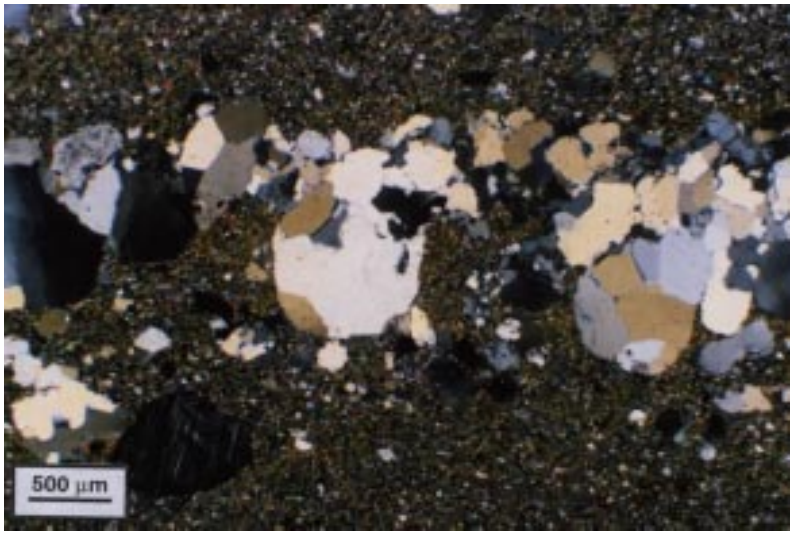

33

34a

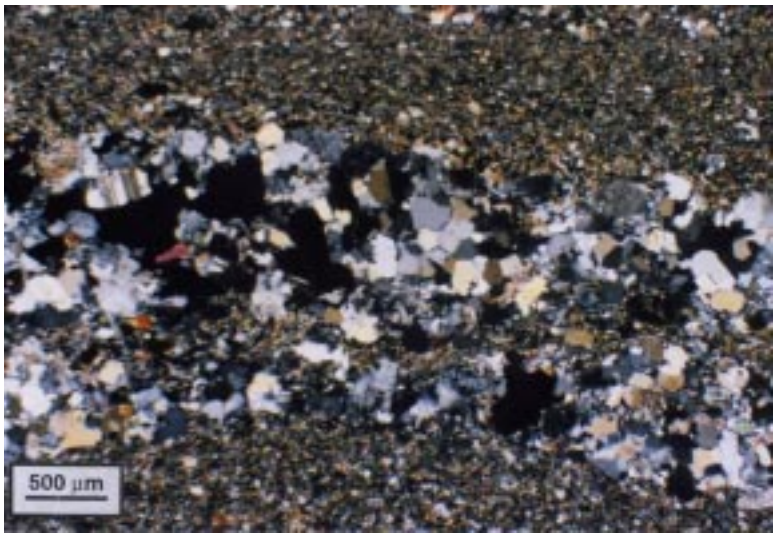

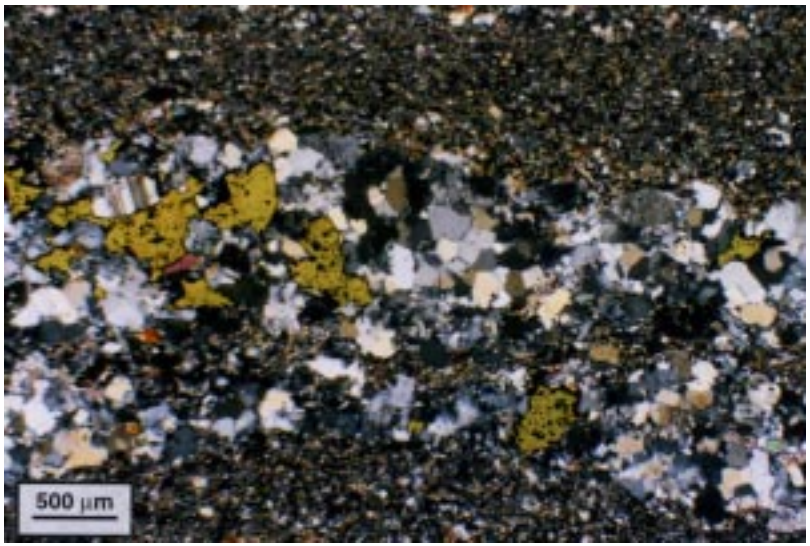

34b

Carbonate-biotite-quartz schist facies

Figure 35

Figure 36

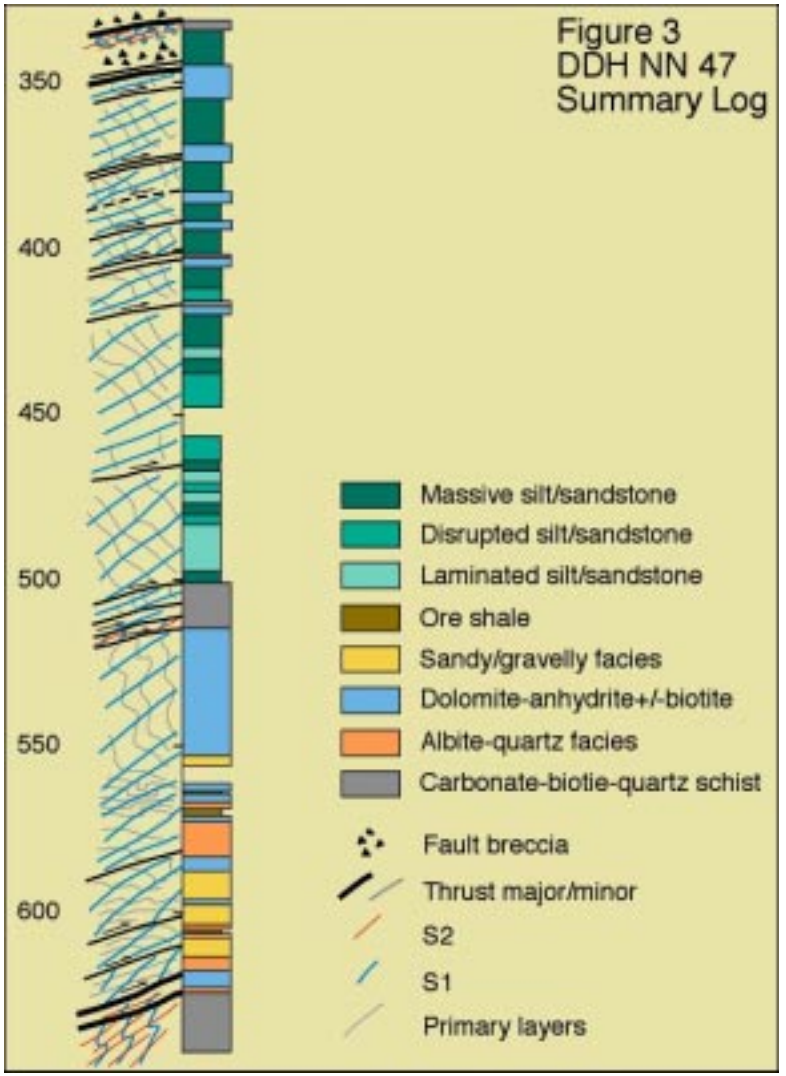

Carbonate-biotite-quartz schist facies

Lufubu Schist

Hand specimen; dark green/grey/black biotite calcite schist

Thin section; felted mass of biotite & chlorite with patches/stringers of carbonate & quartz

Clusters of small epidote crystals with associated brown biotite may represent remnants of an Fe-rich phase

37

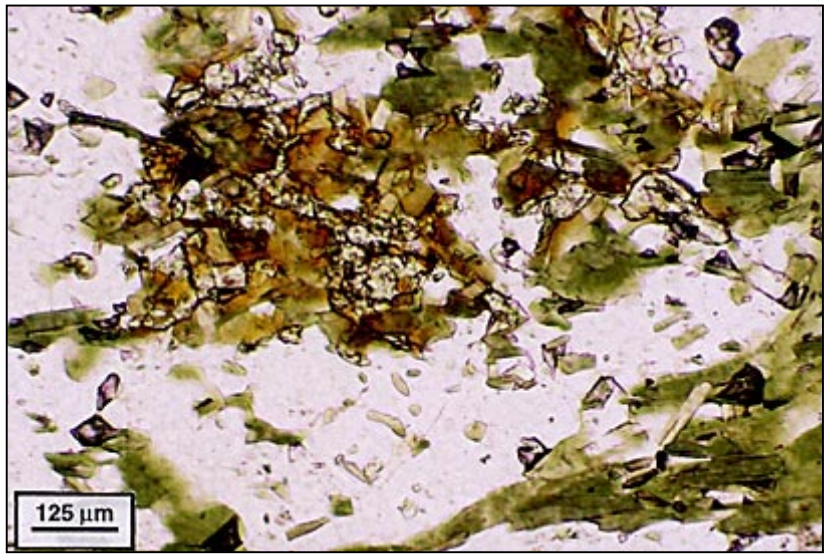

38

Carbonate-biotite-quartz schist facies

Upper Schists

Hand specimen; salt & pepper textured biotite calcite schist

Thin section; equant framework of carbonate & biotite with patches/stringers of quartz & anhydrite

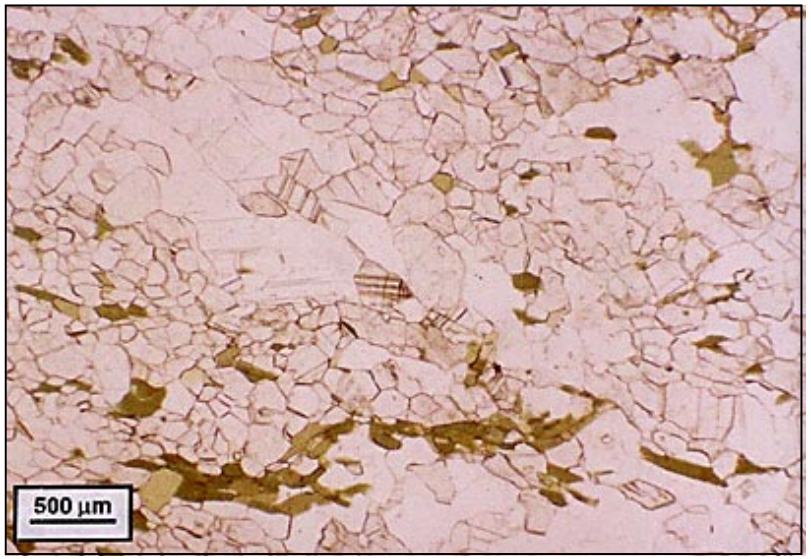

39a

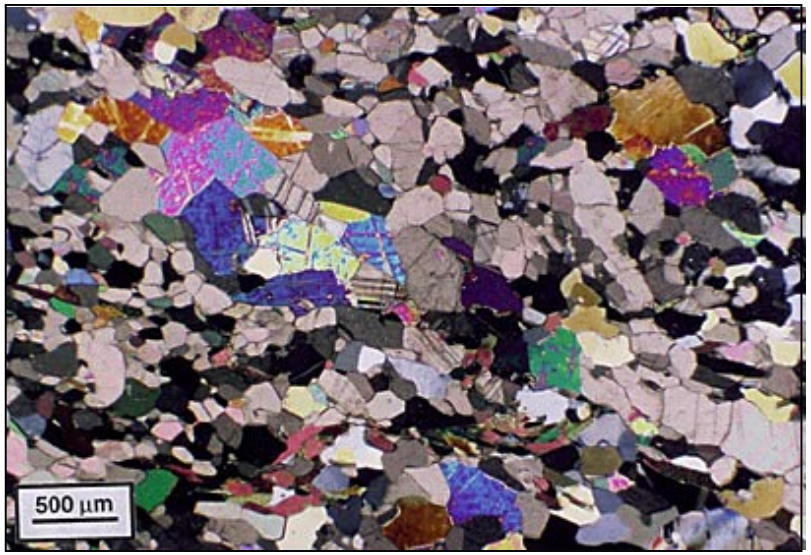

39b

Implications for metamorphism

Biotite is stable throughout the hole =
Lufubu Schist not basement in a metamorphic sense

Several factors suggest the lower end of the 300°–500°C range for biotite stability including;

- ▲ High flourine values in biotite
- ▲ Absence of +400° metamorphic phases (eg. garnet or cordierite/andalusite)
- ▲ Absence of contact skarn assembalges (tremolite-talc etc) at carbonate - siliceous boundaries
- ▲ Often patchy/zoned nature of biotite (Fig. 39c) suggesting low T &/or rapid cooling

39c

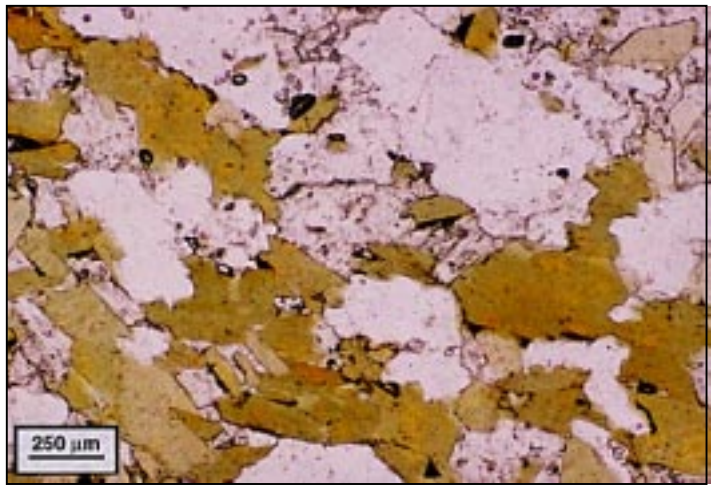

Carbonate-biotite-quartz schist facies

Figure 40

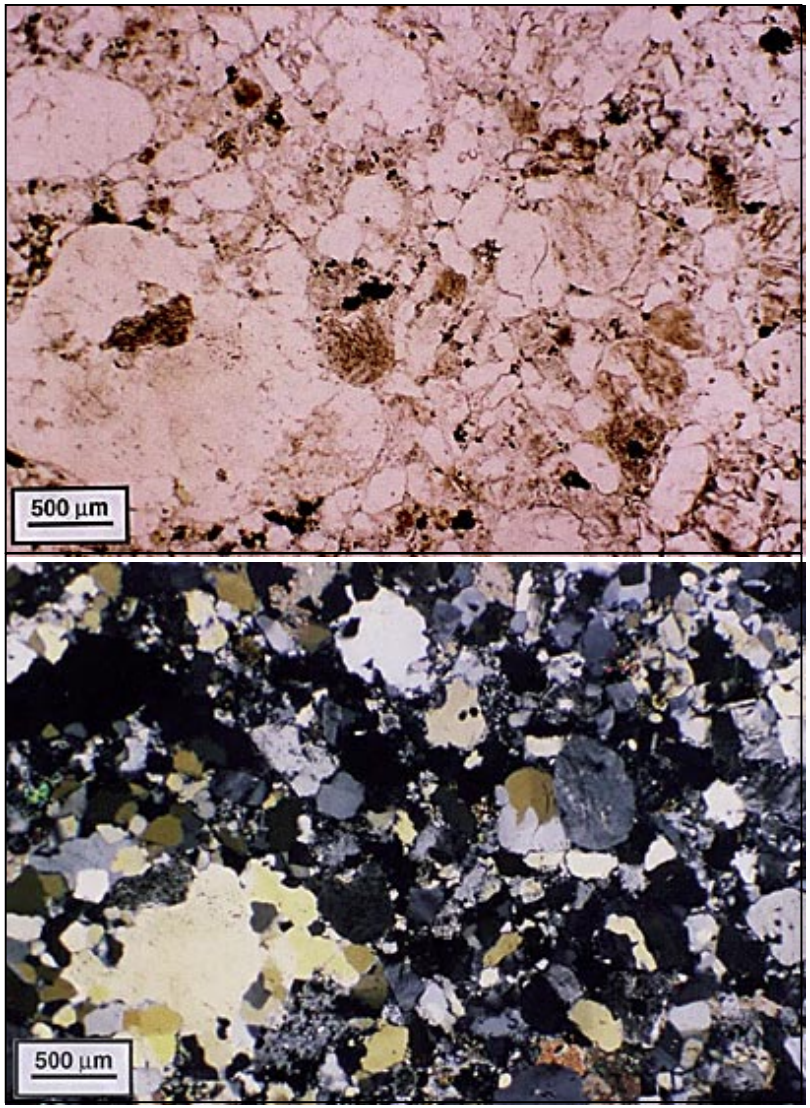

41a

41b

Carbonate-biotite-quartz schist facies

42a

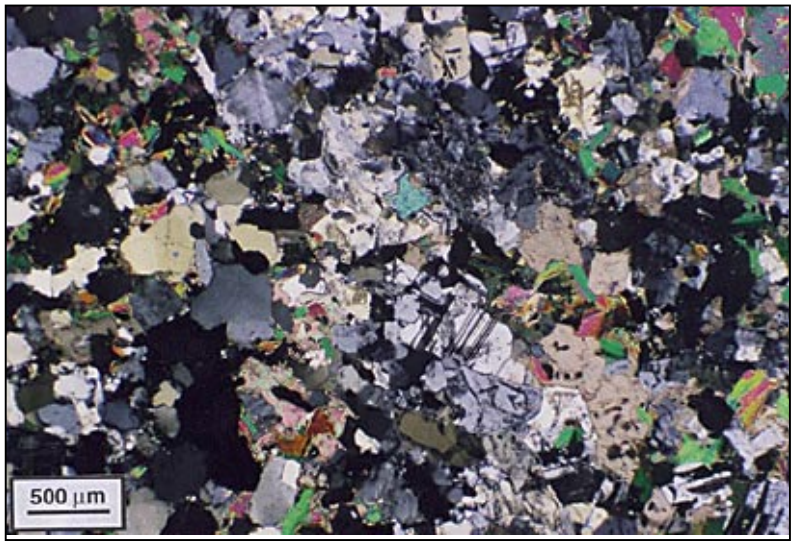

42b

Carbonate-biotite-quartz schist facies

Figure 40

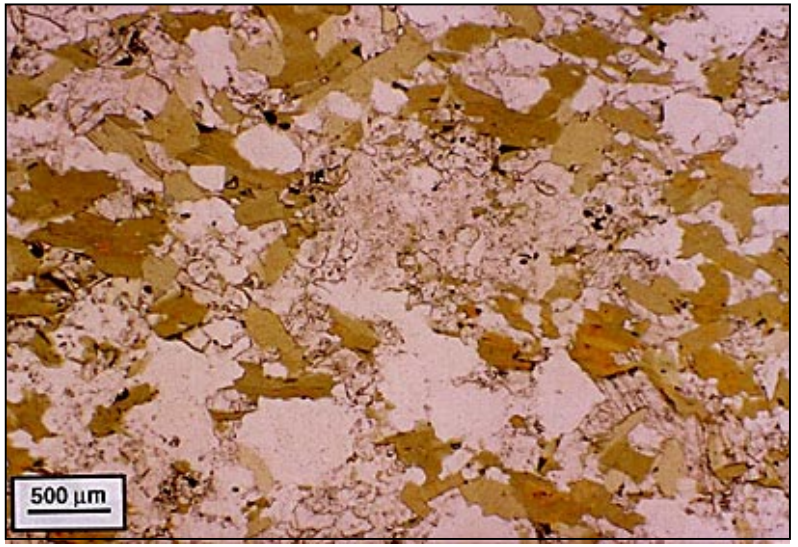

43a

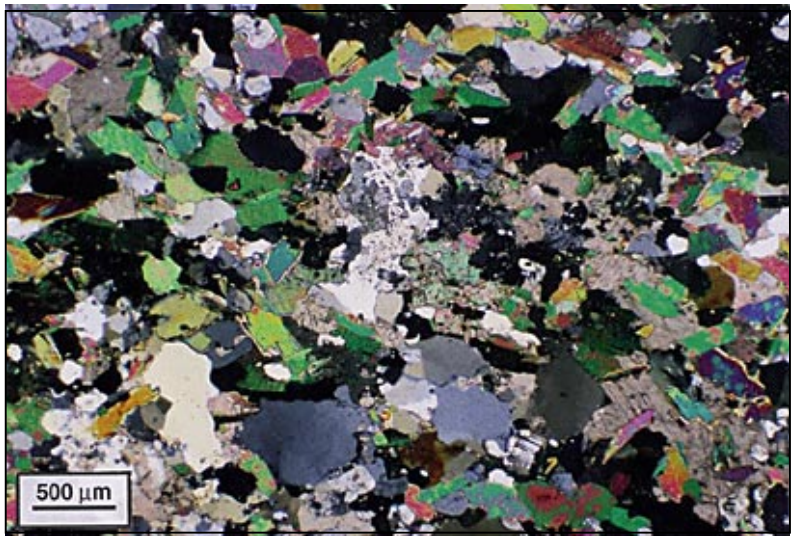

43b

Carbonate-anhydrite±biotite facies

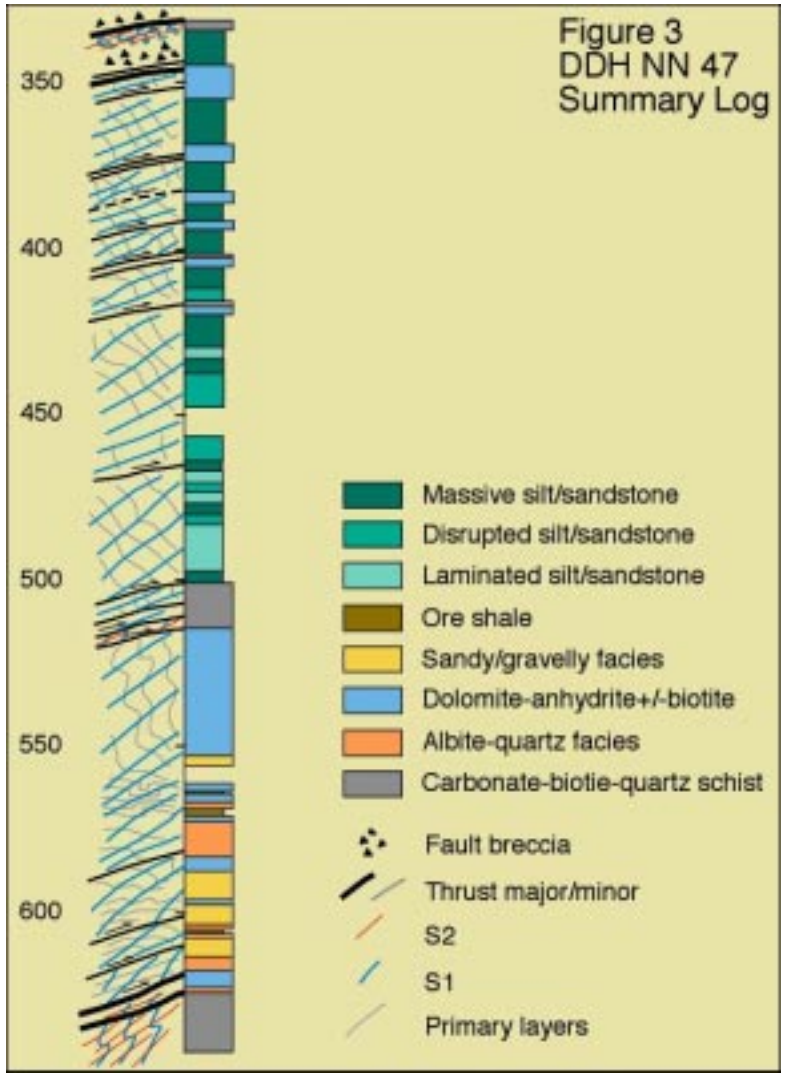

Carbonate-anhydrite±biotite facies

Thin section description

Coarse-grained aggregate of carbonate & anhydrite

May have patches of poly crystalline quartz &/or scattered biotite

May be metamorphically recrystallised carbonate sediments (lack of zircons) or wholesale alteration/metasomatism of clastic protolith

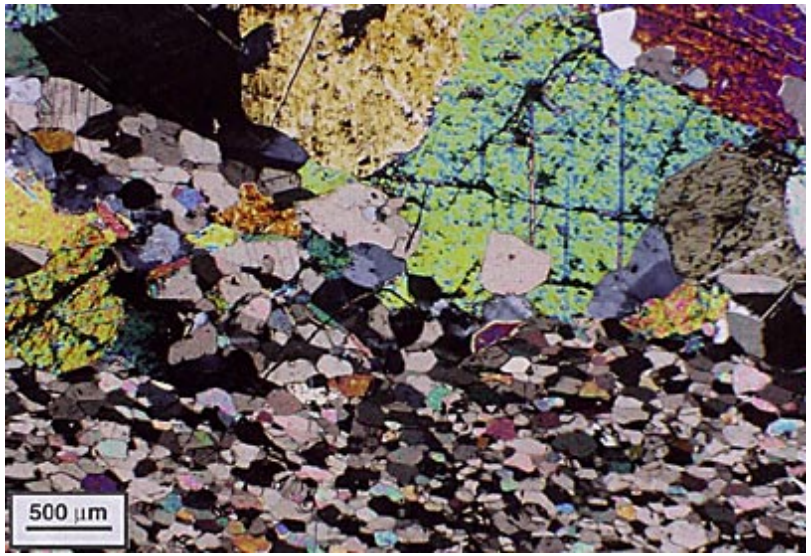

45

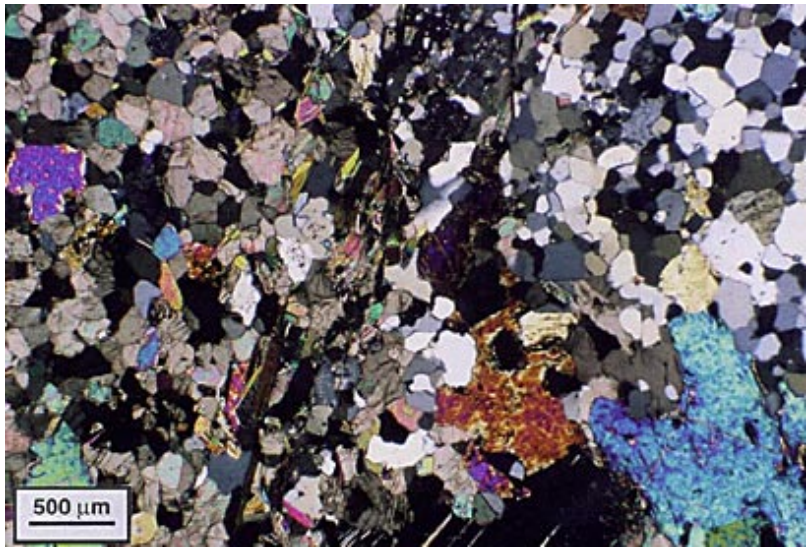

46

Summary

Basal Lufubu Schist is not basement in a metamorphic (or structural) sense

Lower Roan is dominated by a coarse-grained arkosic protolith

Upper Roan is dominated by a finer-grained protolith of similar provenance

Both are partly to completely metamorphically recrystallised &/or altered/metasomatised to assemblages of poly-crystalline quartz, anhydrite, plagioclase (albite?), and mica (sericite/muscovite/chlorite/biotite)

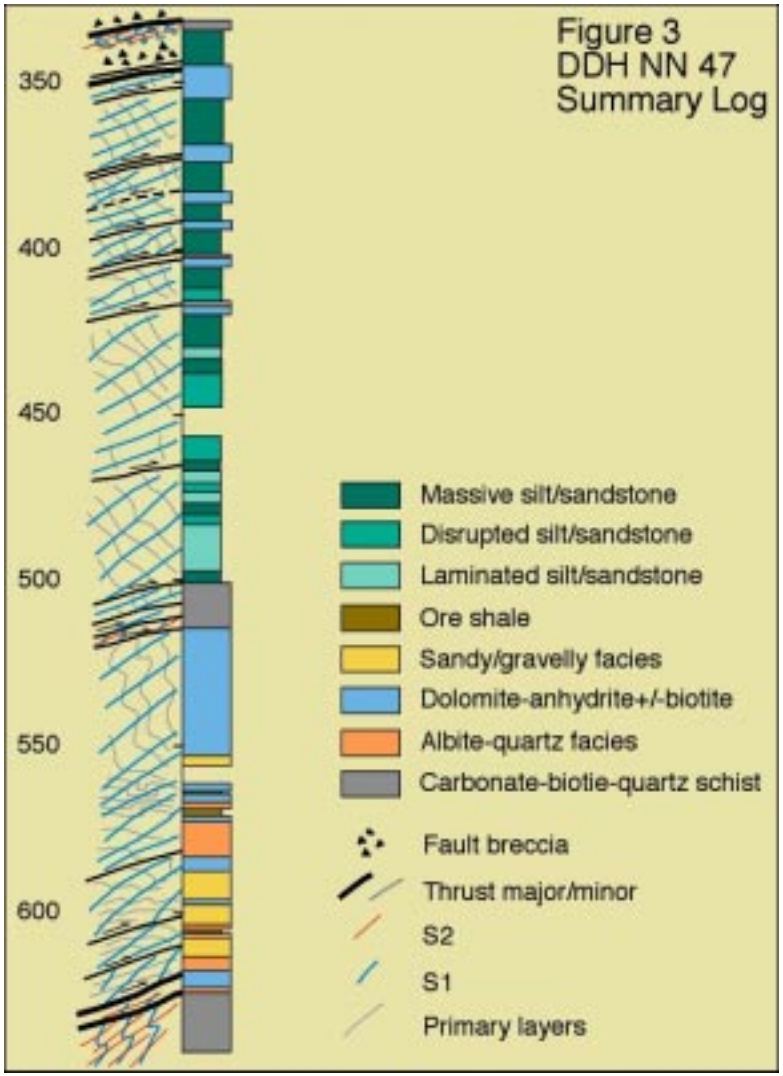

Structural Geometry

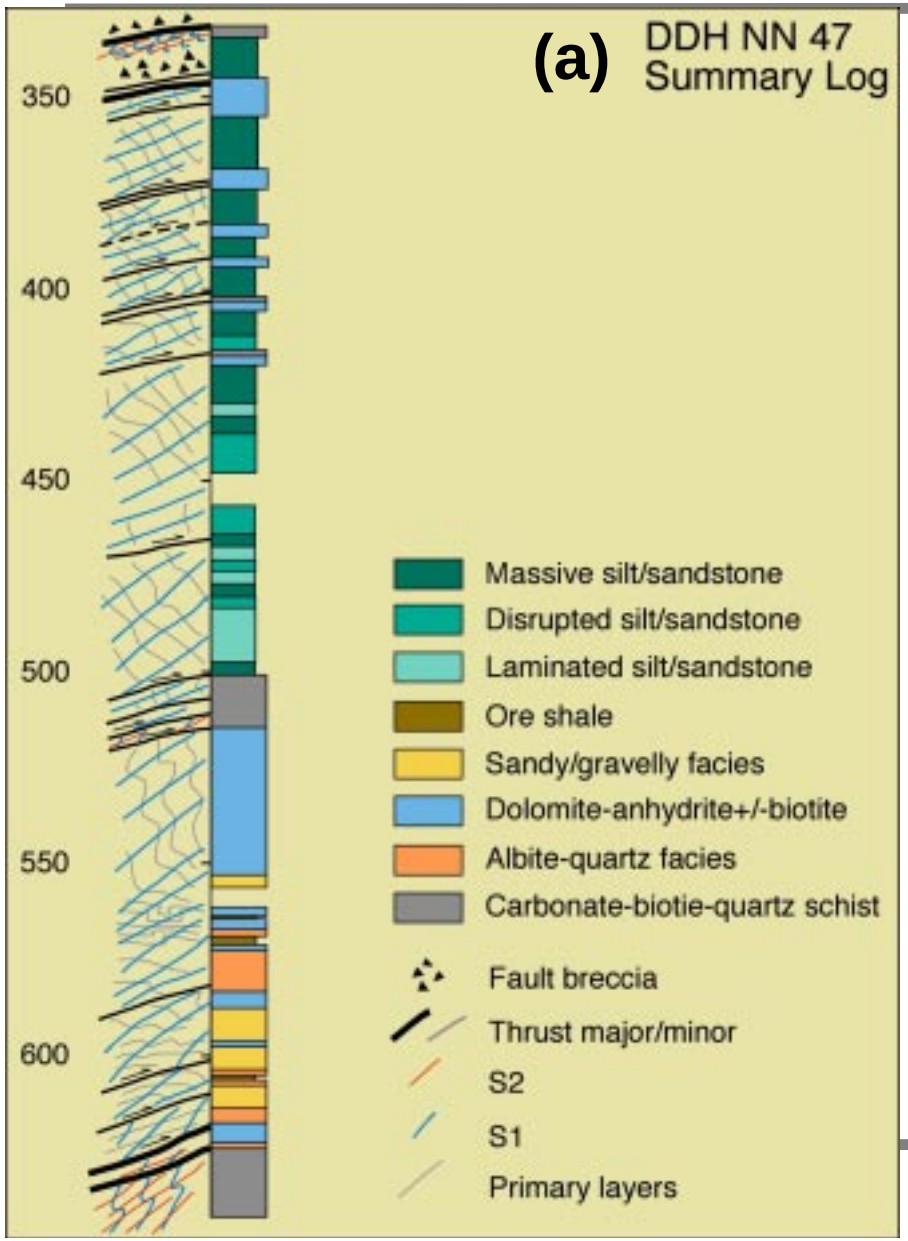

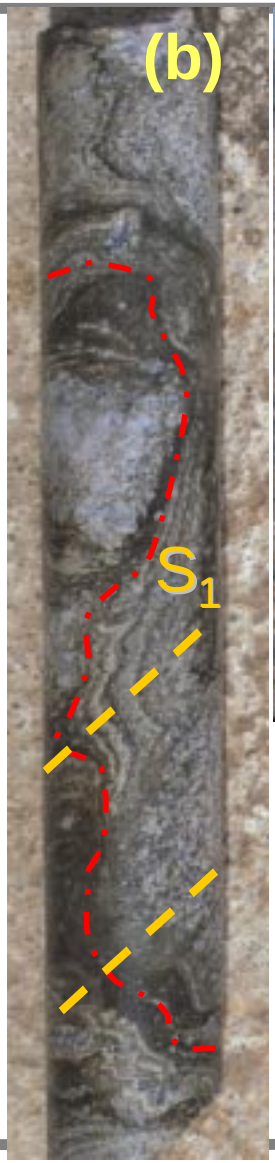

- thrust-bounded Roan
- asymmetric fold geometry
- progressive N-directed fold and thrust event

Fig. 47

Pre-Cleavage Deformation

Fluidization

- clastic dykes
- occupy fold hinges
- oriented within S1

Origins

1) pre-lithification features, deformed by subsequent shortening

2) syn-metamorphic fluidization

Transected Folds

- pre-cleavage fold generation(s)
- opposing vergence to main folding event

Fig. 48

Assemblage 1

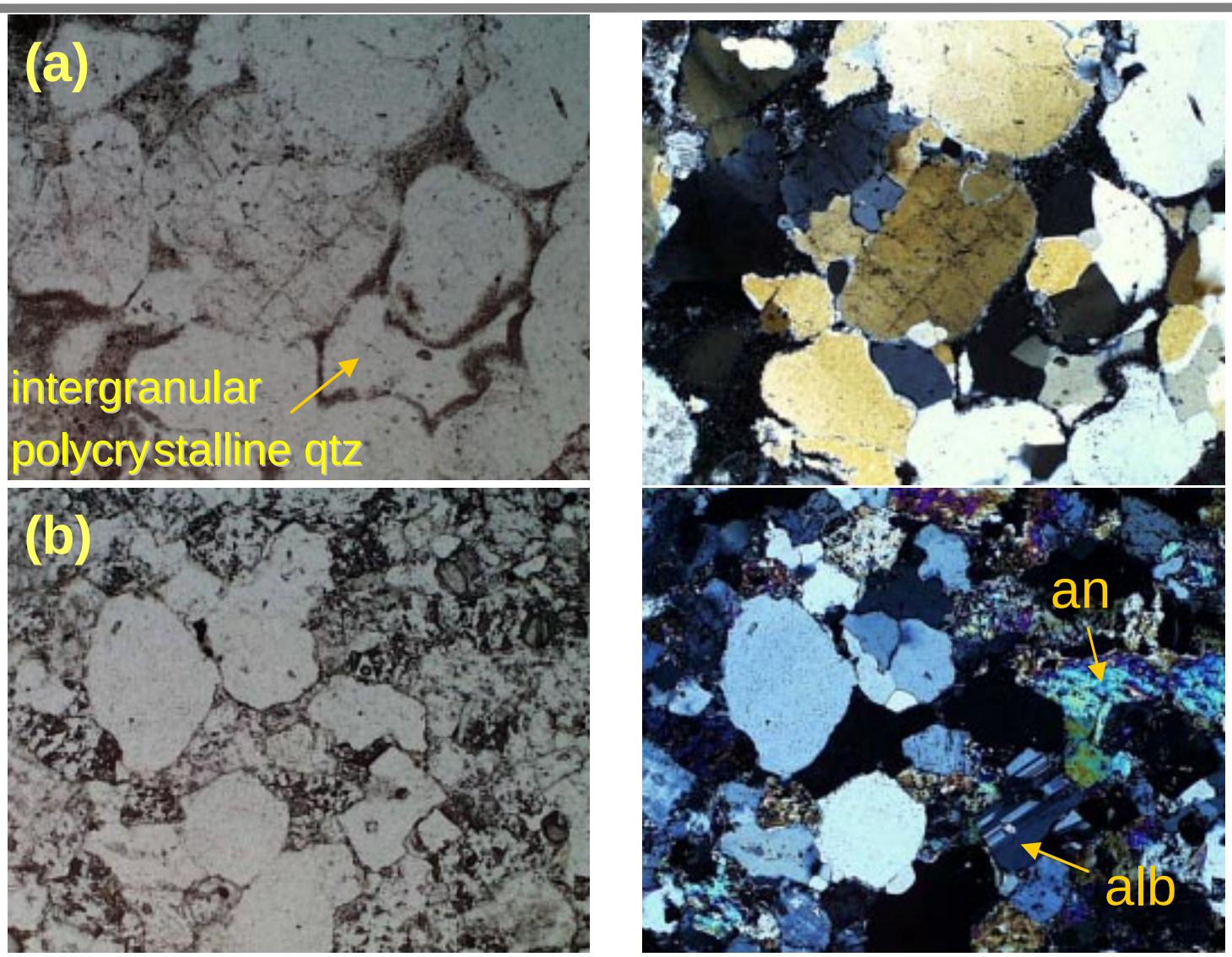

Fig. 49

Assemblage 1

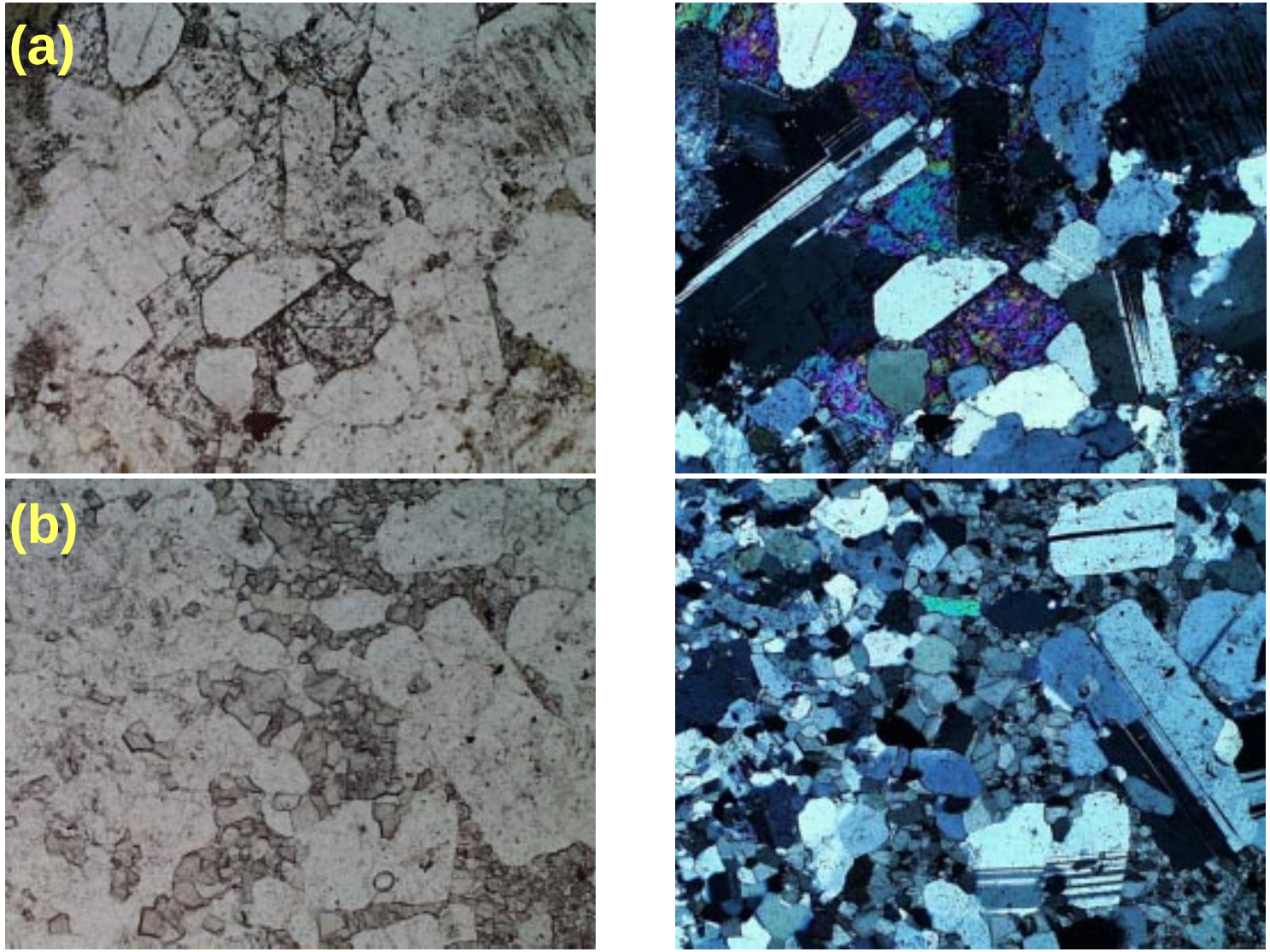

Fig. 50

Layer-parallel shear → *Cataclasis*

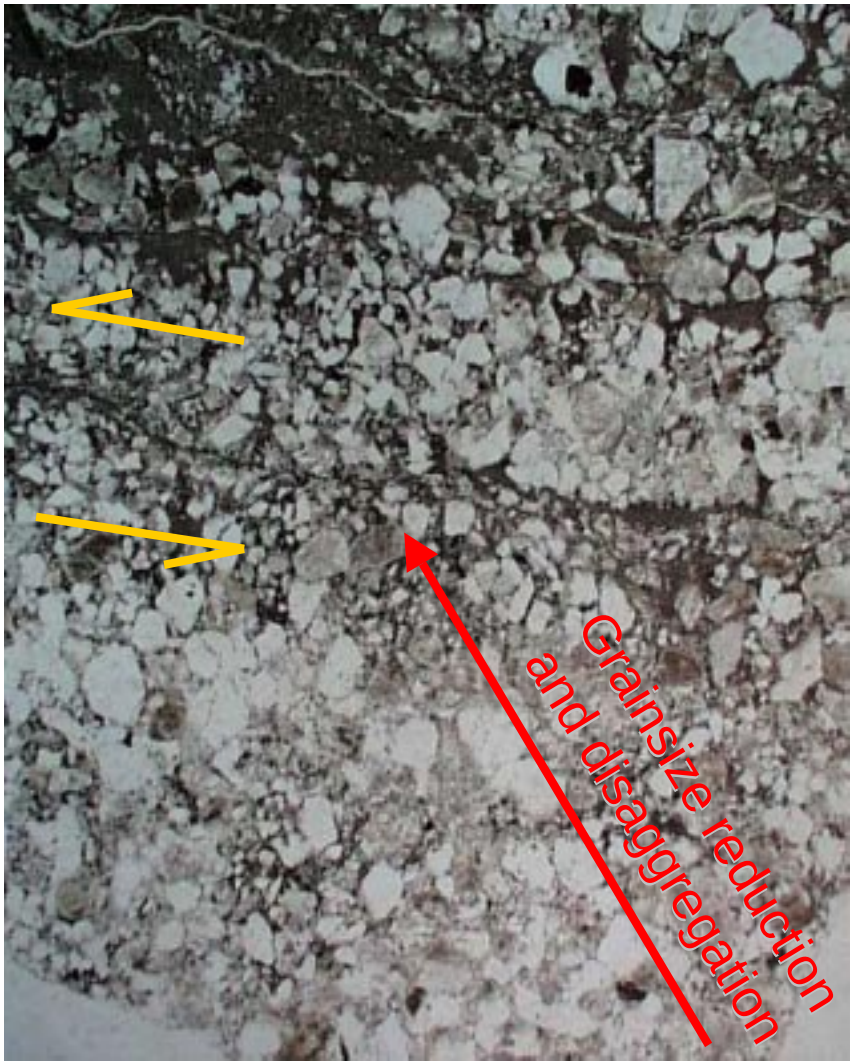

Assemblage 1: Grain-scale textures

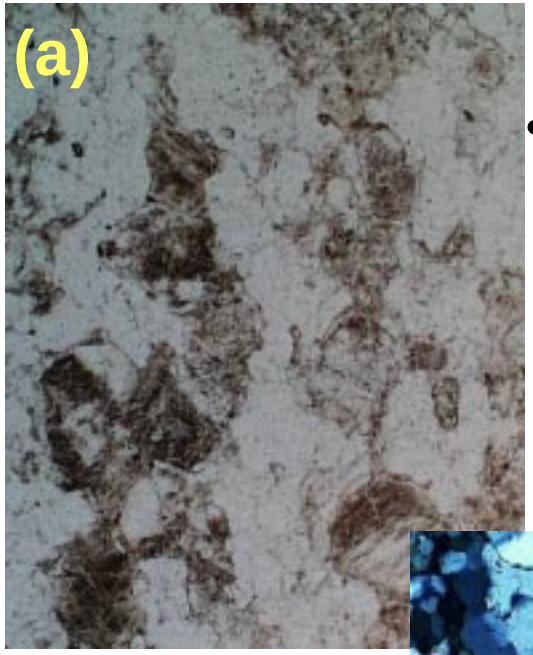

Low Strain

- detrital textures preserved

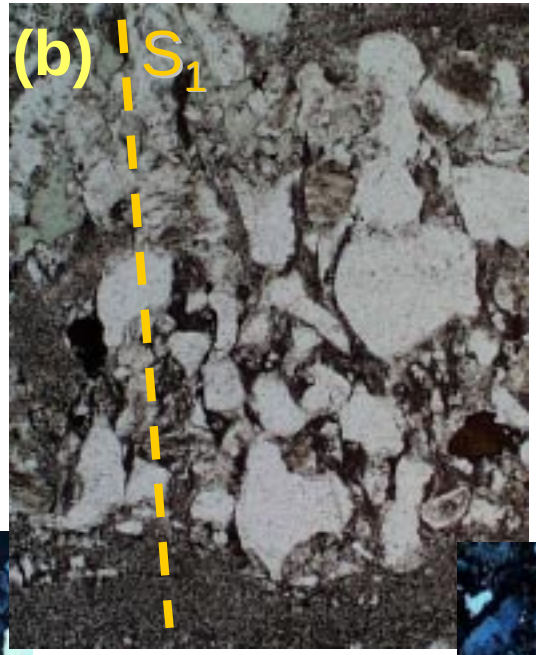

High Strain

- disaggregation
- angular, “shard”-like grains
- cryptocrystalline *assemblage 1* groundmass

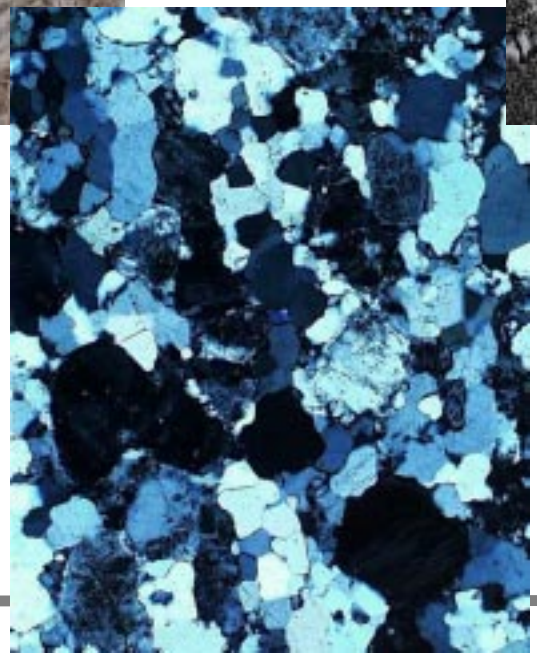

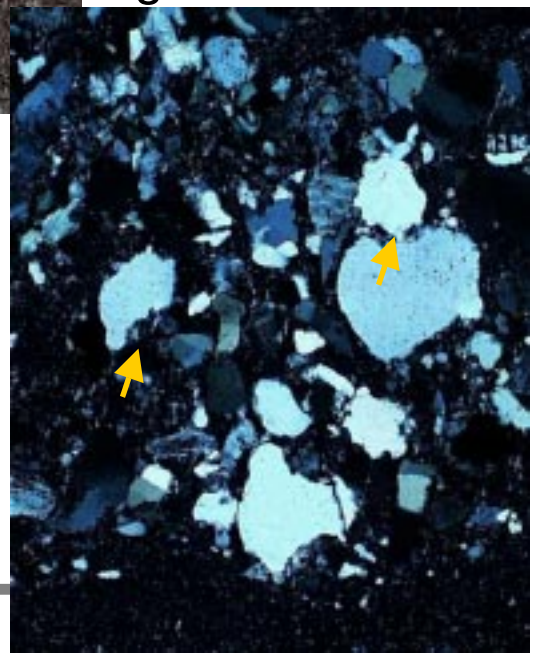

Fig. 52

Assemblage 1: Grain-scale textures

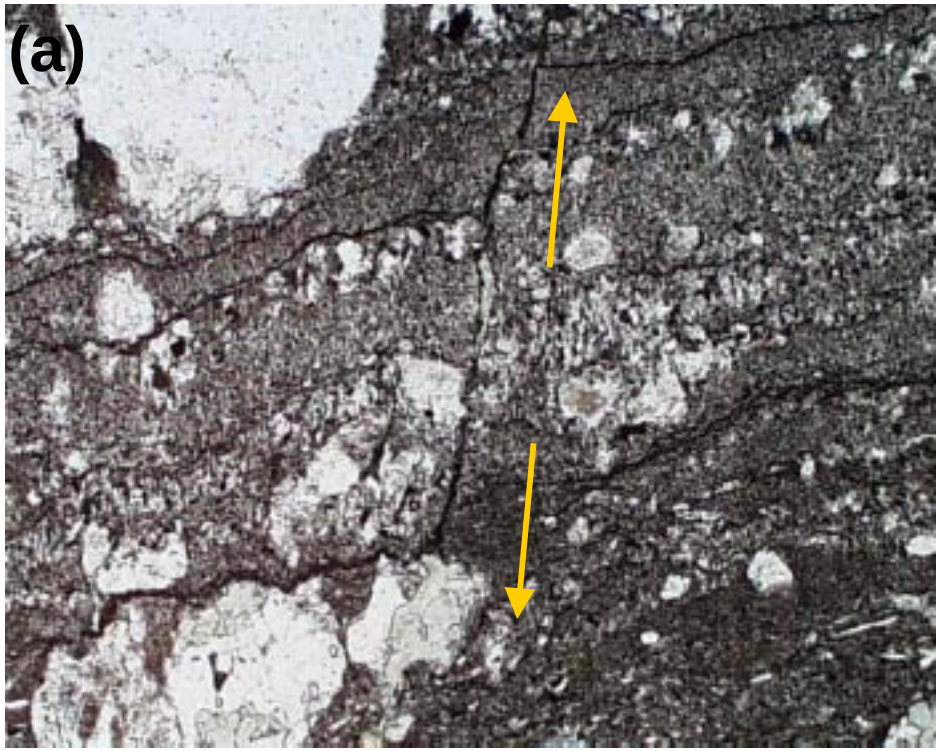

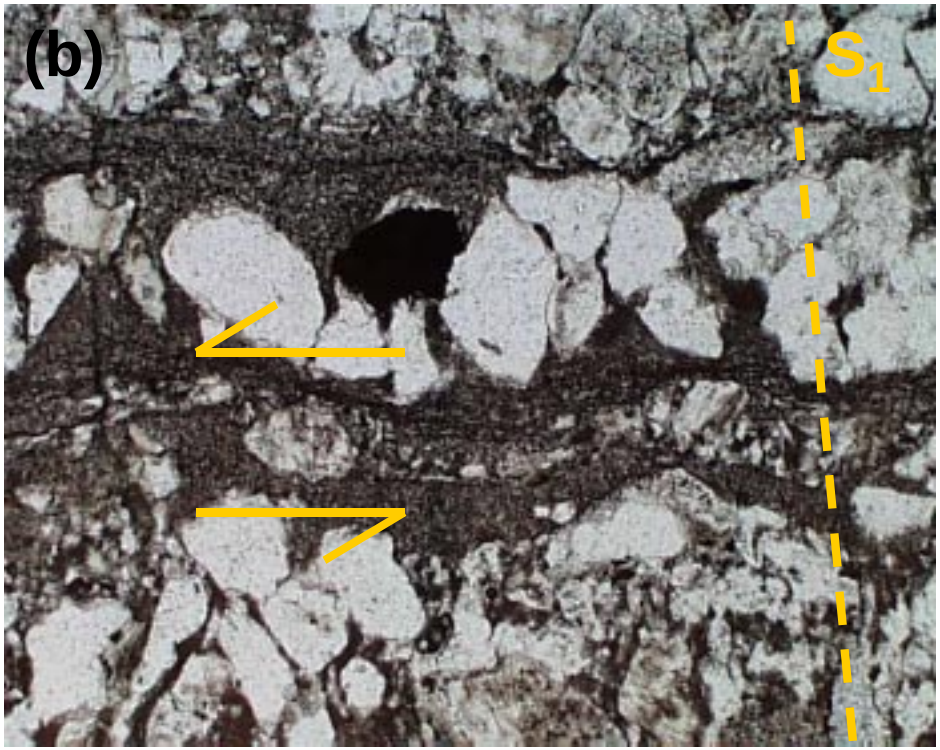

- layer-parallel fibre veins
- fibres track S1

- layer-parallel shear
- granulated or recrystallized tails at grain margins

Assemblage 2: sericite “flooding”

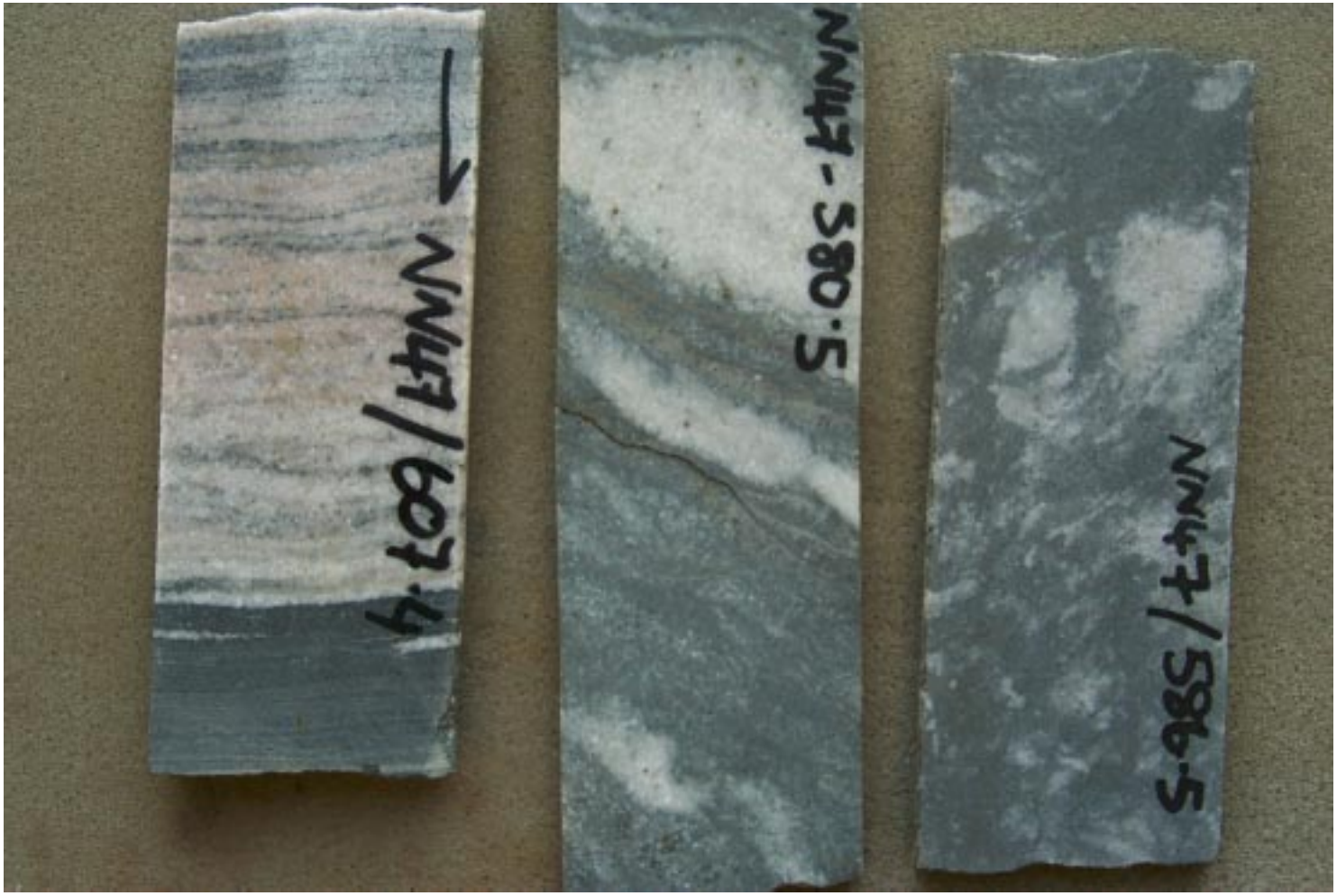

sericite content increasing with disruption

Assemblage 2: overgrowth textures

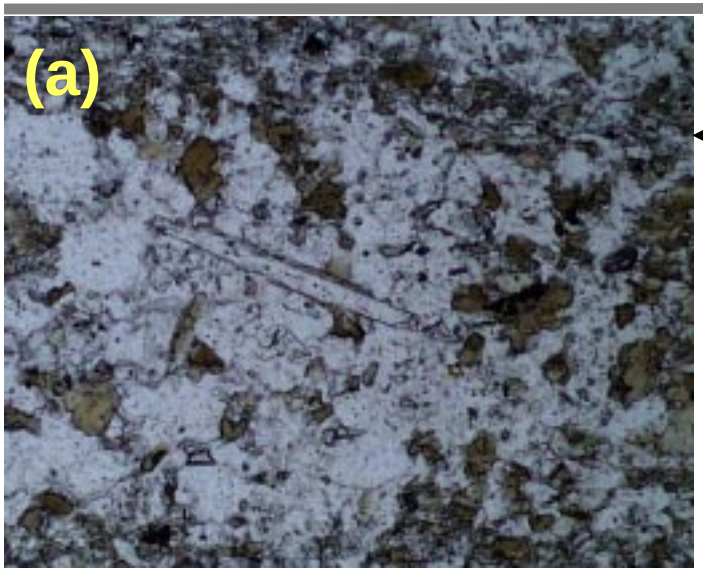

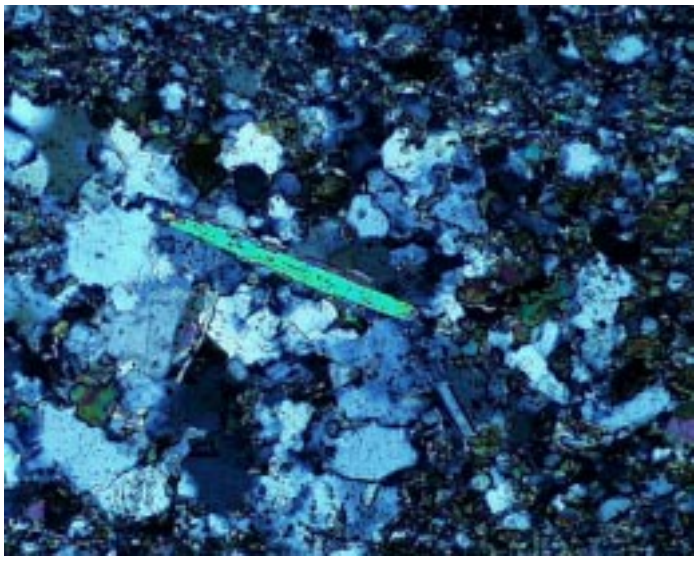

muscovite overprinting *assemblage 1* polycrystalline quartz and albite

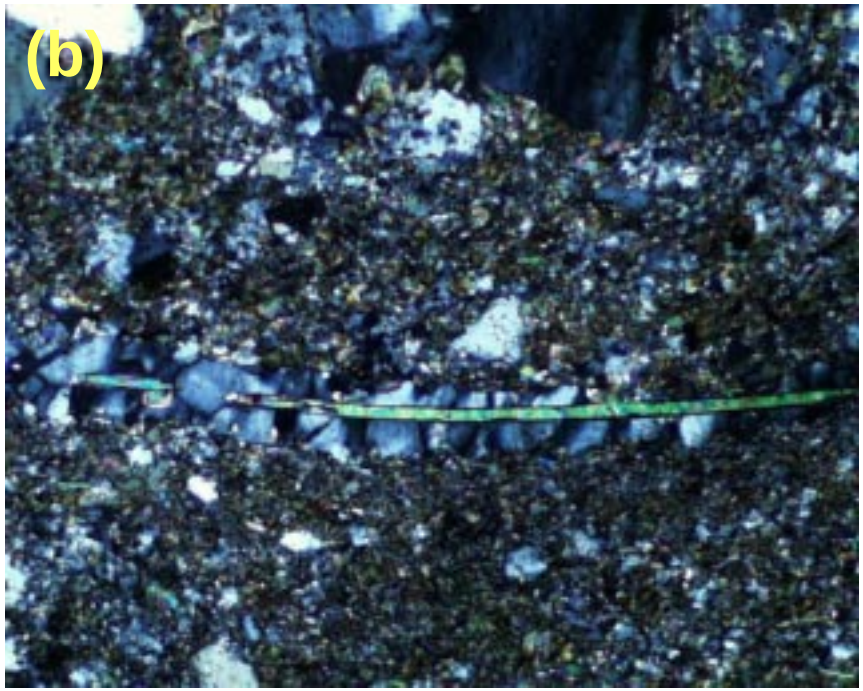

fibrous “beards” on elongate muscovite

Assemblage 2: domains of grain-scale disaggregation

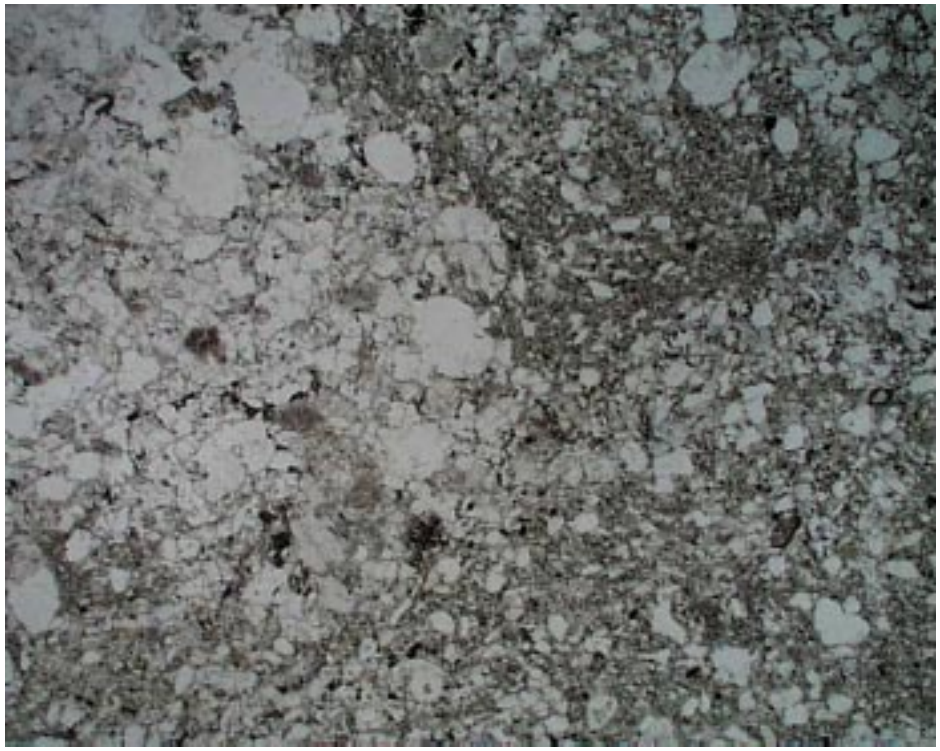

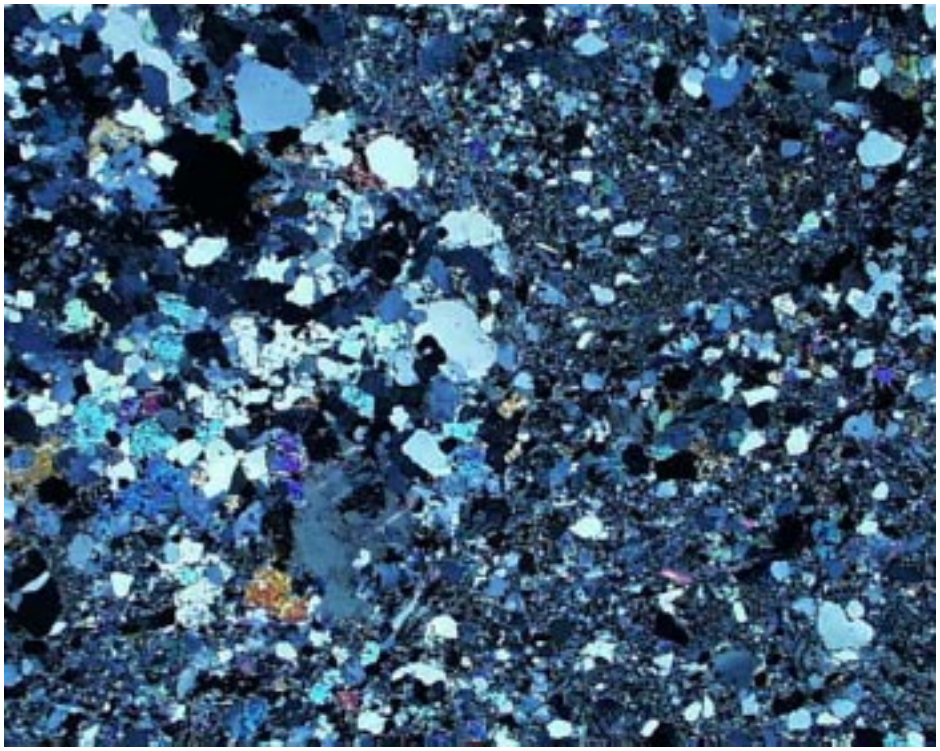

- relict pod of *assemblage 1* alteration enclosed by finer-grained, sericitic sandstone

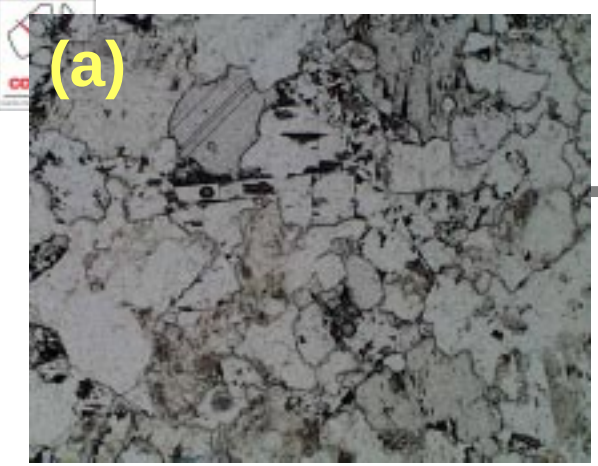

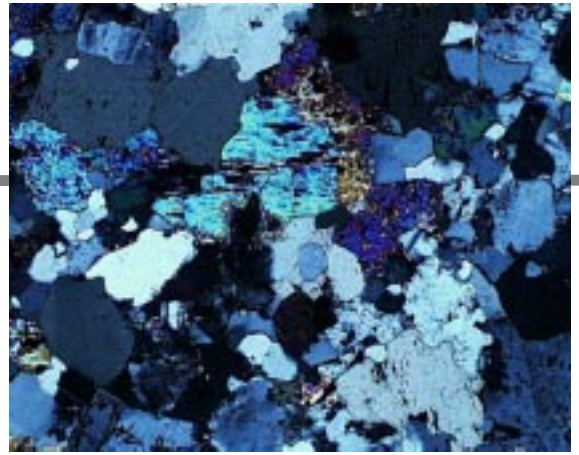

Assemblage 2: white mica content increases with disaggregation

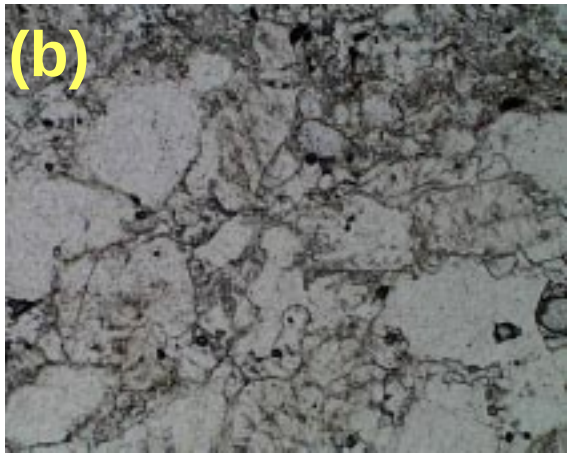

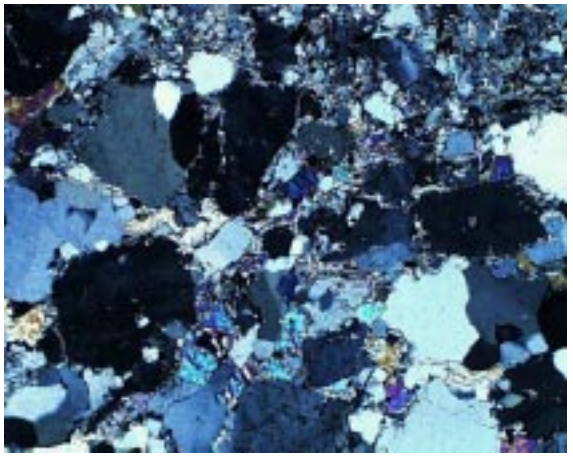

increasing disaggregation

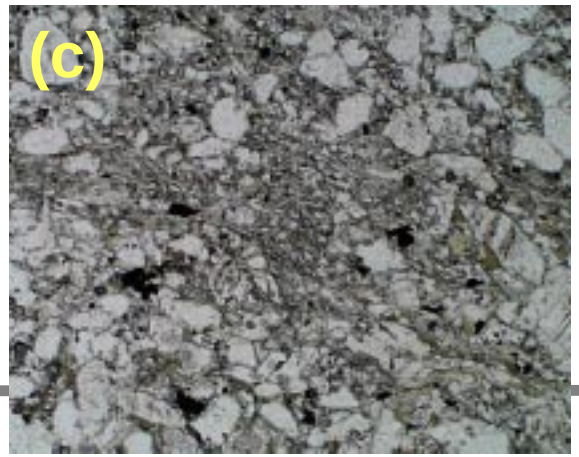

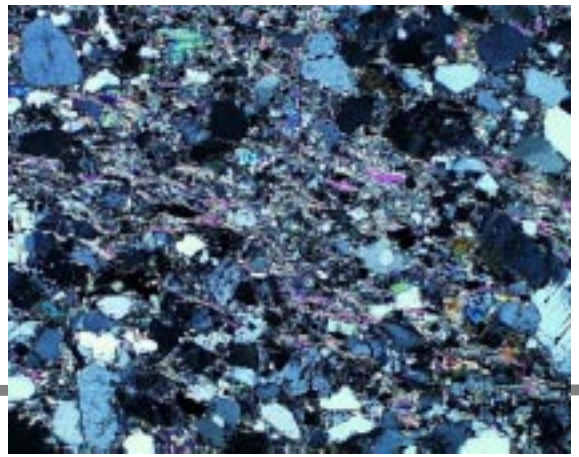

Fig. 57

Assemblage 2: overgrowth textures

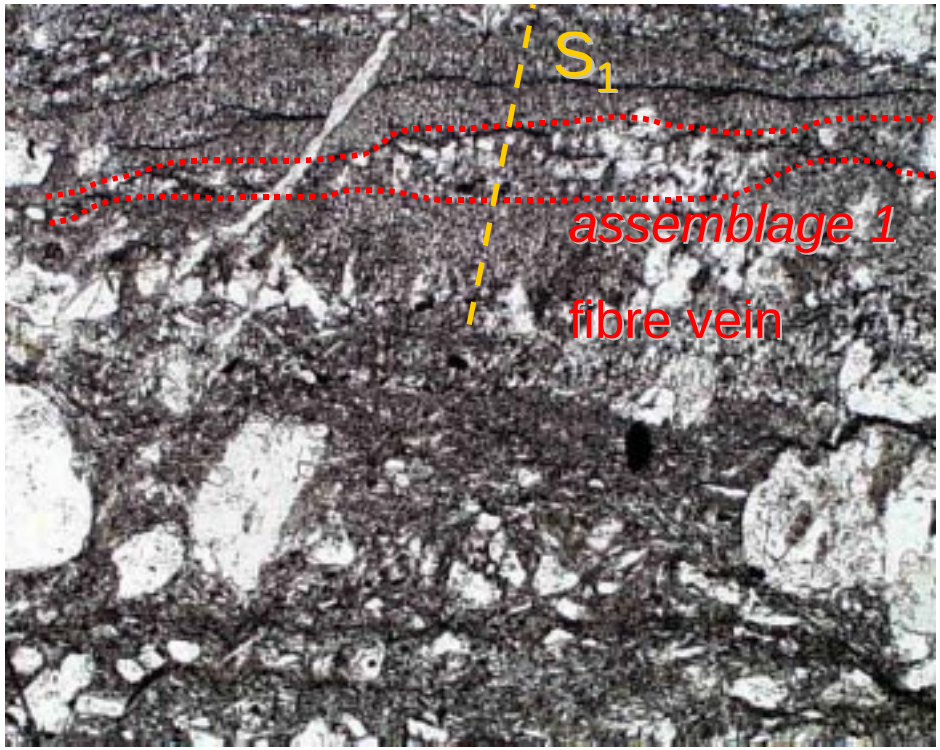

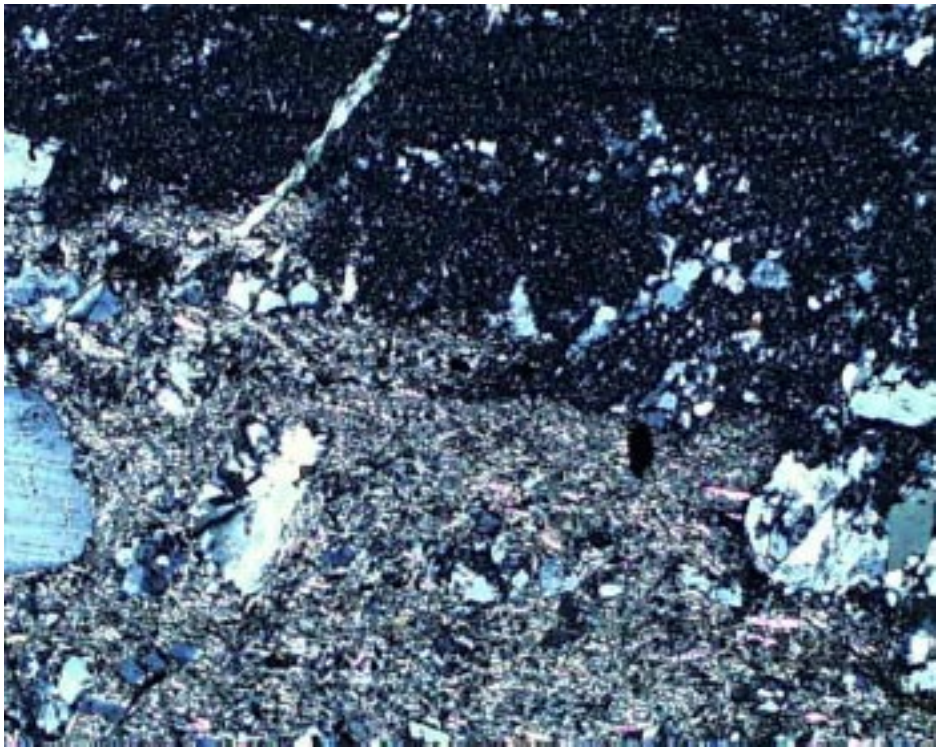

- white mica overprinting *assemblage 1* groundmass and fibre veins with layer-parallel micro-shear

Assemblage 2: Layer-parallel micro-shears

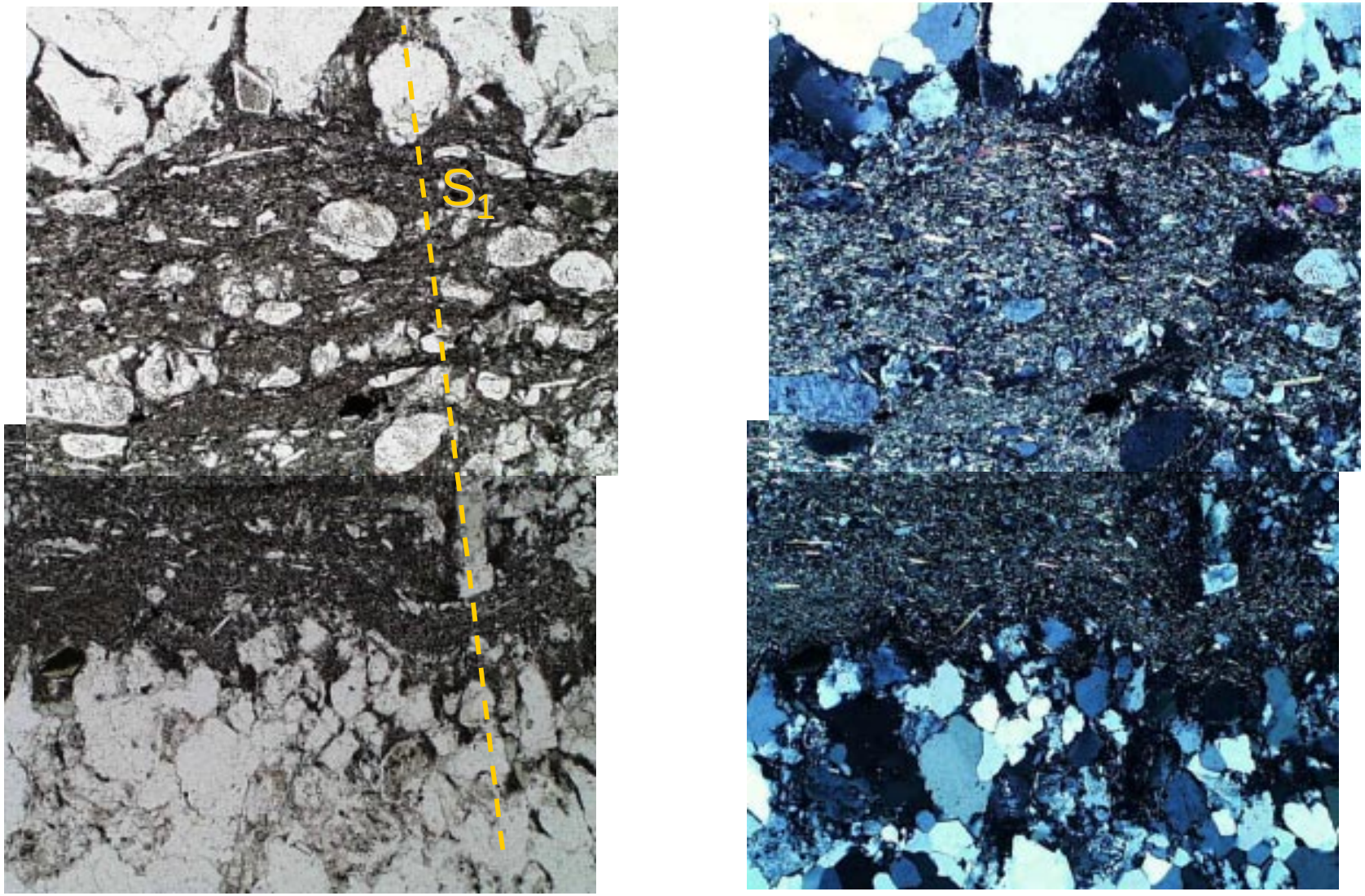

Assemblage 2: Layer-parallel micro-shears

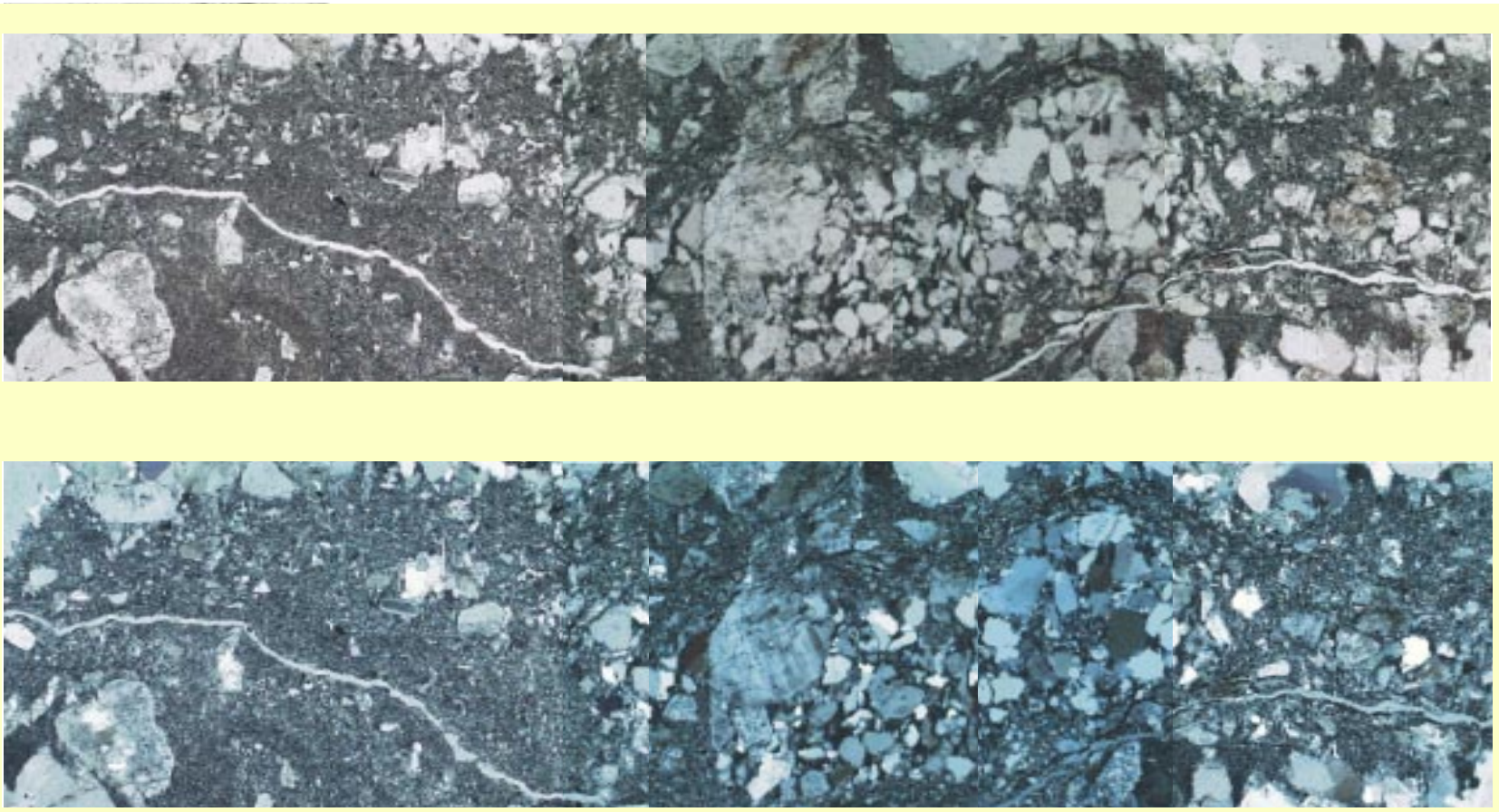

Assemblage 2: orientation of white mica

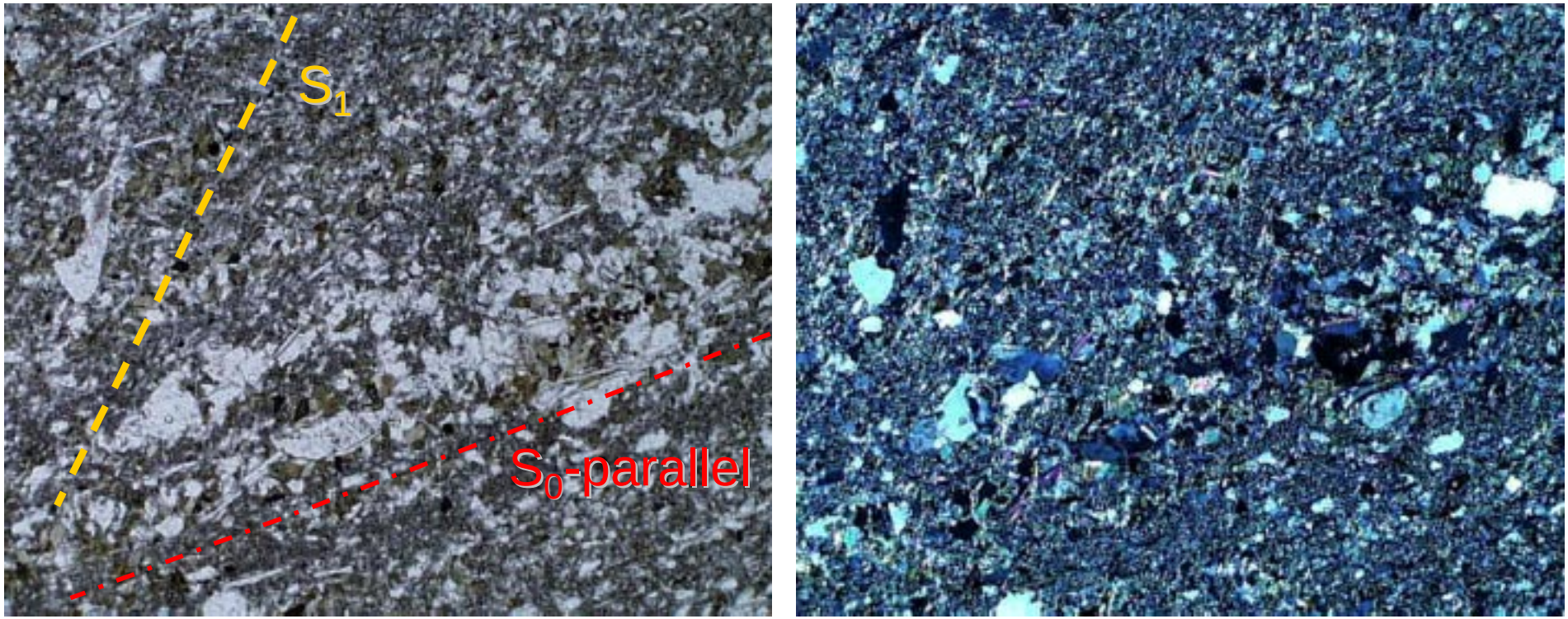

- growth of texturally similar muscovite parallel to both S0 and S1

Assemblage 2: concentration in clastic dykes

semi-coherent layering

clastic dyke

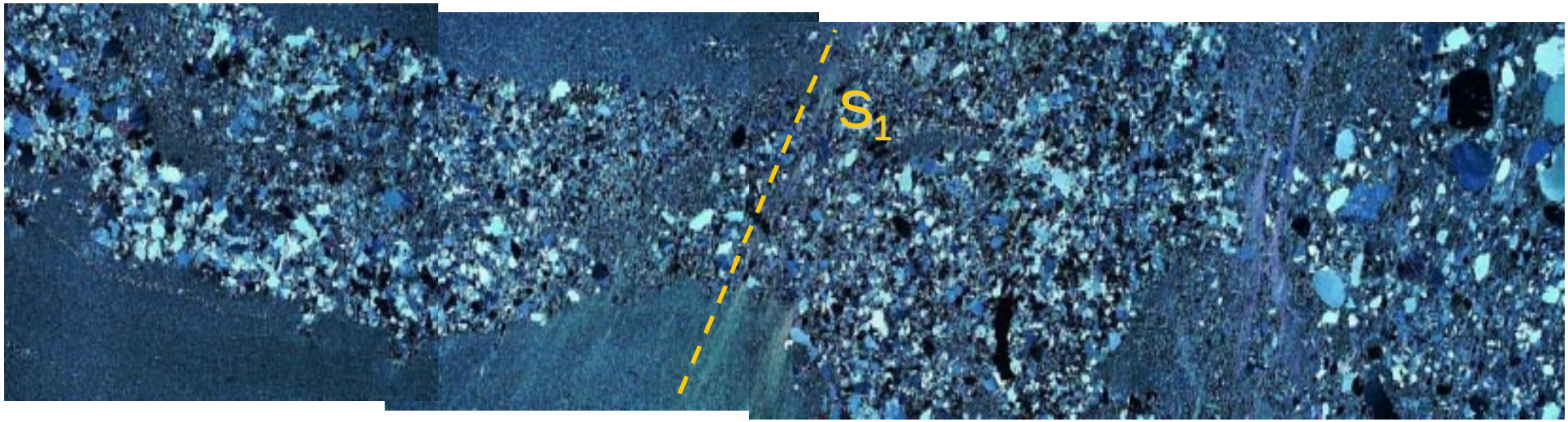

increasing sericite

Assemblage 3: grain-scale textures

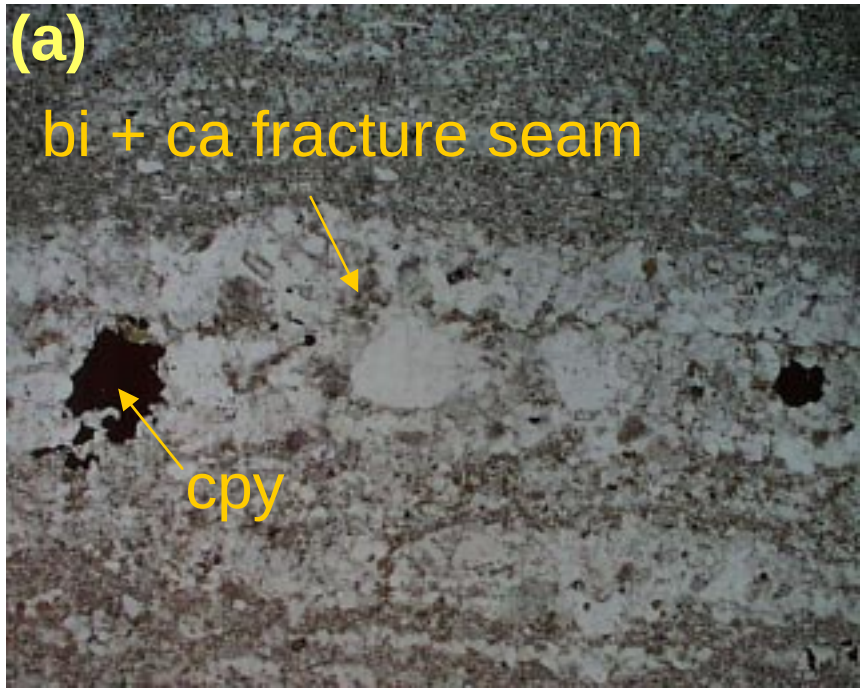

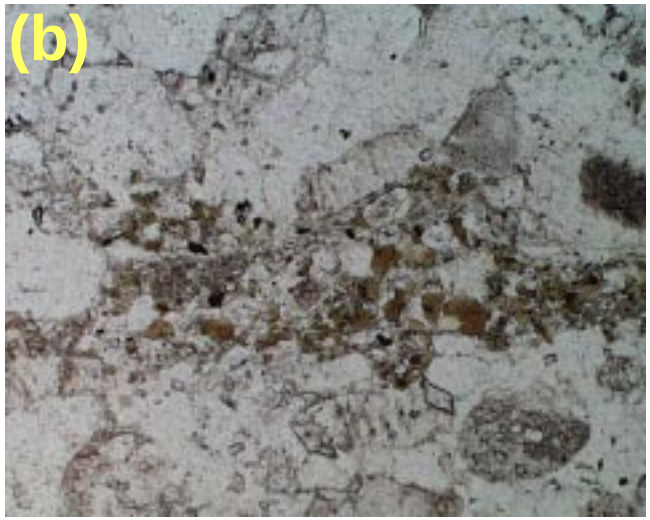

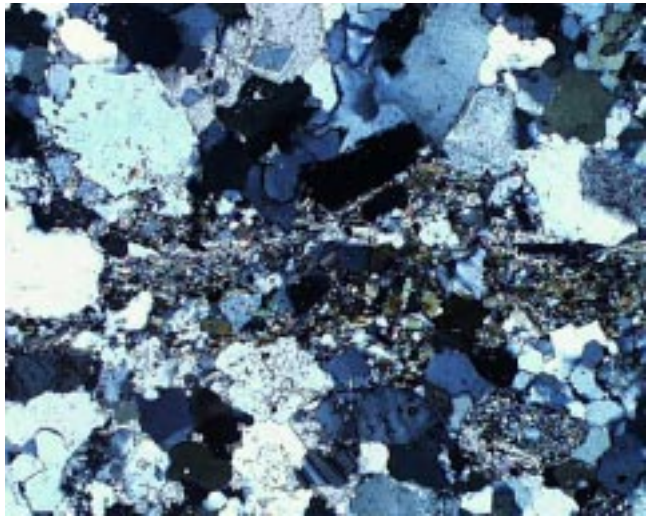

- biotite and carbonate occurs disseminated throughout silty facies and along layer-parallel fracture seams in polycrystalline qtz-albite domains

Assemblage 3: vein morphology

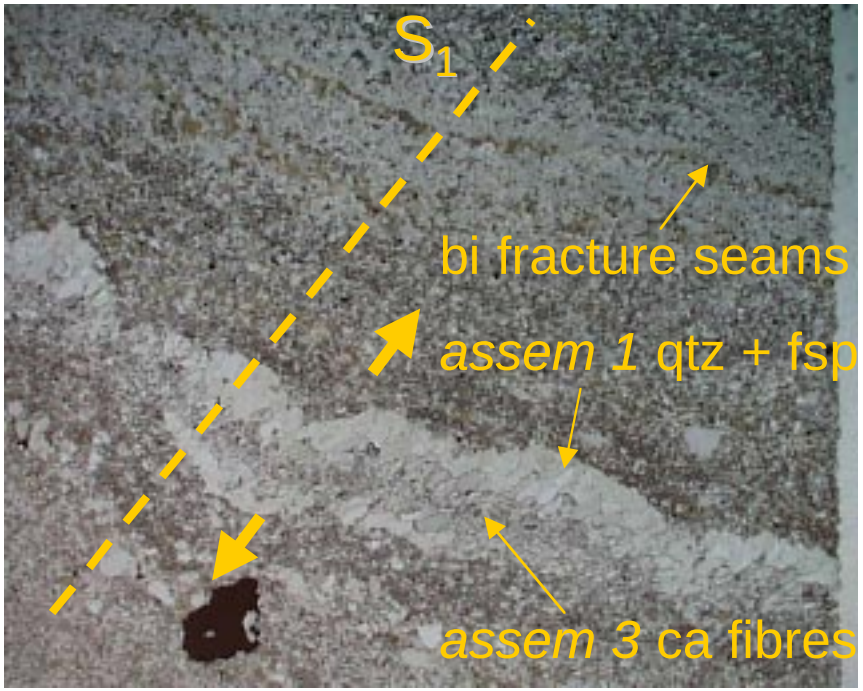

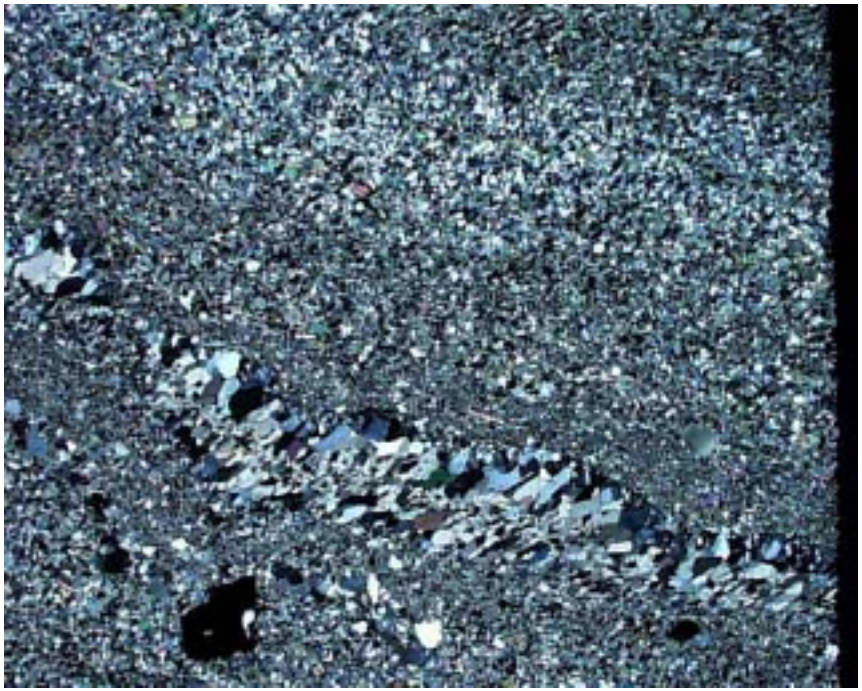

- dilation of layer-parallel *assemblage 1* “veins” or recrystallised domains
- *assemblage 3* fibre veins track the trace of the S1 cleavage

Assemblage 3: Cu-sulphides

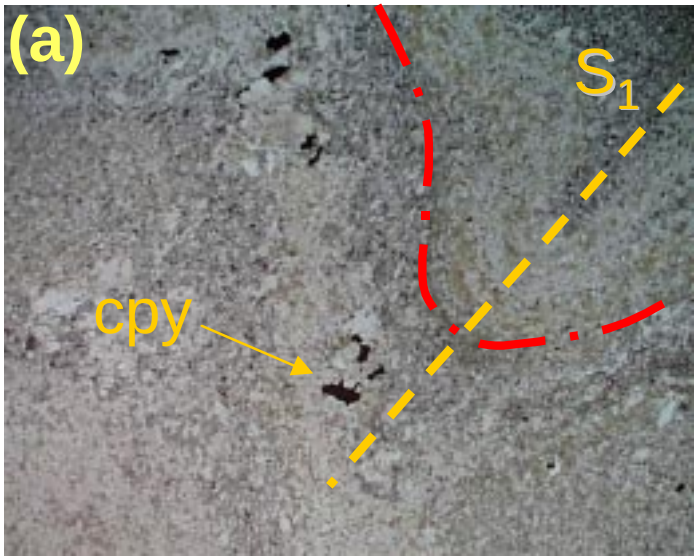

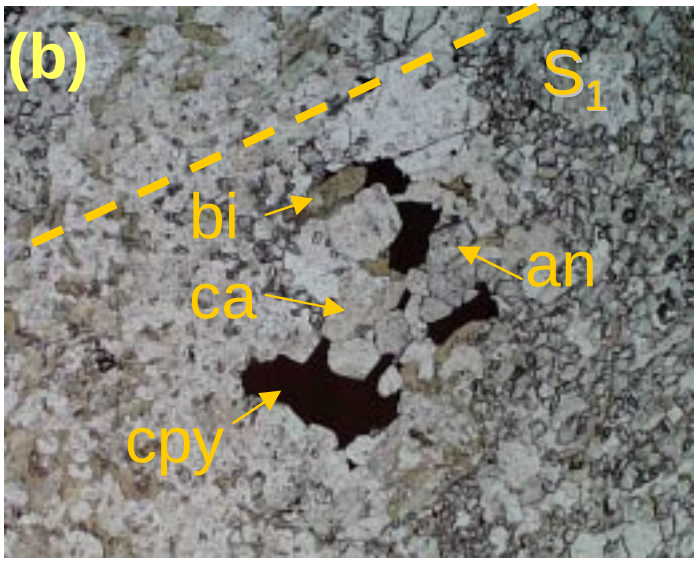

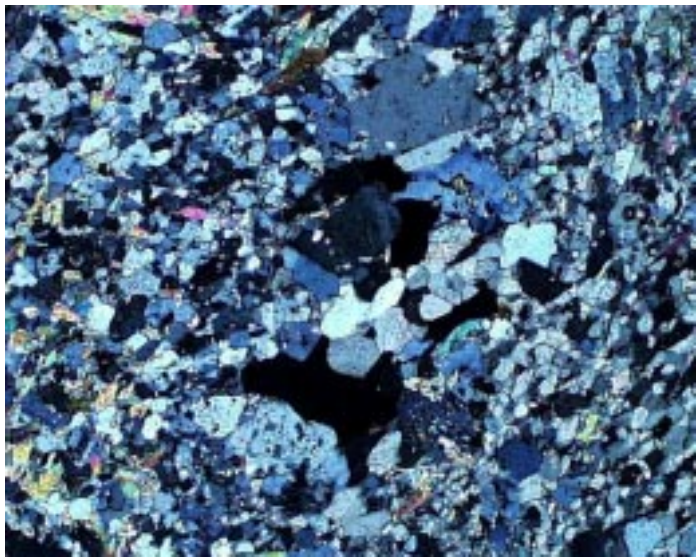

- chalcopyrite intergrown with biotite, carbonate and anhydrite
- overprints *assemblage 1* layer-parallel "vein" in F1 forelimb

Fig. 65

Assemblage 3: overgrowth textures

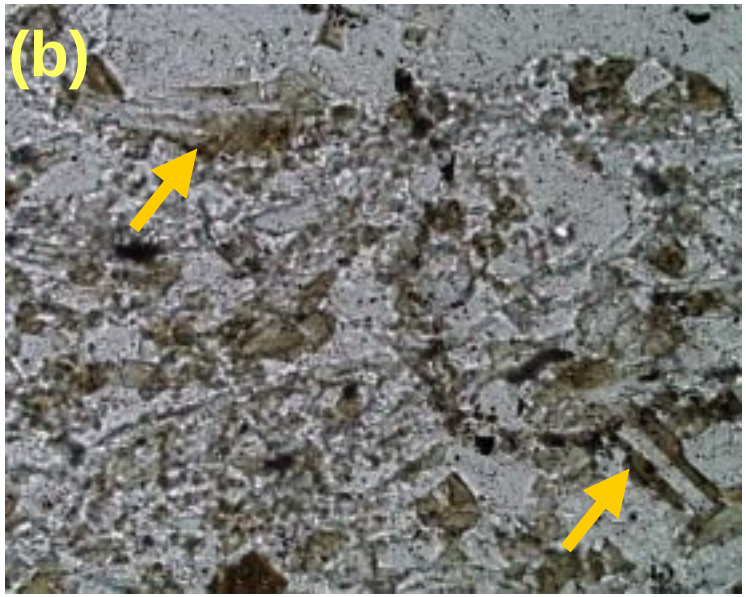

- biotite-carbonate overgrowths on *assemblage 1* albite (right) and *assemblage 2* muscovite (above)

Assemblage 3: overgrowth textures

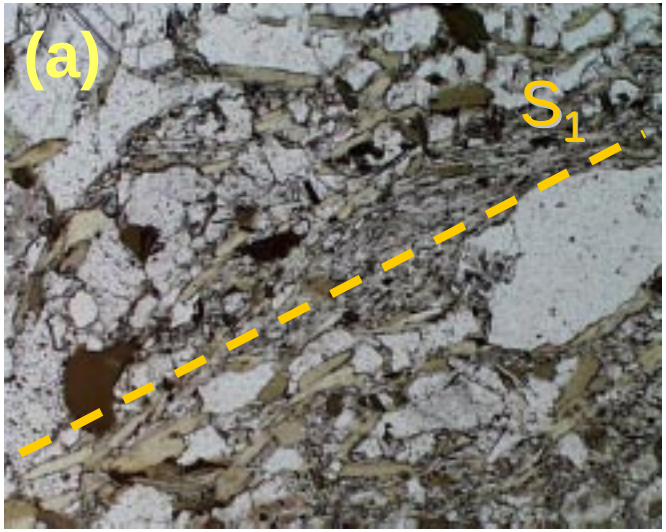

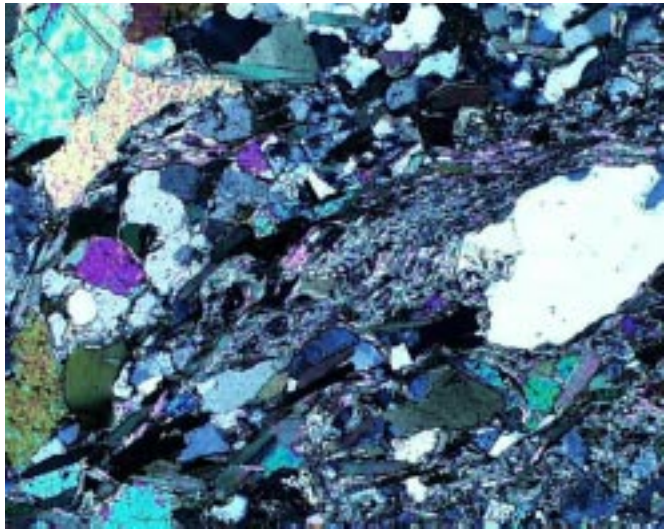

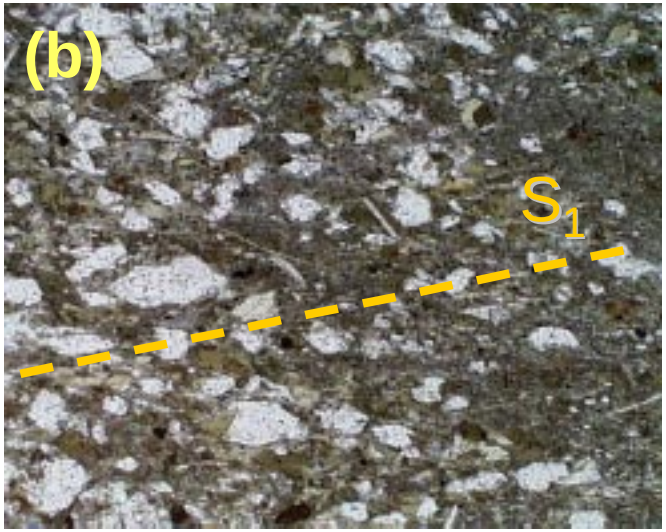

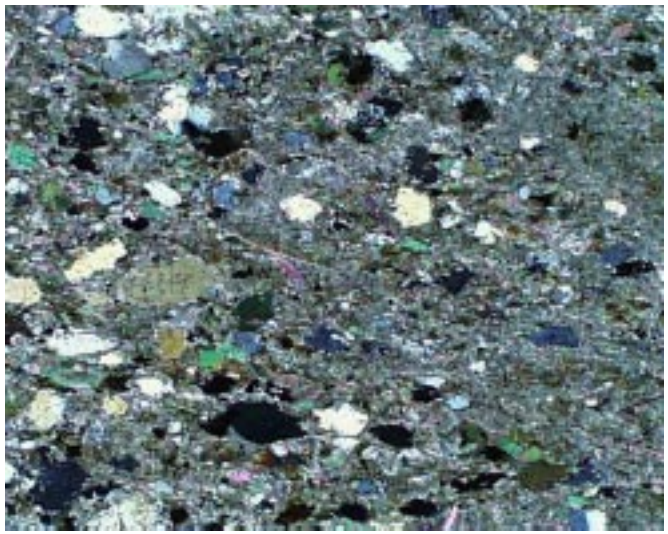

- biotite overprints sericite-muscovite in disaggregated sandstones

Zircon concentration via cataclasis

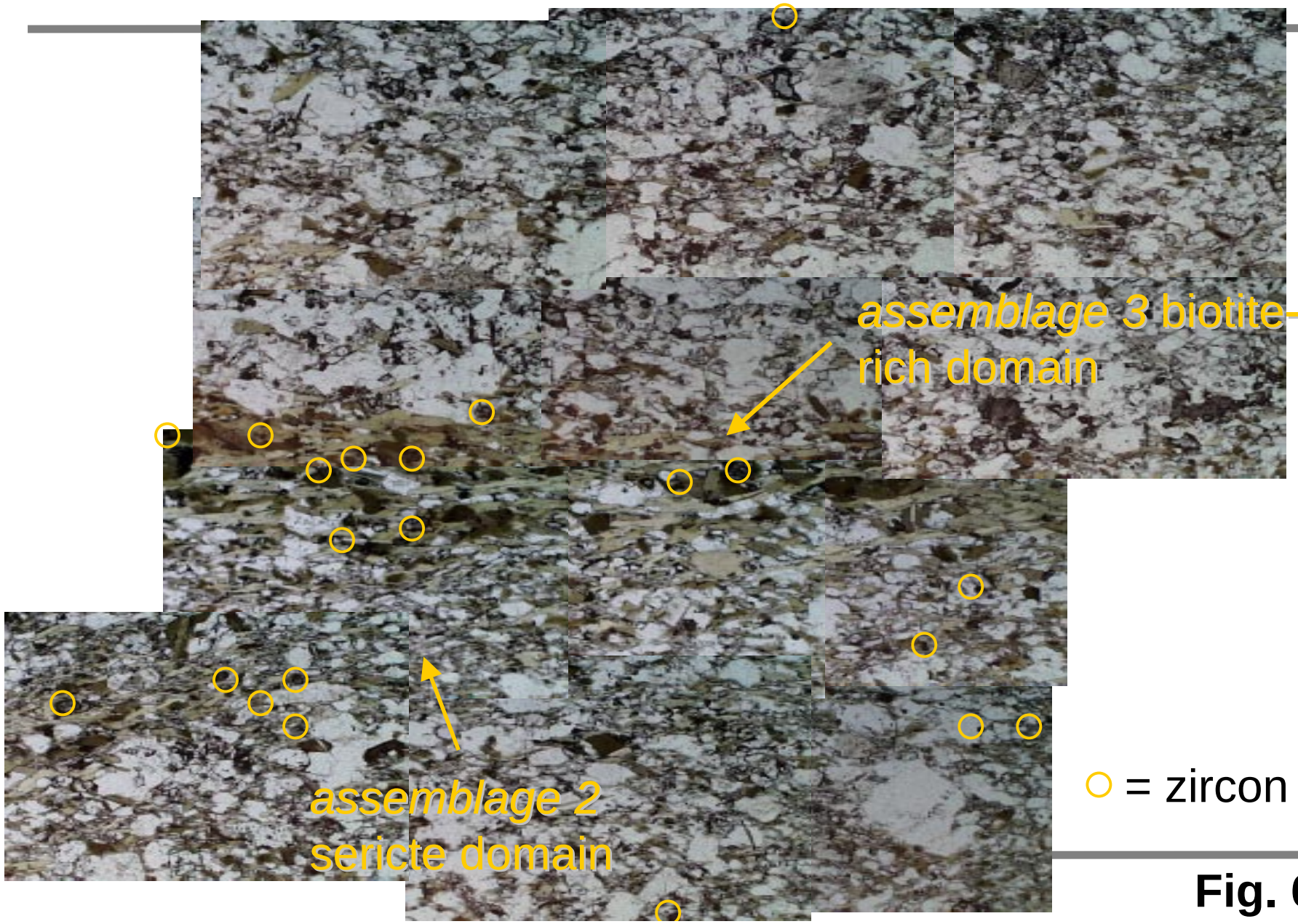

Fig. 68

Zircon morphology: biotite domains

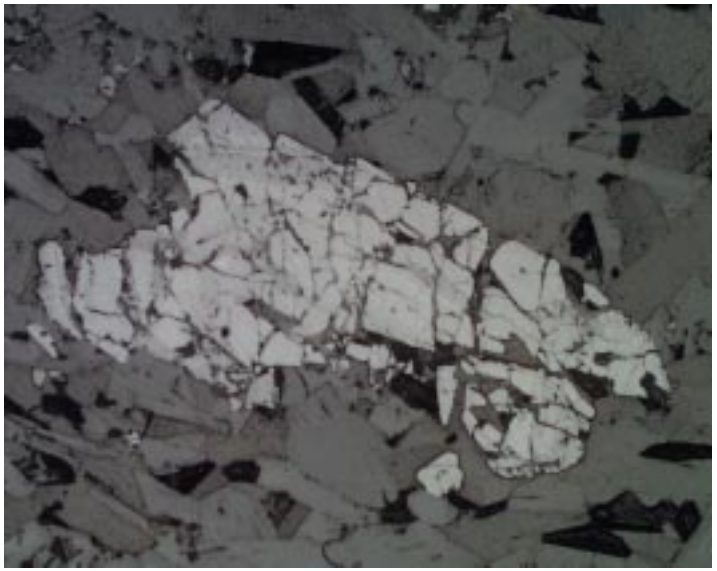

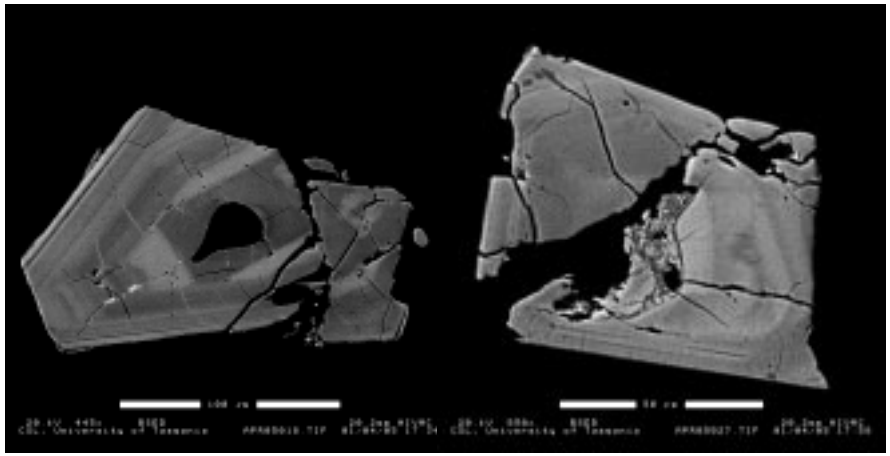

Assemblage 3: macroscopic structural control

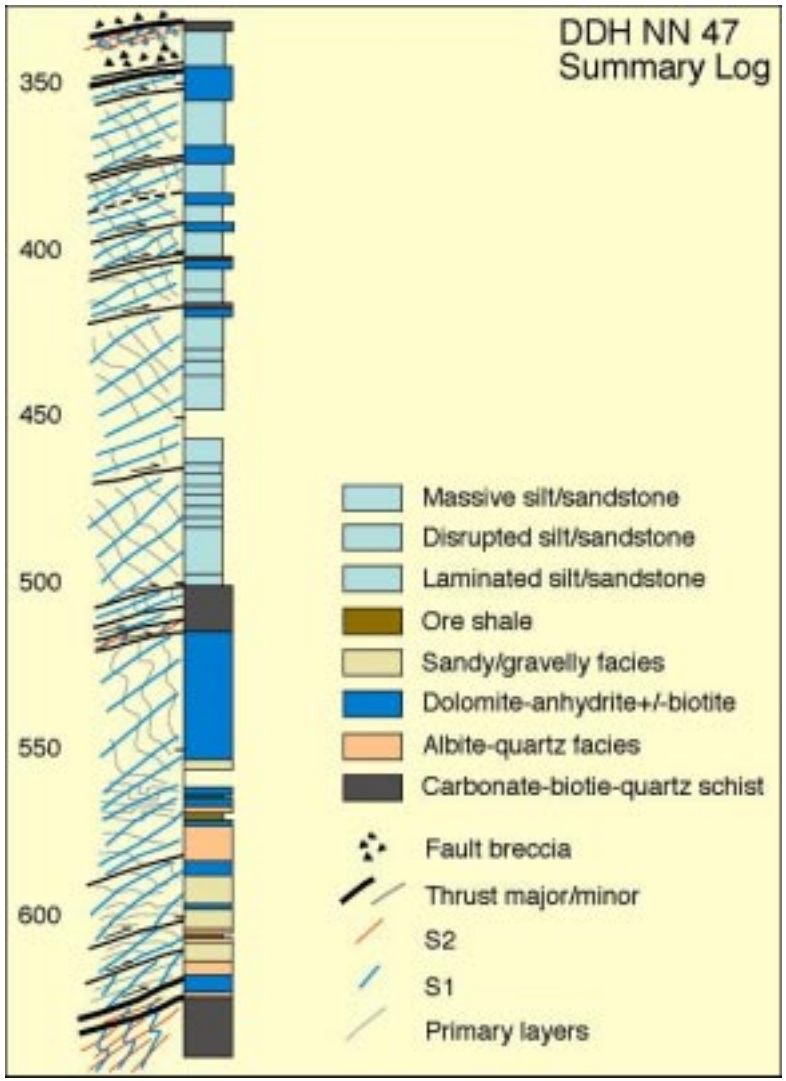

- *assemblage 3* = "dolomite-anhydrite-biotite" & "carbonate-biotite-quartz schist" facies
- partitioning of alteration assemblage within steepened forelimbs of macroscopic folds and shear zones

Assemblage 3: “flooding” domains

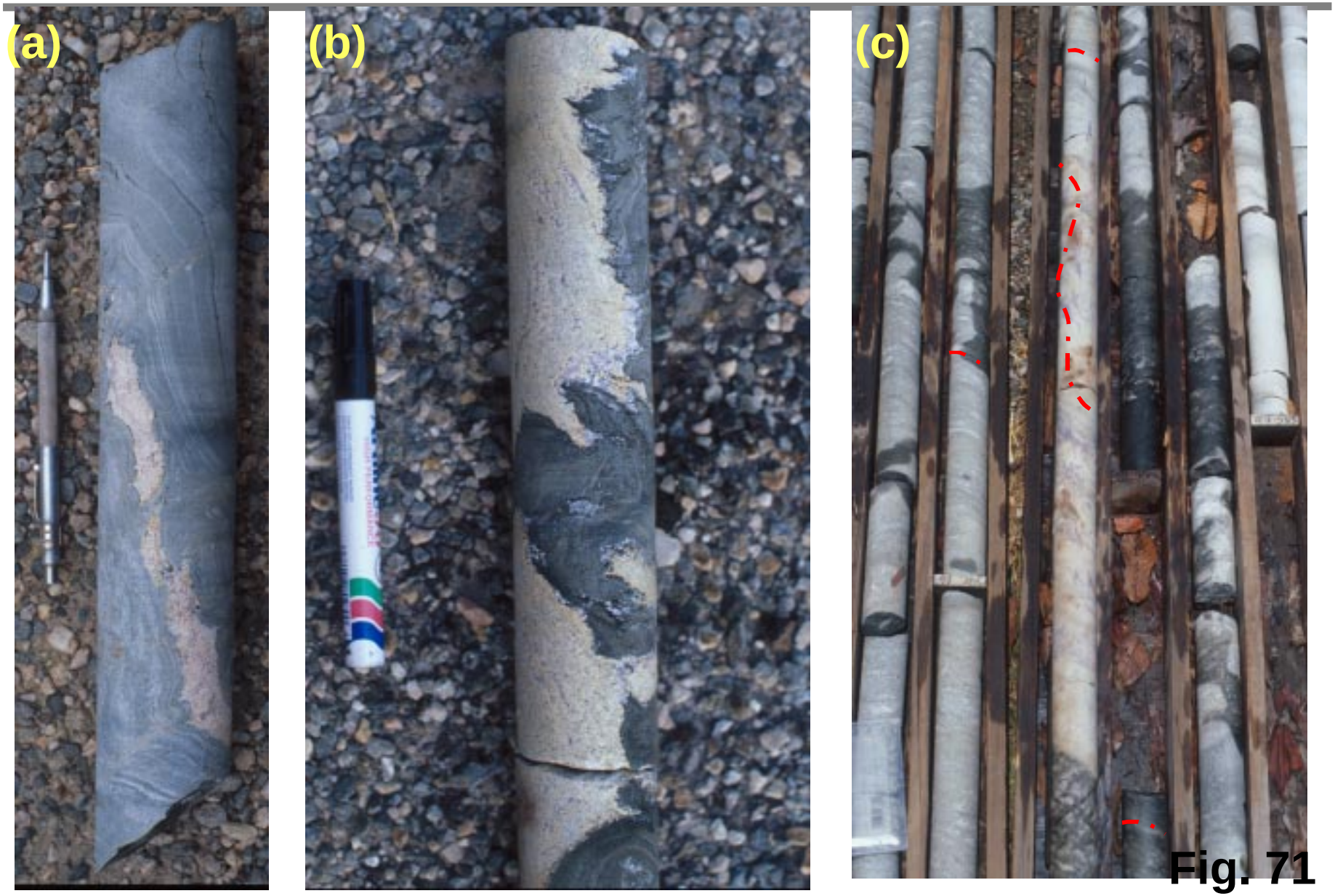

Fig. 71

Biotite morphology: multiple cleavage domains

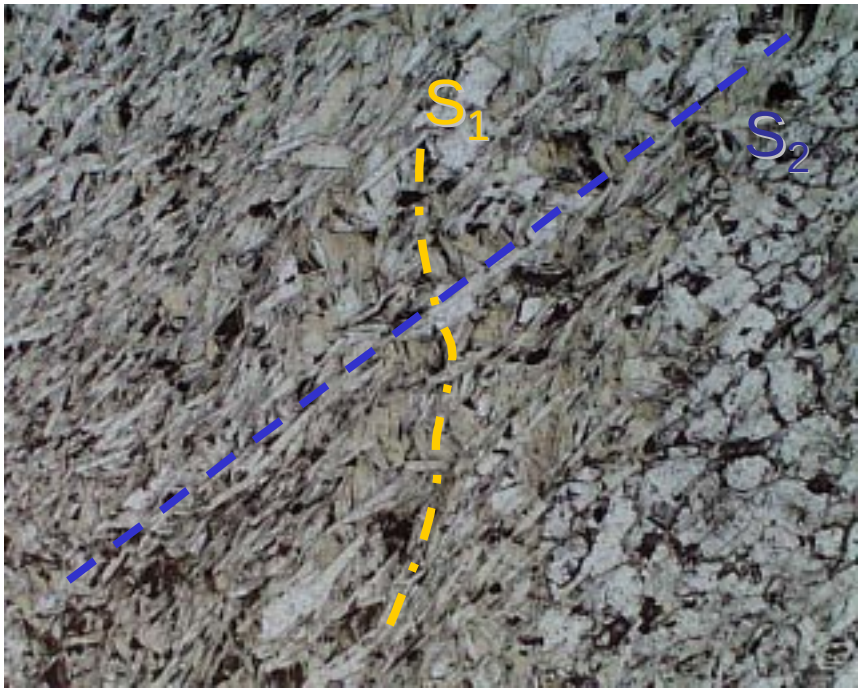

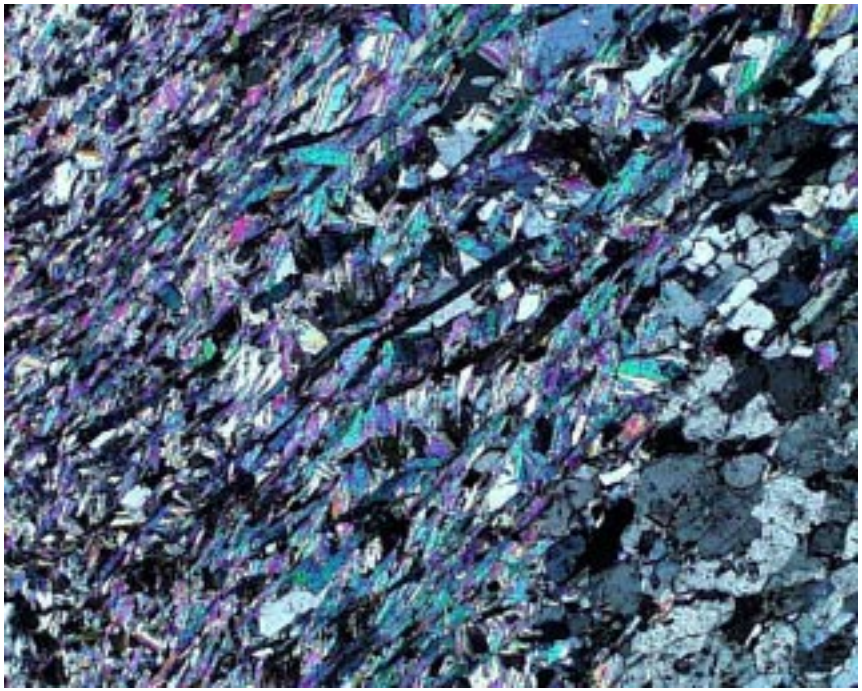

- multiple cleavage development in phlogopite-carbonate “flooded” F2 forelimb
- texturally and compositionally similar micas define both cleavage sets

U-Pb Age Dating (Laser ICPMS) on Zircons

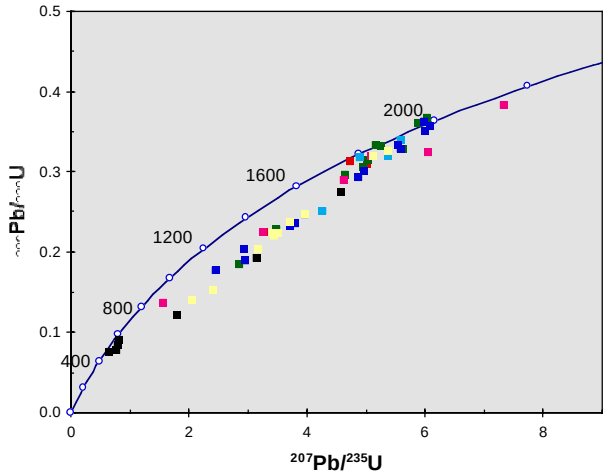

- "basement" indistinguishable from "Roan" in terms of age spectra
- Resetting of Palaeoproterozoic zircons by an Ordovician hydrothermal/metamorphic event

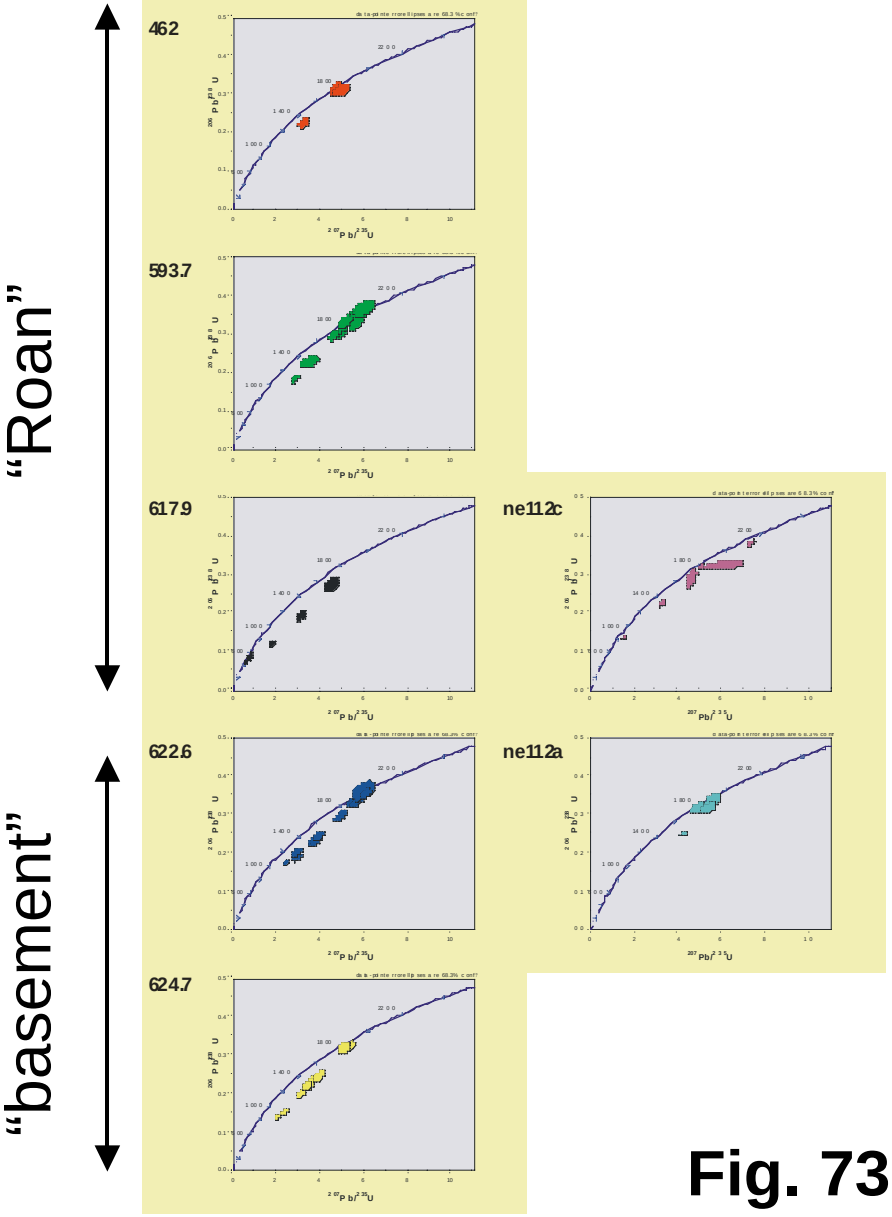

Fig. 73

U-Pb Age Dating (Laser ICPMS) on Zircons

Sample 617.9

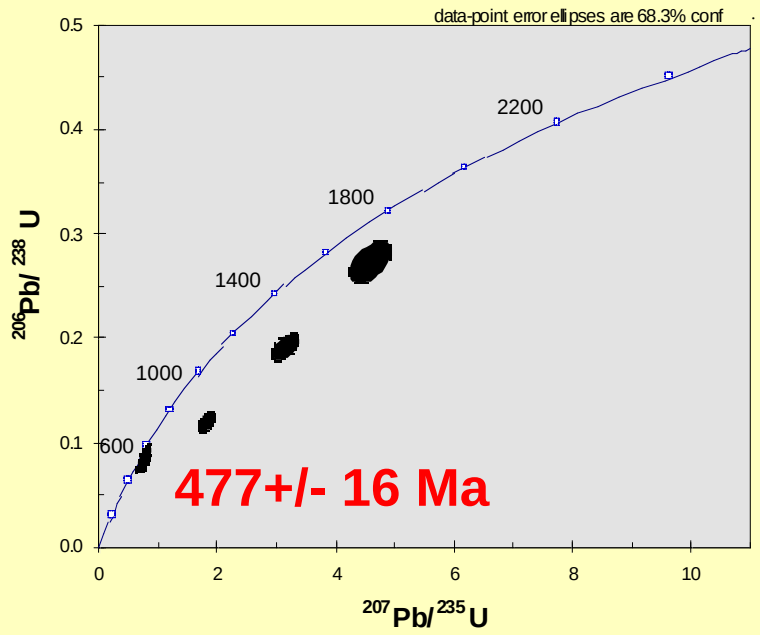

- intense albitic alteration
- concordant age dates from fractured phlogopitic domains
- hydrothermal overgrowths?

Structural - Metasomatic Evolution

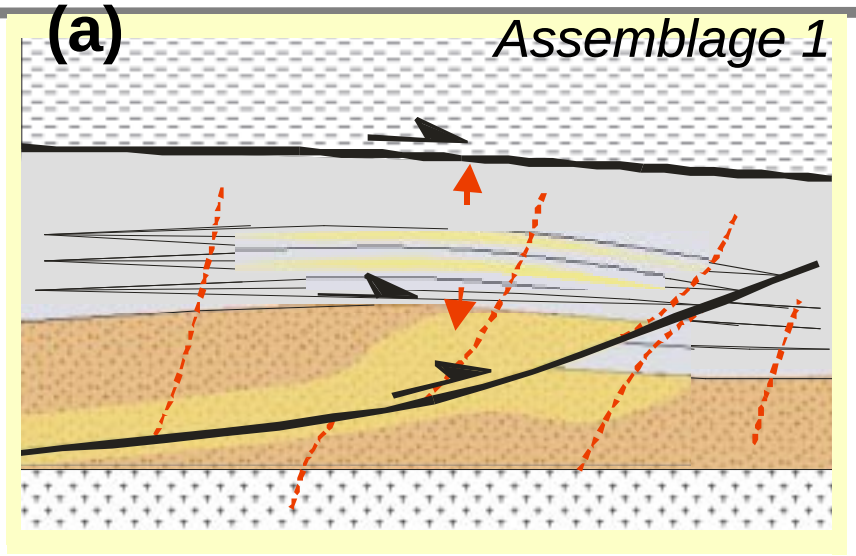

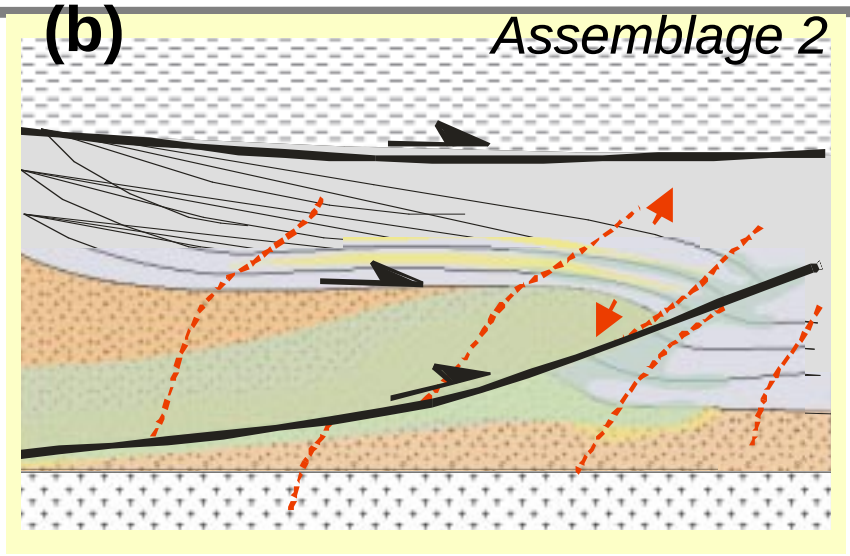

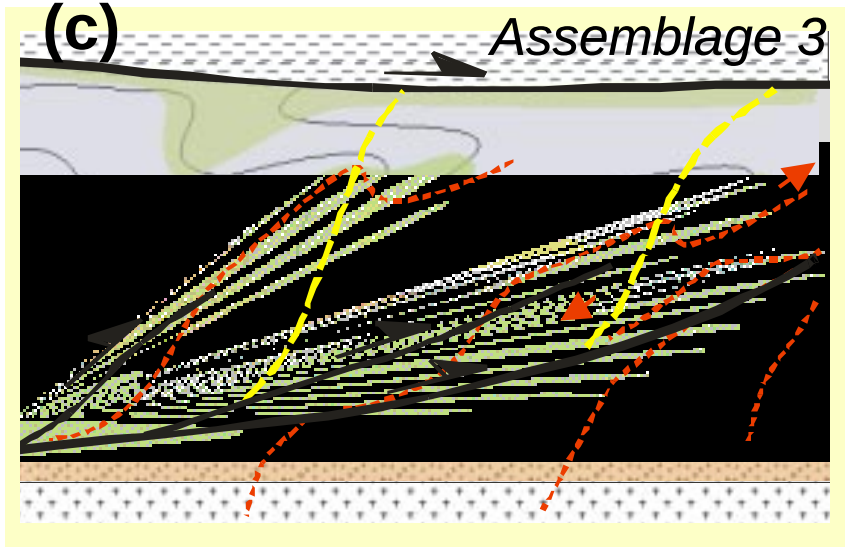

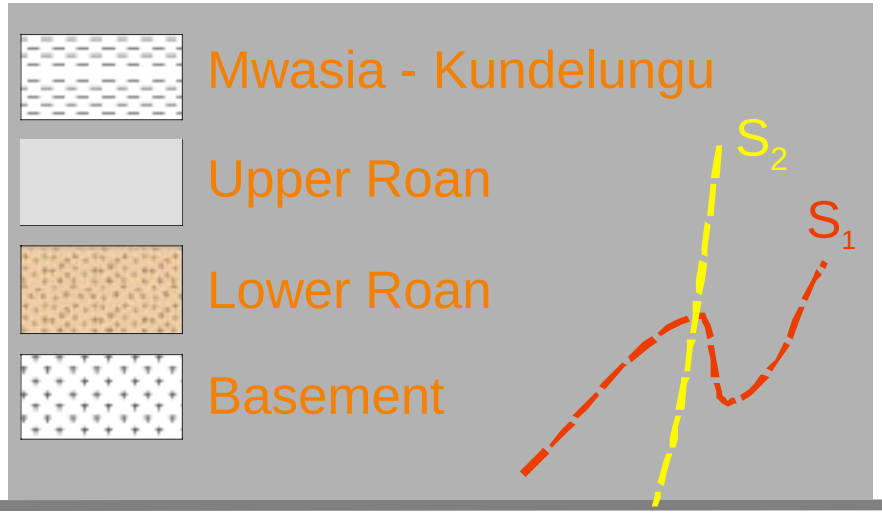

Fig. 75

AMIRA PROJECT P544
SEDIMENT-HOSTED COPPER DEPOSITS

Progress Report – June, 2001

David Broughton, Murray Hitzman
Dept. of Geology and Geological Engineering, Colorado School of Mines, Golden, CO, 80401 USA

Research undertaken at Colorado School of Mines since completion of field work at the end of 2000 includes petrographic study of lithologies and alteration throughout the stratigraphic section, preliminary C and O isotopic characterization of the carbonate stratigraphy bracketing the Grand Conglomerate, and initial S isotopic studies of anhydrite, gypsum and pyrite distal to the Copperbelt ore zones.

Petrographic work has focused on examination of lithologies above and below the "ore shale" section. Biotite is ubiquitous throughout the section, indicating that upper greenschist metamorphism affected the entire Katangan sequence. Epidote, although not as consistently present, has also been found in all parts of the section. Below the ore shale, the sediments are dominantly arkoses containing rounded to angular quartz, plagioclase and K-feldspar grains that commonly lack overgrowth textures. These are petrographically and megascopically similar to grains within the basement Lufubu Schist and apparently weathered basement granite, and it can be difficult to distinguish amongst them. The data suggest that the Lower Roan may have been deposited on pre-existing schists and granites, but does not preclude more complex structural relationships.

The Upper Roan consists of interbedded dolomites, siltstones, gritty siltstones and lesser sandstones, and contains structures indicative of pre-existing evaporites. Petrographically, the dolomites are impure and contain quartz, plagioclase, mica, and scapolite. The overlying Mwashia consists of more thinly bedded siltstones and uppermost dolomites and generally lacks coarser sedimentary material. In broad terms the overall section therefore reflects a fining upwards sequence. Preliminary work suggests that the abundance of detrital feldspar, probably derived from the basement granites, declines up section and is absent in the Mwashia. Megascopic rounded and broken quartz grains are present throughout the Roan and show a variety of strain effects within the same petrographic section, suggesting derivation from a variably deformed basement terrane. The megascopically distinctive blue quartz is difficult to distinguish from normal grains in thin section.

The Grand Conglomerate is characterized petrographically by abraded to broken quartz, plagioclase and feldspar grains and generally rounded lithoclasts within a carbonate-rich matrix (Plate 1). Clast varieties include dolomite and chert; the latter is absent from the local Katangan section and indicates a wider, or otherwise different provenance.

A distinctive breccia is present at the base of the Mwashia and was tentatively interpreted as a thrust breccia during the 2000 field season. Petrographic examination confirms that the unit contains deformed carbonate-rich clasts of possible Upper Roan derivation, within an undeformed carbonate-quartz-plagioclase matrix. In some samples the matrix has abundant plagioclase and a distinct igneous texture (Plate 2), however it is unclear whether this reflects incorporated clasts of gabbro or a primary igneous origin. Further study will be directed at tracing and interpreting this still-enigmatic unit.

Core logging during 2000 demonstrated the

importance of small-scale (mm to cm) "dewatering" structures, which are now termed "diapiric." Petrographic work indicates that these structures are filled with silt to sand-size grains, not mud (Plates 3, 4). This suggests that diapirism occurred after initial diagenesis of mud-rich rocks but prior to dewatering, and diagenetic cementation, of coarser layers. The diapiric textures observed in the Upper Roan are somewhat similar to dewatering structures observed today in the South Caspian Basin. This basin is characterized by up to 25 km of sediment with more than 10km of this fill deposited in the last 6 m.y. (Devlin et al., 1999). While the known thickness of the Roan succession in Zambia is believed to be a fraction of that in the Caspian, the key may be the rate of original sedimentation. Perhaps the dewatering structures indicate extremely rapid sediment deposition. These data may give us a better handle on the depositional system and tectonic regime responsible for the Katangan sequence and allow us to more critically compare basinal settings elsewhere in the world for Copperbelt-type potential.

The dewatering observed in the Katangan sequence could also be related to the glaciogenic deposits which have been recognized in the Katangan succession. Glacial loading and sub-glacial deformation of the Mwashia and Roan sediments may have been responsible for the pre-lithification folds (Plate 5) and small-scale diapirs found throughout the lower Katangan. Abnormally high depostional rates of 40 metres per thousand years are recorded in the cap carbonates, due to extreme greenhouse conditions during the glaciation aftermath (Hoffman et al., 1998), and may have contributed to early deformation.

The importance of the dewatering structures to sulphide mineralization is still difficult to determine. Work to date suggests that the sulphides currently observed post-date the dewatering structures and were probably precipitated during metamorphism. However, the dewatering structures do provide a large number of fluid pathways, and do contain sulphide (Plate 4). They also suggest that the basin contained large amounts of fluid. Finally, diapiric structures in the Caspian are the result of the escape of large amounts of natural gas as well as aqueous fluids. Natural gas in the Katangan sequence may have been, along with evaporitic sulphate, an important source of sulphur for sulphide precipitation.

Petrographic alteration studies were aimed at broadly defining the nature and extent of alteration within the Katangan section. Preliminary observations indicate that fine-grained hematite and weathered iron species, rather than K-feldspar, are responsible for much of the distinctive red colouration in the Katangan section. Alteration defined by visible bleaching and associated with contacts and veins is characterized petrographically by dolomitization, silicification and plagioclase alteration (Plate 6). Veins commonly contain plagioclase and/or K-feldspar, as well as quartz and carbonate. This alteration appears similar to that known at the vein-hosted Kansanshi deposit, west of the Copperbelt, where mineralization has been dated at circa 500 Ma (Torrealday et al, 2000). The copper sulphides observed in thin sections from Konkola and Nkana are commonly intergrown with metamorphic biotite (Plate 7) and appear metamorphic or metamorphically remobilized.

One of the continuing difficulties in the Katangan sequence in the Copperbelt area has been to accurately determine absolute stratigraphic position. The Katangan sequence contains several conglomerate layers which are thought to be glacial diamictites. In particular, the Grand Conglomerate is thought to correlate with similar deposits in Namibia and around the world. The glacial diamictites record a series of late Proterozoic global glaciations that covered even the equatorial regions – the Snowball Earth. Hoffman et al. (1998) and others have documented distinctive negative C isotopic excursions associated with the Sturtian–aged (~760 – 700 Ma) Ghaub and Chuos diamictites in Namibia, recorded in the underlying and overlying (cap) limestones. Sedimentological differences between the two cap limestones are reflected in their respective C signatures.

In the Copperbelt, the Grand Conglomerate is overlain by the Kakontwe Limestone, a +100 metre thick meta-dolomite, and underlain by similar meta-dolomites of the Mwashia Group. Greenschist

metamorphism has obliterated any sedimentary structures, making it impossible to visually distinguish one carbonate from another. However, the whole-rock isotopic compositions of samples from three drill holes in the Nchanga-Konkola area record a –2 to –5 per mil C excursion associated with the Grand Conglomerate, and an isotopically heavier C signature for the Kakontwe versus the Mwashia dolomites. The O isotopic signatures are similar but somewhat less robust. The results suggest that the Grand Conglomerate and Kakontwe Limestone correlate with the Chuos diamictite and Rasthof Limestone in Namibia, and encourage the use of simple whole-rock C and O isotopes for stratigraphic correlation within the Copperbelt and regionally within the Katangan. This should allow more precise stratigraphic correlation throughout the Lufilian Arc, even in areas containing incomplete sections.

Anhydrite and gypsum are present in varying amounts in the Copperbelt rocks and suggest that evaporates were present in the original stratigraphic section. This has important implications for deformational history, character of basinal and ore-forming fluids, and ultimately, deposit genesis. The sulphates commonly occur in late structural and metamorphic structures, rather than in preserved sedimentary structures such as nodules, which reflects their ease of mobility and replacement by carbonate and/or quartz. Isotopic compositions of sulphate were analysed to determine whether distinctions could be made between different stratigraphic intervals, to characterize the provenance of the sulphate. The majority of the anhydrite and gypsum has a heavy $\delta^{34}S$ signature of +18 to +21.5 per mil, including samples from weakly mineralized zones laterally equivalent to the Copperbelt ore zones. However, samples from the uppermost part of the Mwashia have a lighter signature of +12 to +13 per mil, both in metamorphic and preserved, clearly evaporitic textures. Although the data are limited, this suggests that $\delta^{34}S$ values may be helpful in correlating sequences within the Copperbelt.

Preliminary $\delta^{34}S$ results have been received for disseminated and vein pyrite occurring in barren and weakly mineralized zones distal to the Copperbelt ores. Results range from +6 to +16 per mil, consistently heavier than the isotopically light (-10 to +5 per mil) values for sulphides within the ores. The distal pyrite is isotopically too heavy to be bacterial, and may have been derived from the dissolution of primary sulphates during diagenesis or metamorphism. The results suggest a lateral gradient may be present between the distal and proximal parts of the mineralizing system, which could be a powerful exploration vector. Results are pending on chalcopyrite analyses from these same distal zones.

Research during June through August, 2001 will focus on fieldwork to complete collection of stratigraphic sections throughout the Copperbelt and begin to piece together a more three-dimensional picture of facies variability. The work will also seek to constrain large-scale structural disruption of the sedimentary sequence building upon the recognition of the regional-scale, low-angle breccia structure during the 2000 field season. Results to date will be integrated with the more detailed structural and ore deposit-focused studies of the CODES group. This will be facilitated by having both the CSM and CODES teams on the ground in Zambia simultaneously. The preliminary petrographic and isotopic work will allow us to better focus sampling during the 2001 field season and move towards answering specific questions, particularly whether broad-scale alteration halos to the Copperbelt sulfide bodies can be identified petrographically or isotopically.

References

Devlin, W.J., Cogswell, J.M., Gaskins, G.M., Isaksen, G.H., Pitcher, D.M., Puls, D.P., Stanley, K.O., and Wall, G.R.T., 1999, South Caspian Basin: Young, Cool and Full of Promise; GSA Today, v. 9, No. 7, pp. 1-9.

Hoffman, P.F., Kaufman, A.J., Halverson, G.P., and Schrag, D.P., 1998, A Neoproterozoic Snowball Earth; Science, v. 281, pp. 1342-1346.

Torrealday, H.T., Hitzman, M.W., Stein, H.J., Markley, R.J., Armstrong, R., and Broughton, D., 2000, Re-Os and U-Pb Dating of the Vein-Hosted Mineralization at the Kansanshi Copper Deposit, Northern Zambia; Economic Geology, v. 95, pp. 1165-1170.

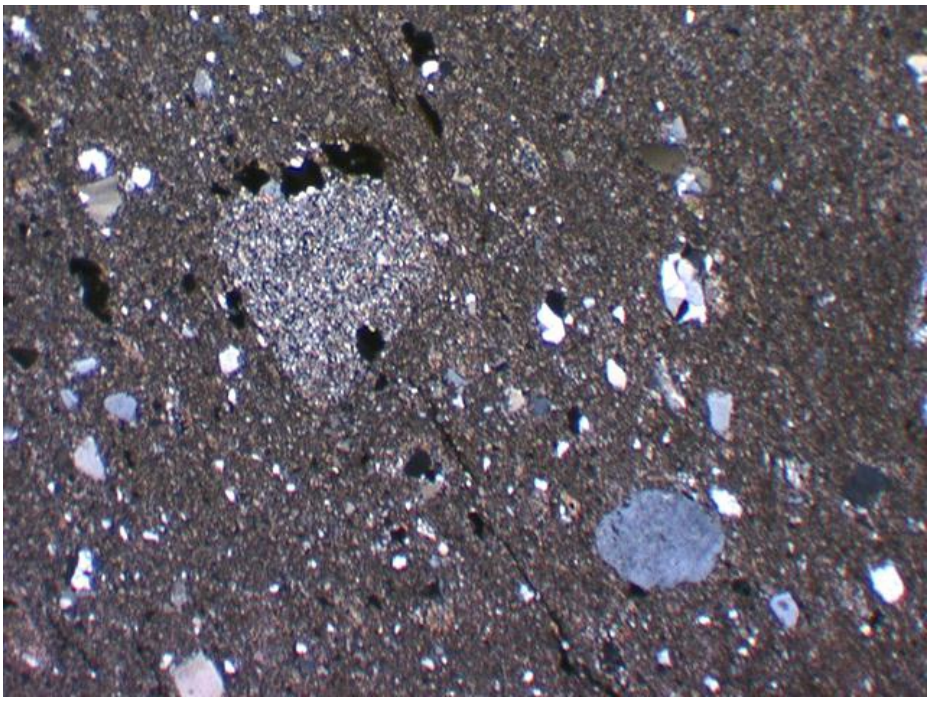

Plate 1. Grand Conglomerate, showing clasts of chert, quartz and feldspar in fine sand to silt-sized matrix of rock fragments, carbonate. Field of view about 3 mm.

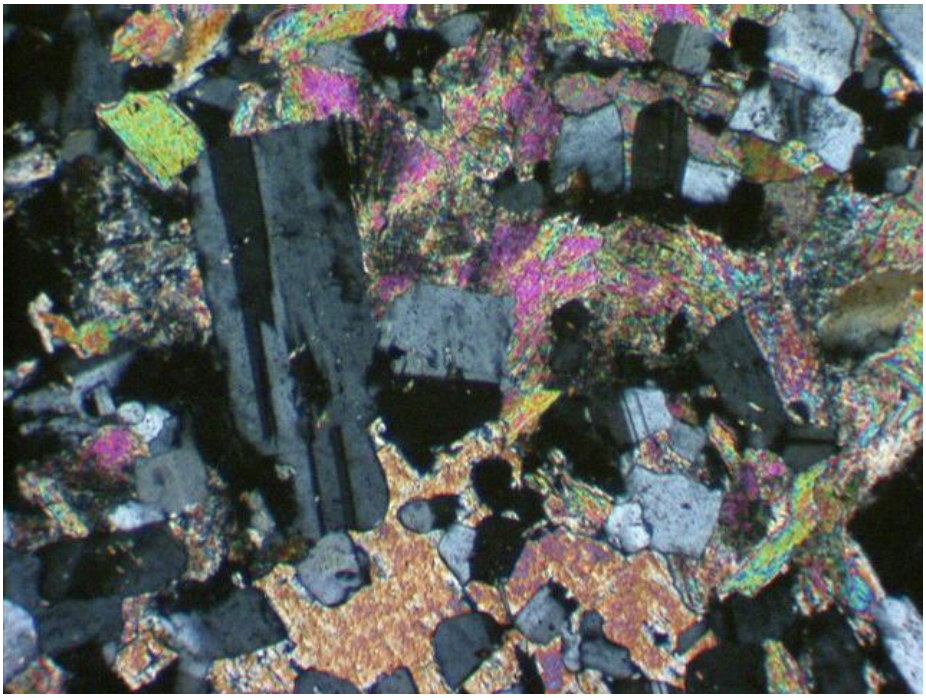

Plate 2. Breccia at base of Mwashia, showing well-developed plagioclase and biotite in a carbonate matrix. Field of view about 3 mm.

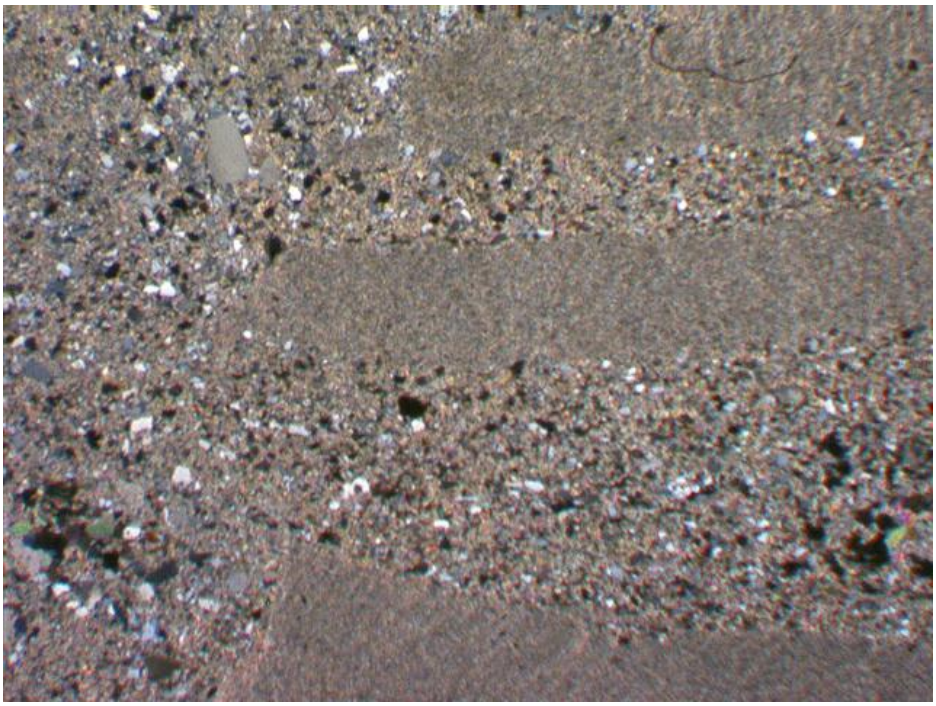

Plate 3. Sand-filled diapiric structure (left) truncates fine-grained beds but is continuous with coarse-grained beds. Lower Roan, field of view about 1 cm.

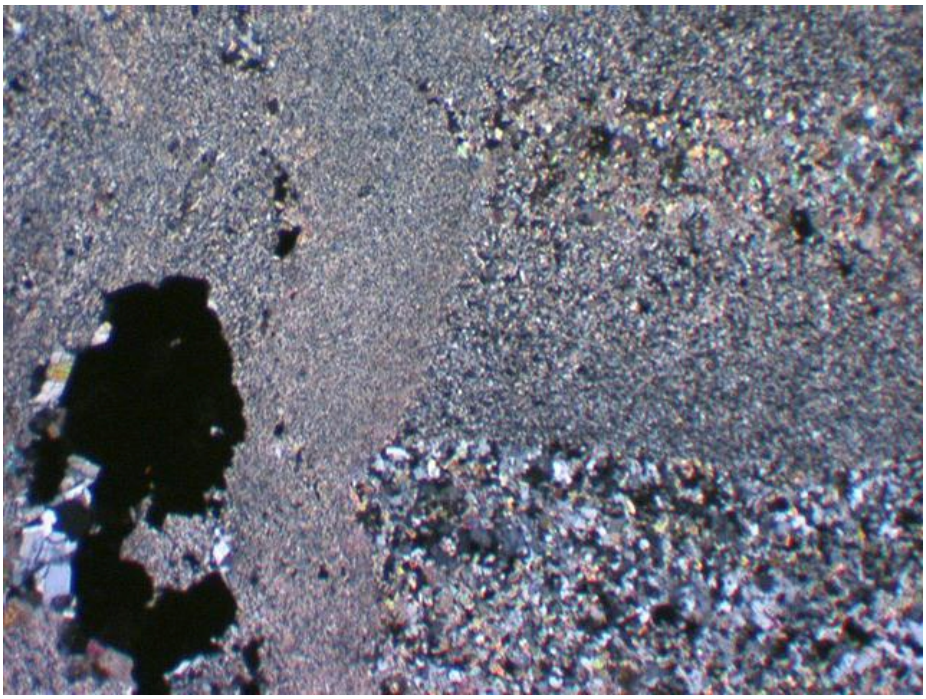

Plate 4. Silt-filled diapiric structure with coarse pyrite, cutting bedded sandstones and siltstones. Upper Roan, field of view about 1 cm.

Plate 5. Prelithification fold, Lower Roan Shale-with-Grit. Note lack of axial cleavage. Field of view about 1 cm.

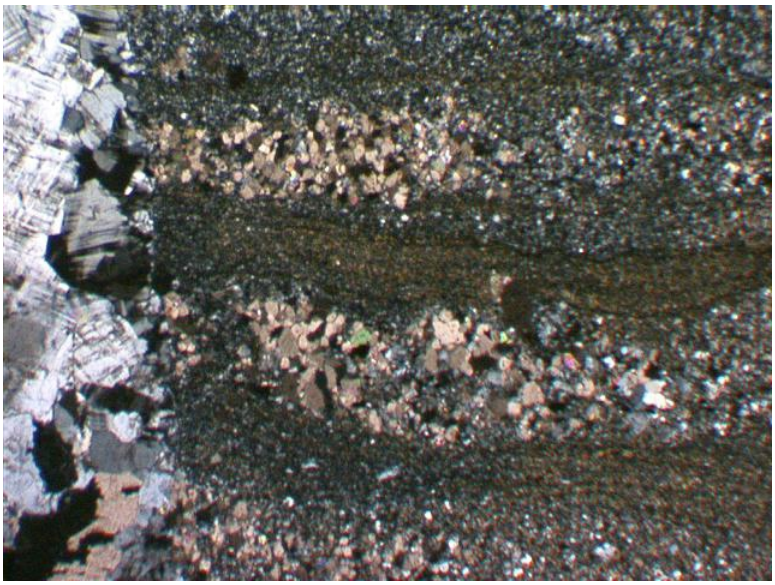

Plate 6. Alteration associated with high-angle microcline-plagioclase-quartz-ferroan dolomite veinlet. Dolomite alteration predominates in coarse-grained beds, grey silicification and feldspathization in finer beds. Lower Roan, field of view about 1 cm.

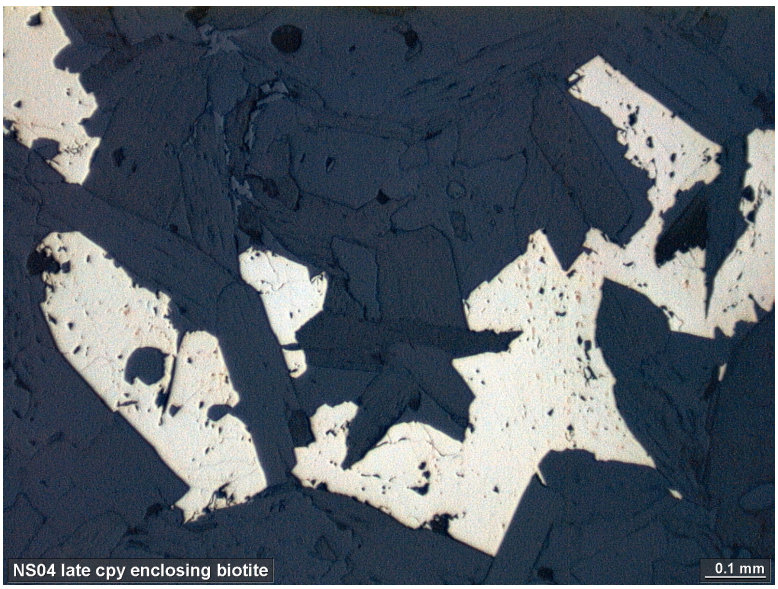

Plate 7. Chalcopyrite enclosing and intergrown with metamorphic biotite.

Nkana PhD

Geology and genesis of the Nkana copper deposits —

Mawson Croaker

Aims

- **Document the diversity and gross distribution of ore type in the Mindola–Nkana North–Nkana South (MNNN) line of orebodies**
- **Review sedimentology of the host sequence (including the 'barren gaps') and the relationship between basement rocks and the Lower Roan, including sedimentological controls on sulfide distribution**
- **Document the macro- and meso-scale structures of the MNN system**
- **Document the nature and timing of metamorphic and hydrothermal processes that have affected the Lower Roan rocks**
- **Ultimately, to produce an empirical/descriptive model for the MNN deposits and to discuss the genetic aspects of this model**

Nkana PhD (cont)

Research Plan and Methods

- Techniques used for this study will include underground mapping, core logging and review of existing mine plans, sections and core logs
- In order to target key underground exposure and suitable drill-core, initial planning for this project will need to be done in close consultation with mine staff and other First Quantum-Mopani geologists
- Fringes of mineralisation and 'barren gaps' will be carefully examined, as these are likely to be key areas for deciphering ore-forming processes

Nkana PhD (cont)

Research Plan and Methods (cont)

- Structural mapping (will be carried out on both underground exposures and drill-core)
- Conventional petrographic and geochemical techniques will be used to characterise samples from MNN deposits and will complement similar work being carried out elsewhere in the Copperbelt in AMIRA P544
- Stable isotope (S,C,O) will be measured on paragenetically well constrained samples in order to gain insight into fluid rock interaction processes and S sources
- Immobile element geochemistry and/or zircon/monazite dating may be used to assists with correlation of sedimentary packages along the line of orebodies

Mufulira PhD

Sedimentology, structure and geochemistry of the Mufulira copper deposit — Nicky Pollington

Aims

- **Document the sedimentology of the host sequence at Mufulira and interpret them using modern facies analysis techniques**
- **Review evidence for sedimentary vs a tectonic origin for structures in the Ore Formation and host sequence**
- **Determine the origin, or origins, of breccias present in the footwall and hangingwall to the Ore Formation**
- **Document the relationship between sulfide and sulfate in the Ore Formation, and their relationship to gross metal zoning**
- **Better understand the lateral and down-dip distribution of sulfides and their relationship to sedimentary facies and structures**
- **Ultimately, to produce an empirical/descriptive model for the Mufulira deposit and to discuss the genetic aspects of this model**

Mufulira PhD (cont)

Research Plan and Methods

- Techniques used for this study will include underground mapping, core logging and review of existing mine plans, sections and core logs
- In order to target key underground exposure and suitable drill-core, initial planning for this project will need to be done in close consultation with mine staff and other First Quantum-Mopani geologists
- Fringes of mineralisation and 'barren gaps' will be carefully examined, as these are likely to be key areas for deciphering ore-forming processes

Mufulira PhD (cont)

Research Plan and Methods (cont)

- Initially the work will focus on drill-core, with limited underground mapping, but access to new development underground (particularly at 'fringe' ore positions) may become more important as work progresses
- Conventional petrographic and geochemical techniques will be used to characterise samples from Mufulira and will complement similar work being carried out elsewhere in the Copperbelt in AMIRA P544
- Stable isotope (S,C,O) will be measured on paragenetically well constrained samples in order to gain insight into fluid rock interaction processes and S sources
- Immobile element geochemistry and/or zircon/monazite dating may be used to assists with correlation of sedimentary packages along the line of orebodies

Xenotime, Monazite and Zircon SHRIMP Geochronology:

Methods for refining the Precambrian time scale and understanding basin evolution

---

Presented by Galvin Dawson

Centre for Global Metallogeny,
University of Western Australia

Outline

- What is Xenotime?
- Forms of Xenotime
- Applications of U-Pb dating
  - Basin evolution
  - Chronostratigraphy
- SHRIMP geochronology
- Application to the Zambian Copperbelt
  - Project details

What is Xenotime and when does it form?

- Xenotime - YPO_4
- Xenotime forms during:
  - Early Diagenesis
  - Burial Diagenesis
  - Metamorphism
  - Alteration
  - Mineralisation

Authigenic Xenotime

- **Xenotime forms during diagenesis in the first few metres to tens of metres of burial**
  - **Phosphate and Y from seawater and organics are adsorbed onto clays and Fe- (hydr-) oxides**
- **Zircon & Xenotime are isostructural**
  - **Bacterial reduction release P and Y to form xenotime as pyramidal shaped overgrowths on detrital zircons**
- **Authigenic xenotime forms overgrowths on detrital zircon grains in ~50% of all siliciclastic rocks so far studied**
  - **inc. mudstones, sandstones and conglomerates**

What is Xenotime and when does it form?

- Xenotime - YPO_4
- Xenotime forms during:
  - Early Diagenesis
  - Burial Diagenesis
  - Metamorphism
  - Alteration
  - Mineralisation

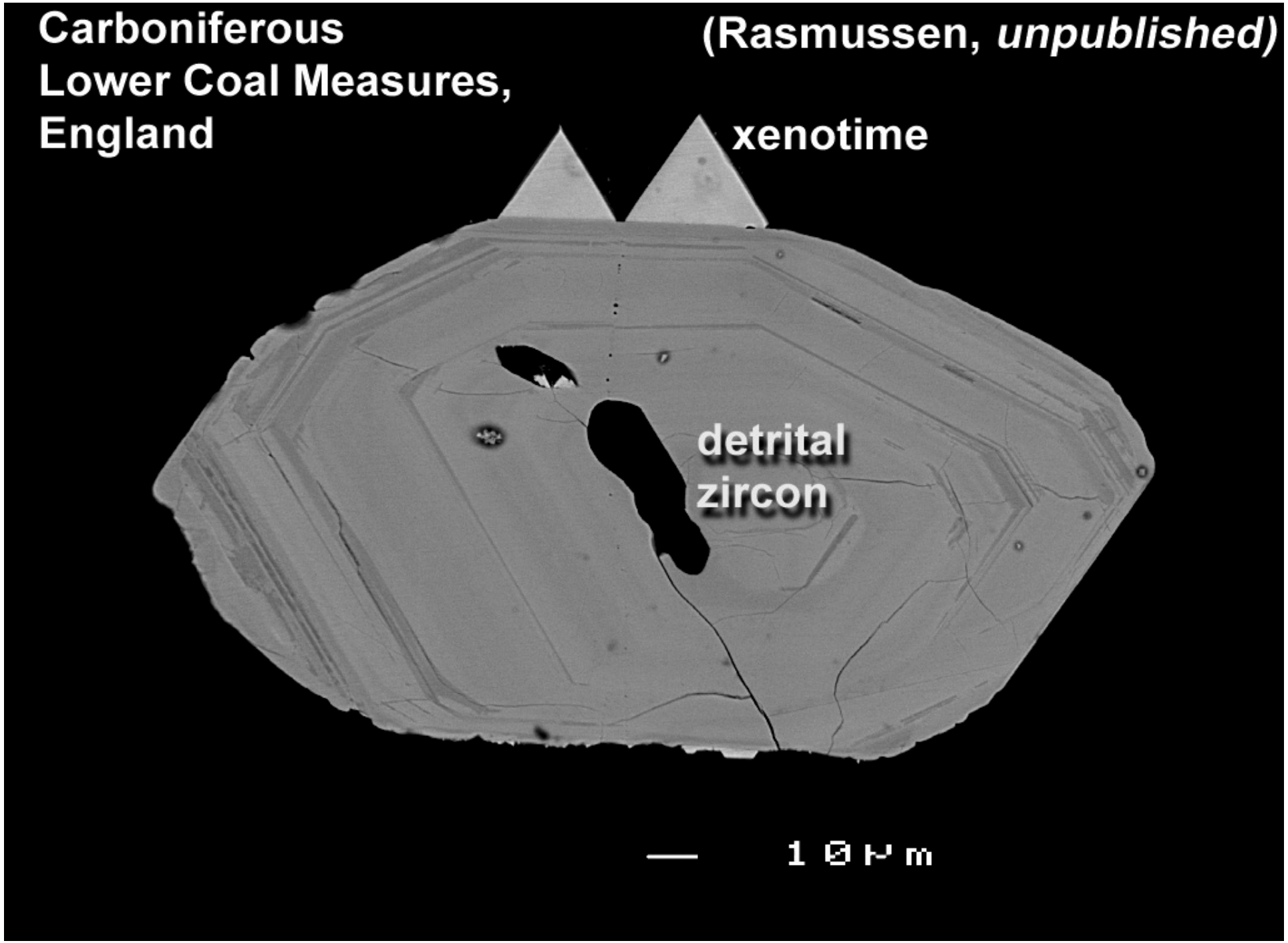
Carboniferous
Lower Coal Measures,
England
(Rasmussen, *unpublished)*
xenotime
detrital
zircon
10 µm

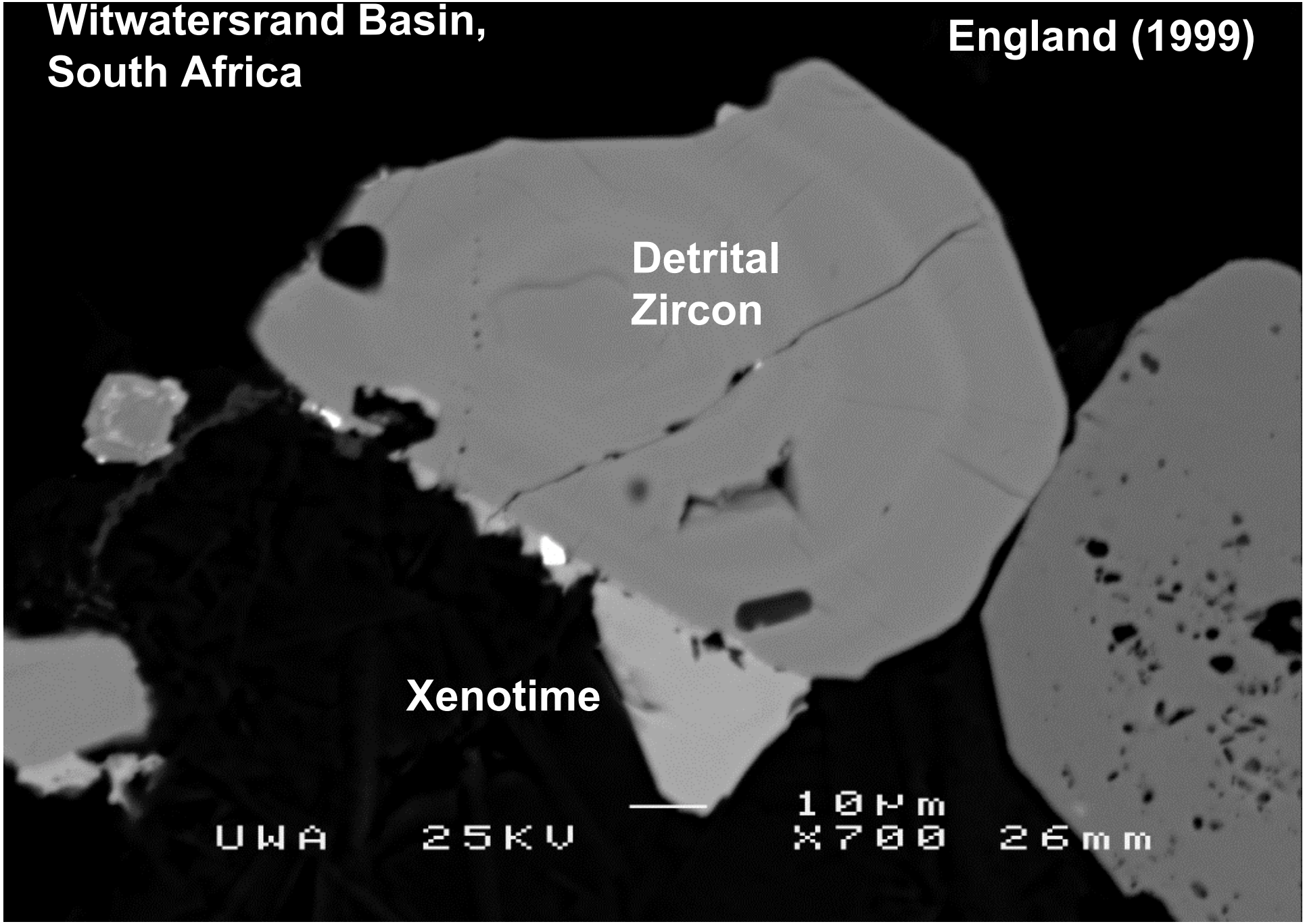
Witwatersrand Basin,
South Africa
England (1999)
Detrital
Zircon
Xenotime
10µm
UWA 25KV X700 26mm

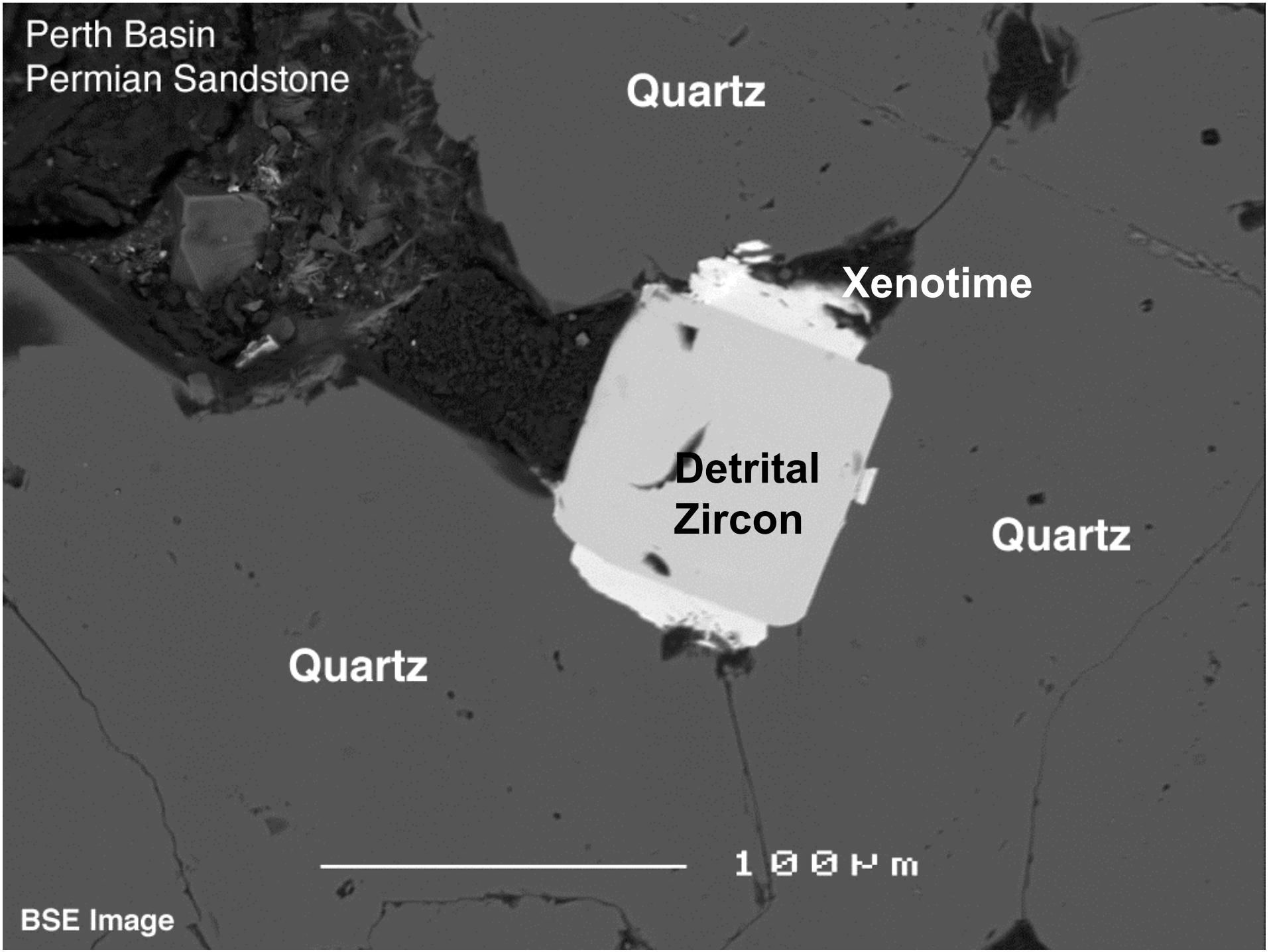
Perth Basin
Permian Sandstone
Quartz
Xenotime
Detrital
Zircon
Quartz
Quartz
100 µm
BSE Image

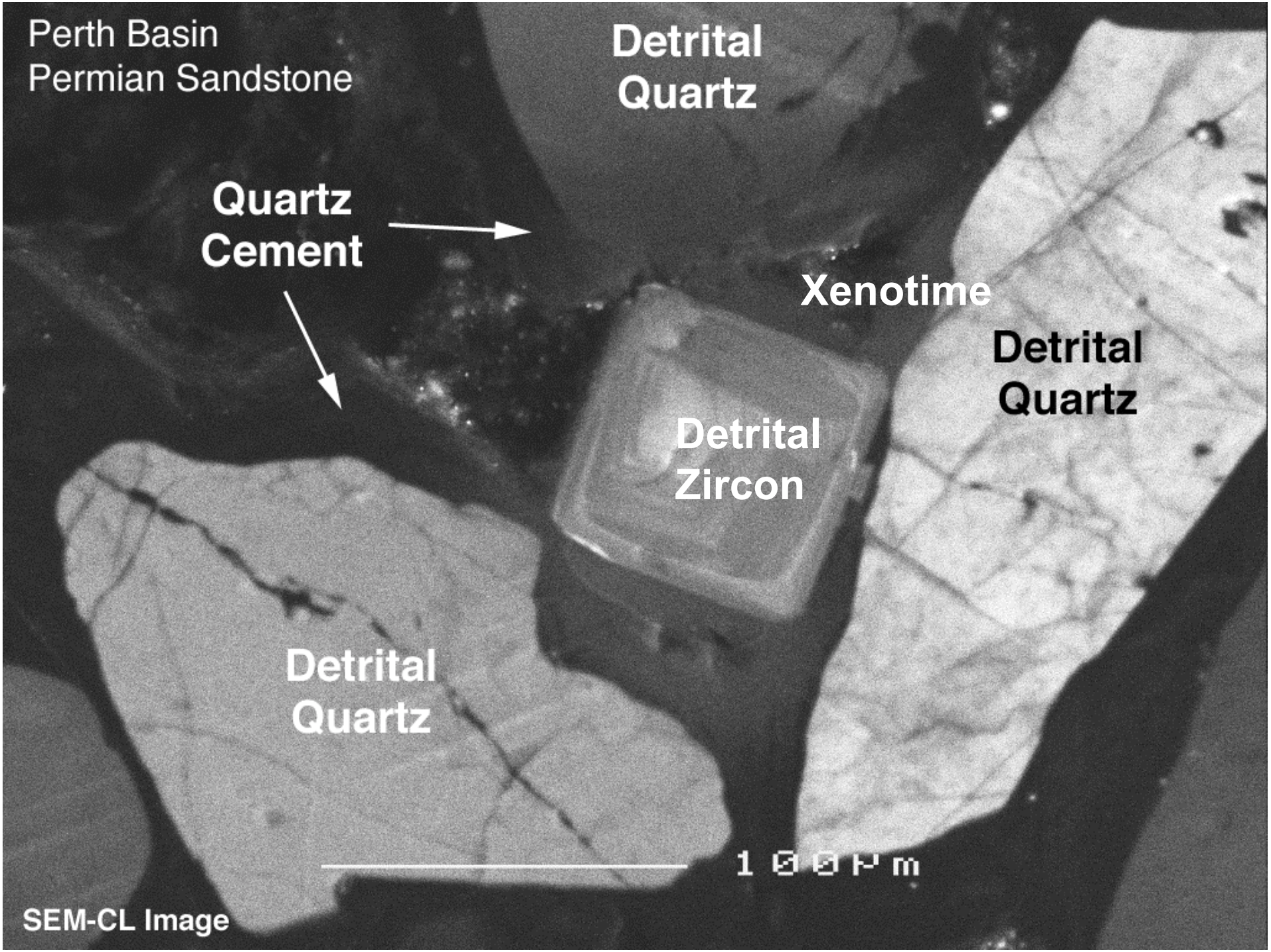
Perth Basin
Permian Sandstone
Detrital
Quartz
Quartz
Cement
Xenotime
Detrital
Quartz
Detrital
Zircon
Detrital
Quartz
100 µm
SEM-CL Image

What is Xenotime and when does it form?

- Xenotime - YPO_4.
- Xenotime forms during:
  - Early Diagenesis
  - Burial Diagenesis
  - Metamorphism
  - Alteration
  - Mineralisation

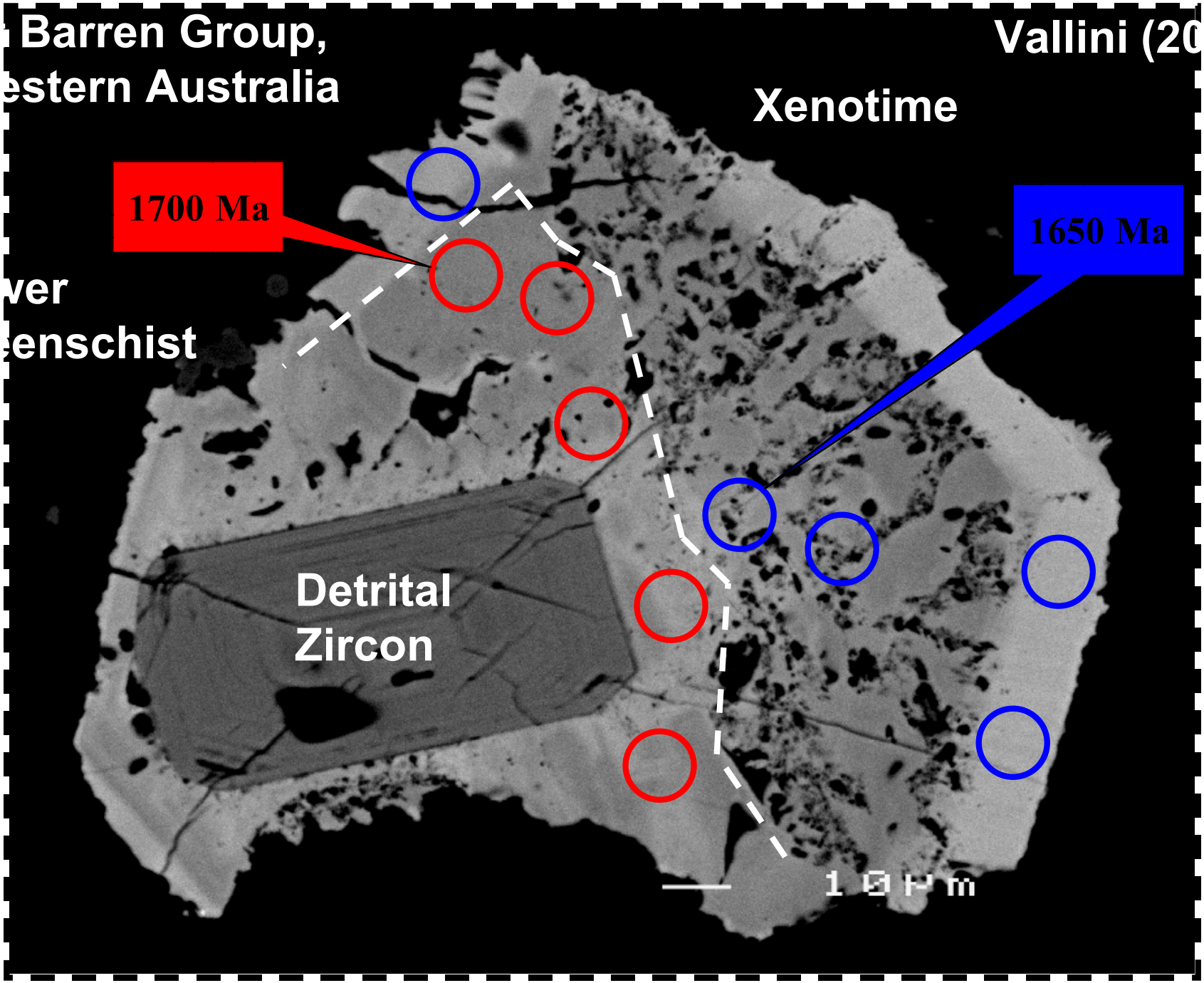
Barren Group,
estern Australia
Vallini (20
Xenotime
1700 Ma
1650 Ma
ver
enschist
Detrital
Zircon
10 µm

What is Xenotime and when does it form?

- Xenotime - YPO_4.
- Xenotime forms during:
  - Early Diagenesis
  - Burial Diagenesis
  - Metamorphism
  - Alteration
  - Mineralisation

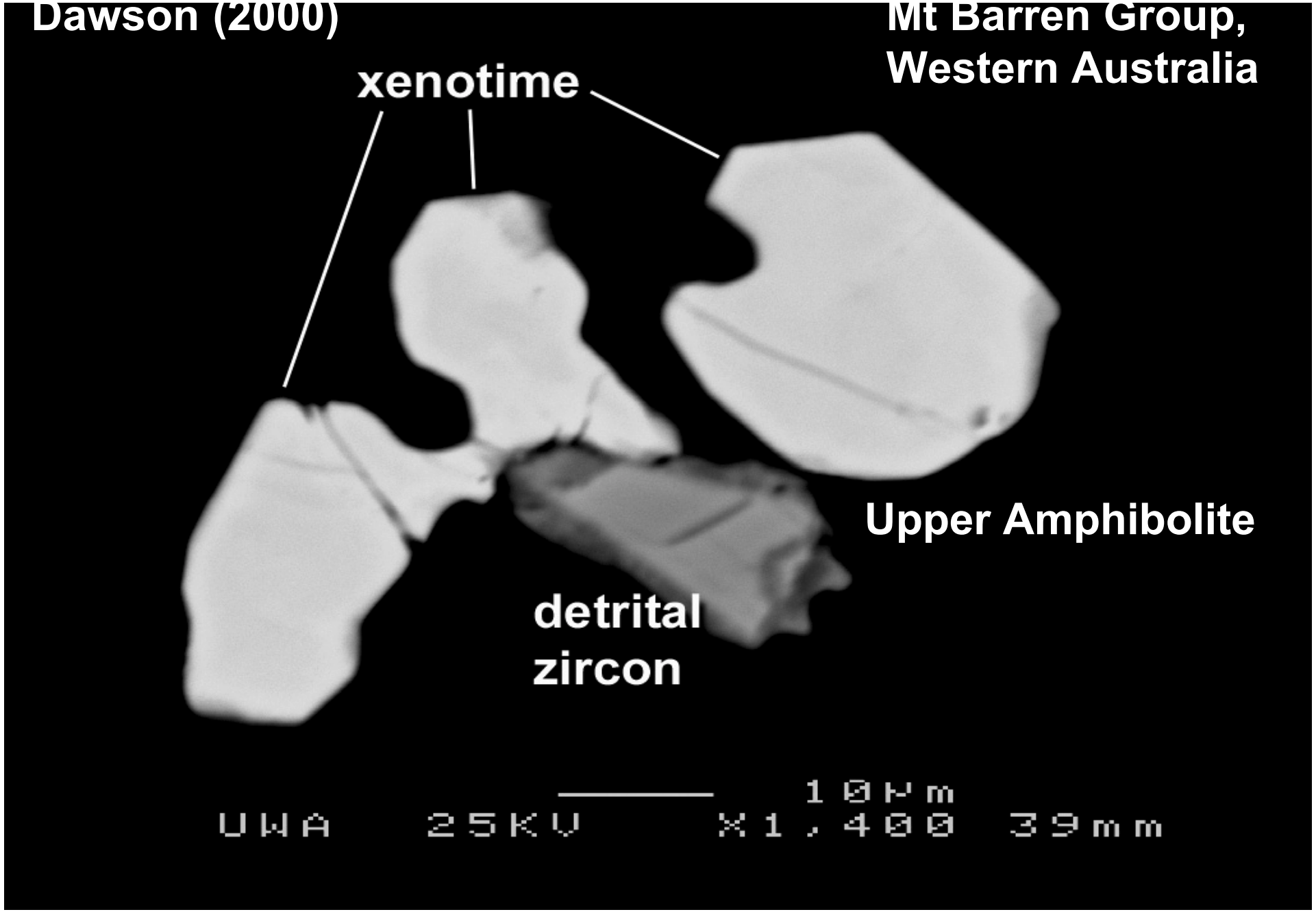
Dawson (2000)
Mt Barren Group,
Western Australia
xenotime
Upper Amphibolite
detrital
zircon
10µm
UWA 25KV X1,400 39mm

What is Xenotime and when does it form?

- Xenotime - YPO_4.
- Xenotime forms during:
  - Early Diagenesis
  - Burial Diagenesis
  - Metamorphism
  - Alteration
  - Mineralisation

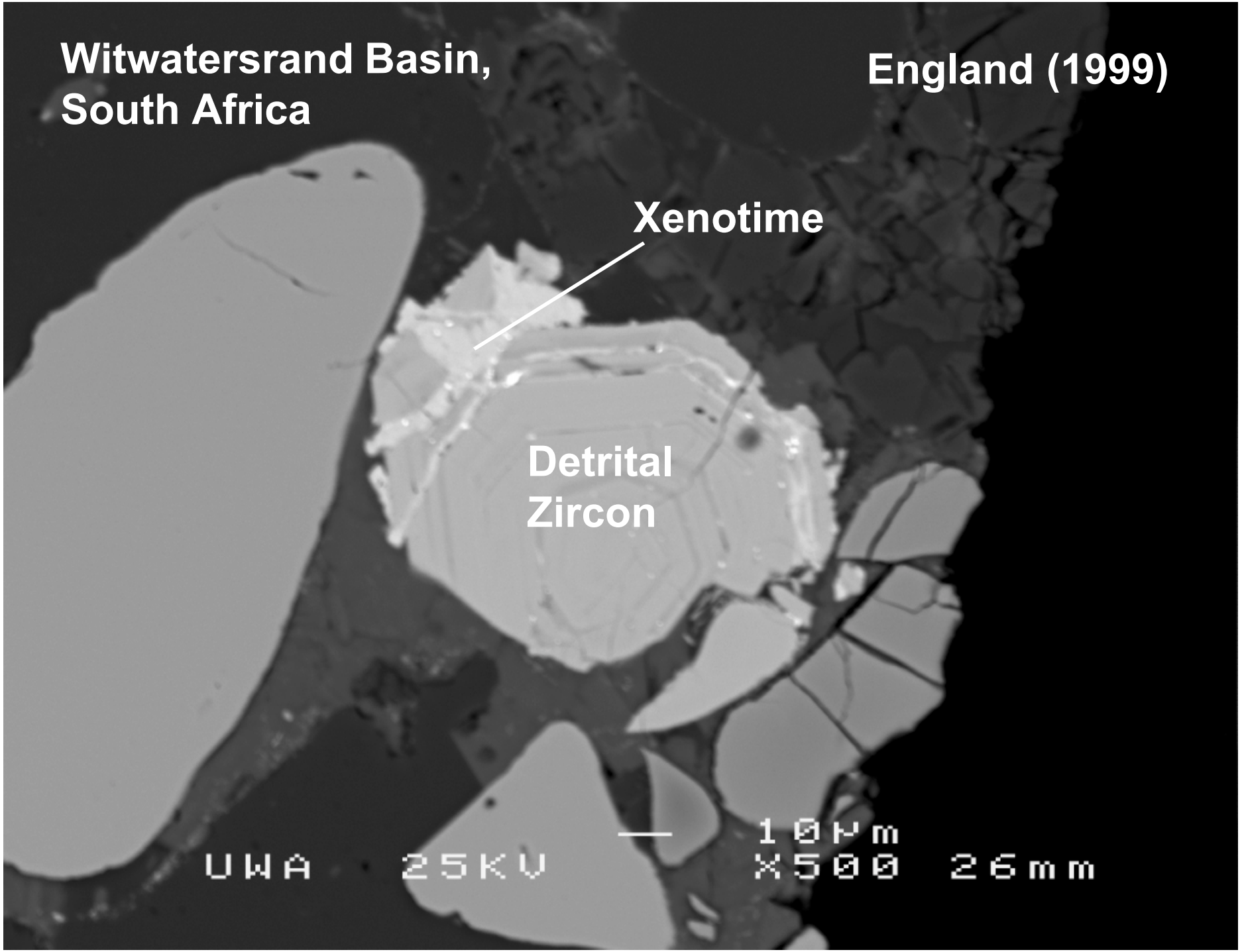
Witwatersrand Basin,
South Africa
England (1999)
Xenotime
Detrital
Zircon
UWA 25KV
10µm
X500 26mm

What is Xenotime and when does it form?

- Xenotime - YPO_4.
- Xenotime forms during:
  - Early Diagenesis
  - Burial Diagenesis
  - Metamorphism
  - Alteration
  - Mineralisation

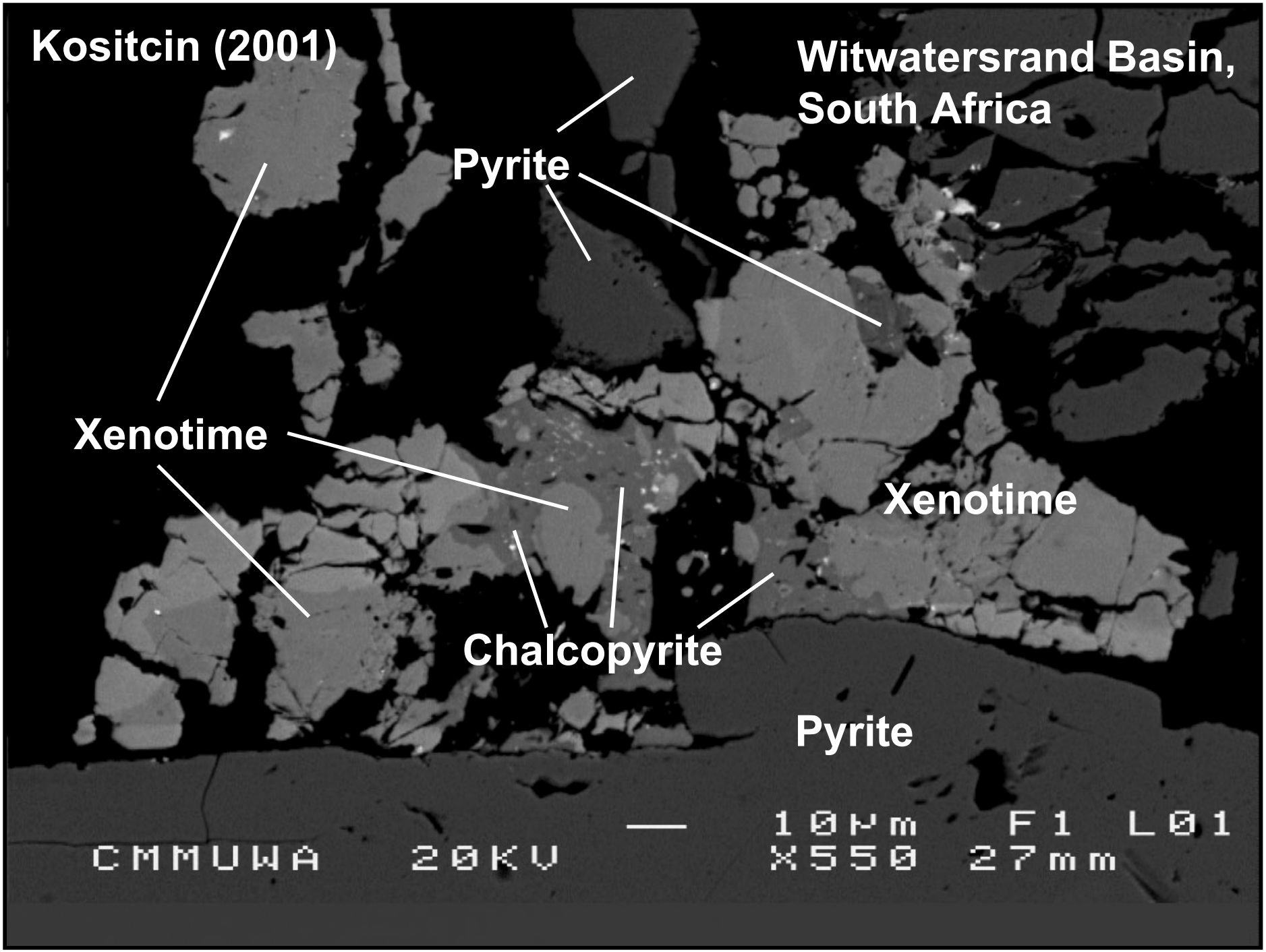
Kositcin (2001)
Witwatersrand Basin,
South Africa
Pyrite
Xenotime
Xenotime
Chalcopyrite
Pyrite
10µm F1 L01
CMMUWA 20KV X550 27mm

Applications:
Basin Evolution

- **Detrital zircons - Maximum age for sedimentation**
- **Authigenic Xenotime - Minimum age for sedimentation**
  - **A good approximation of the age of deposition**
- **Xenotime and Monazite - Metamorphism, alteration and/or mineralisation**

Applications: Chronostratigraphy

- Poor fossil record in Precambrian
- Dating methods for the Precambrian
  - Volcanics: U-Pb in zircons
    - May give poor constraints
- Diagenetic Geochronology
  - A new tool for Precambrian basin studies was developed at the University of Western Australia

SHRIMP Geochronology

- **SHRIMP - Sensitive high resolution ion microprobe**
  - **Best spatial resolution**
- **Xenotime is better than zircon!**
  - **Doesn’t become metamict like zircon**
  - **Higher U-content -> better age precision**

SHRIMP applications to the Zambian Copperbelt: PhD project outline

---

1. Chronostratigraphy: Xenotime

The age of the Katangan sequence is constrained between ca 870 Ma to ca 600 Ma

2. Other events: Xenotime and Monazite

Metamorphism and hydrothermal events

3. Sediment sources: Detrital zircons

Tectonic regimes

PhD study on the Zambian Copperbelt

“Temporal framework of the Zambian Copperbelt”

- Study funded through through the ARC Large Grant Scheme
- Research in AMIRA P544 will provide firm geological constraints to SHRIMP dating work
- Results to be reported in the first instance to AMIRA P544 sponsors and researchers
- Results will be more widely reported (at conferences and in scientific papers) after consultation with P544 sponsors

PhD Project: Sedimentology and structure of the Callanna Group, Willouran Ranges

Wallace Mackay
Centre for Ore Deposit Research, University of Tasmania

Aims of the Project

The project will study the Callanna Group sediments cropping out in the Willouran Range, with emphasis on the breccias and the evaporitic units within the Callanna Group. There are four major topics to be considered;

- the overall structure of the Callanna Group,
- the structure and origin of the breccias,
- that nature of the evaporites,
- the influence of the Callanna Group on the chemistry, timing and flow paths on basinal fluid flow.

Previous work within the Willouran Range has been either more regional in aspect (Burrell, 1977) or focussed on mineral exploration (e.g., Rowland et al., 1981) and has not attempted to develop a detailed understanding of the basin structure at the time of deposition of the Callanna Group and its subsequent structural evolution. The difficulty with understanding the basin structure at the time of deposition arises from the broken nature of the outcrop of the Callanna Group and particularly the brecciation of the presumed Arkaroola Sub-Group.

There has been much work on the breccias and particularly the diapirs within the Adelaide Fold Belt (e.g., Dyson, 1992, 1996; Lemon, 1988). Most of these studies have concentrated on the central Adelaidean Foldbelt, with little detailed study of the breccias in the Willouran Range. At present, three interpretations have been offered for the breccias in the Willouran Range; brecciation of basal Callanna Group along a decollement plane (Burrell, 1977), olistostromes developed by graben foundering (Rowlands et al, 1981) and diapir-related brecciation (Preiss, 1987). These three interpretations infer very different tectonic regimes at the time of brecciation and as such, it becomes important to the outcomes of this project to determine the causes of brecciation.

The nature of the evaporites has been discussed briefly in Preiss, 1987. Halite pseudomorphs are locally abundant (Preiss, 1987), quartz after gypsum has been noted by several authors (Burrell, 1977, Rowlands et al., 1981) and Rowlands et al (1981) have reported quartz and authigenic microcline pseudomorphs after shortite. As part of their exploration for sediment-hosted copper mineralisation, Utah Development Company conducted a sedimentological study and interpreted sabhka-facies sedimentation for at least part of the Curdimurka Sub-group and overlying Burra Group (Rowlands et al., 1981). The nature of the evaporites, and particularly their mineralogy is important when considering their role in fluid generation and the geochemistry of the fluids (see below). Sedimentological, mineralogical and geochemical studies will be used to determine the nature of the evaporites, their original mineralogy, depositional environment and their diagenetic history.

The influence of the Callanna Group on the chemistry, timing and fluid-paths of basinal fluids and their potential to play a role in mineralisation processes is the culmination of the study. If the

brecciation is related to diapirism and the dissolution of evaporite minerals, then evaporite salts will have a major control on the chemistry of basin fluids. The three possibilities for evaporite minerals identified above and their respective abundance's will influence the ability of basin fluids to dissolve, transport and finally deposit metals. The fluid pathways and when they develop will control the access of fluids to source areas for metals and sites suitable for the deposition of metals. Studies to be undertaken will include structural studies to determine the orientation of possible fluid pathways, and geochemical and mineralogical studies to determine the nature of the fluids.

Part of the study will examine mineralisation in the Willouran Range. The known mineralisation is insufficient to form a study in its own right, but it will provide insights to the movement of metals (copper and gold) and the geochemistry of the mineralising fluids.

Methods

Aerial photography interpretation, structural mapping and closed spaced sedimentary logging of key areas will be the basis for initial part in this study.

Laboratory work will involve detailed petrographic work on evaporitic facies with a view to characterising the varieties of evaporite pseudomorphs, and identifying the original minerals.

Petrography will be important for deciphering the nature of the carbonate breccia units.

Later, chemical modelling of basin waters and coeval brines will be used to develop an understanding of (possible) Cu mobilisation early in the history of the northern Adelaide Geosyncline.

Previous Work

Open File Reporting

In terms of work completed and reporting, previous exploration in the Willouran Range is dominated by the work of Utah Exploration in the period 1977 - 1983. Although there has been exploration for Cu since the work of Utah, their work and their reporting is fundamental to work in the Willouran Range. Their mapping and interpretation of their mapping considered the sedimentological setting of the Callanna Group and Burra Groups in particular, as a test for the model of mineralisation they were applying to the area (Sediment-hosted copper mineralisation, within sediments deposited in a sabhka environment, based on the Zambian Copperbelt). While the Utah open file reports do not provide all the data they generated, they do interpret the results of their mapping and drilling in terms of facies analysis and rudimentary sequence stratigraphy. The use local names for stratigraphy in separate project areas has resulted in confusion in correlating work from one area to the next.

M.I.M remapped an area between Mirra Creek in the west and Breaden Hill in the east. The writer of the MIM report considered that "Utah's work was marred by poor geological mapping and the apparent disbelief in faulting or tectonic brecciation" (M.I.M. report, 1992). They also drilled three diamond core holes adjacent to Utah RC drill holes which had intersected mineralisation, and 12 RC holes. The highest grade reported in the diamond core was 1.02% Cu over six metres in dolomitic siltstone of the Tapley Hill Formation. Cross-sections of the drill holes provide some structural information. M.I.M. do provide further interpretative information on some structural aspects in the area in which they explored, particularly with regard to faulting and thrusting.

The work of other companies is still being examined. Much of the geochemical data is of limited use because of its age; limited geochemical suites were used and the assay methods used had high detection limits relative to today, but it will provide information on the extent of mineralisation.

Published Literature

There is an large body of work on the Adelaide Foldbelt as a whole, but the published material on the Willouran Range is limited. The majority of work

on the Willouran Range has been published in PIRSA (and its many past guises) publications (Bulletins, Quarterly Geological Notes, Reports of Investigations, Explanatory Notes, the MESA Journal). There have been few papers written in the general literature (e.g., Rowlands et al., 1981).

Theses

There have been a large number of theses completed on the Adelaide Fold Belt at the University of Adelaide. Two PhD theses in particular are thought to be relevant, Paul (1997) and Murrell, (1977). Paul looks primarily at what may affect deformation, including geothermal effects and thickness of sediments and is more relevant to the AMIRA project as a whole. Murrell's thesis was based on a traverse from Andamooka to Marree and therefore covers the area of interest for this project. A number of other PhD theses study aspects of regional geology, or a particular stratigraphic level, but these were not examined in detail. They may become more relevant as the project progresses.

Murrell's thesis is being copied at the moment. Two conclusions to note at this point are: the mapping of basement in the Euromina Window and the interpretation of the breccias within the Willouran Range. The interpretation of there being a basement inlier within the Willouran Range is based on the presence of an essexite intrusion (n.b. essexite is an alkaline gabbro, associated with continental basic magmatism) and an albitite with the contact with the surrounding breccia interpreted to be an unconformity. This interpretation is in part based upon the interpretation of the breccias. Murrell notes that the breccias retain a semblance of layering comparable with the Arkaroola Sub-group, with a basal arenite, a dolomitic unit (the Black Knob Marble) and a volcanic unit (the Noranda Basalt). Murrell considers the breccias to represent a decollement beneath the Curdimurka Sub-group. He also considers there to have been a deformation before deposition of the Burra Group, although whether it was related to compression or extension is not clear at this stage. Both the interpretation of the breccias and the essexite and albitite are questioned by Wolfgang Preiss. A more detailed critique will be prepared when the thesis arrives.

The major areas of mineralisation discussed are those around the Mt Painter Inlier, mainly copper but also lead and zinc, and lead - zinc mineralisation in Cambrian sediments. Mineralisation in or adjacent to diapers is also discussed.

Theses pertaining to mineralisation near Mt Painter are: Buckhorn, 1973; Eberhard, 1973; Docking, 1975; Mayer, 1976; Godsmark, 1993. Other theses discussing the Adelaidean sediments around Mt Painter are: Ashton, 1973; Ambrose, 1973.

Theses discussing mineralisation related to diapers are: McKay, 1968; Hall, 1984.

Theses discussing lead - zinc mineralisation in Cambrian sediments are: Glover, 1968; Mayer, 1976.

One honours thesis, sponsored by Utah Development Company was completed on the Willouran Range; Heathersay, 1979.

A number of other Honours theses on themes more relevant to regional geology and geochemistry were read but are not listed here.

Work to date

This has been limited to a literature search of open file data from exploration within the project area, published material and unpublished theses and a two week field visit to the western part of the area.

Three traverses were completed across the Stony Range; one toward the southern end near Bend Hut, and two about a kilometre either side of the Mulgaria-Witchelina track. The traverses were designed to assess the Norwest Fault and the Curdimurka Sub Group.

The traverses showed that the basal Curdimurka Sub-group in this area is a highly silicified quartz arenite with minor siltstone, shale and carbonate units. Cross-beds are common within the arenite and it is likely that they were originally feldspathic, the feldspars now replaced by quartz or kaolin, depending on the degree of silicification. There are indications that the shale was originally a black, pyritic siltstone, it having weathered to a white kaolinite.

The Norwest Fault does not outcrop but it is interpreted by a change in facing between the arenite of the Curdimurka Sub-group and the overlying arenite of the basal Burra Group. Intense silicification of the Curdimurka Sub-group sediments adjacent to the Norwest Fault suggest that it has been a major conduit for fluid flow.

Future Work

Over the next six months, the intention is to;

- complete the review of published literature and theses on the Willouran Range,
- complete a review of literature on evaporites,
- undertake a field trip to the Willouran Range is planned for September and October to determine the areas for more detailed mapping and to begin the detailed mapping,
- visit sites of mineralisation in the Willouran Range to determine the feasibility of conducting more detailed studies on the mineralisation in the field during year 2 of the project,
- continue the examination of open file data with the intention of identifying diamond core drill holes held by PIRSA, which may be used for more detailed studies in year 2.

South Australia

Progress Report & Forward Program

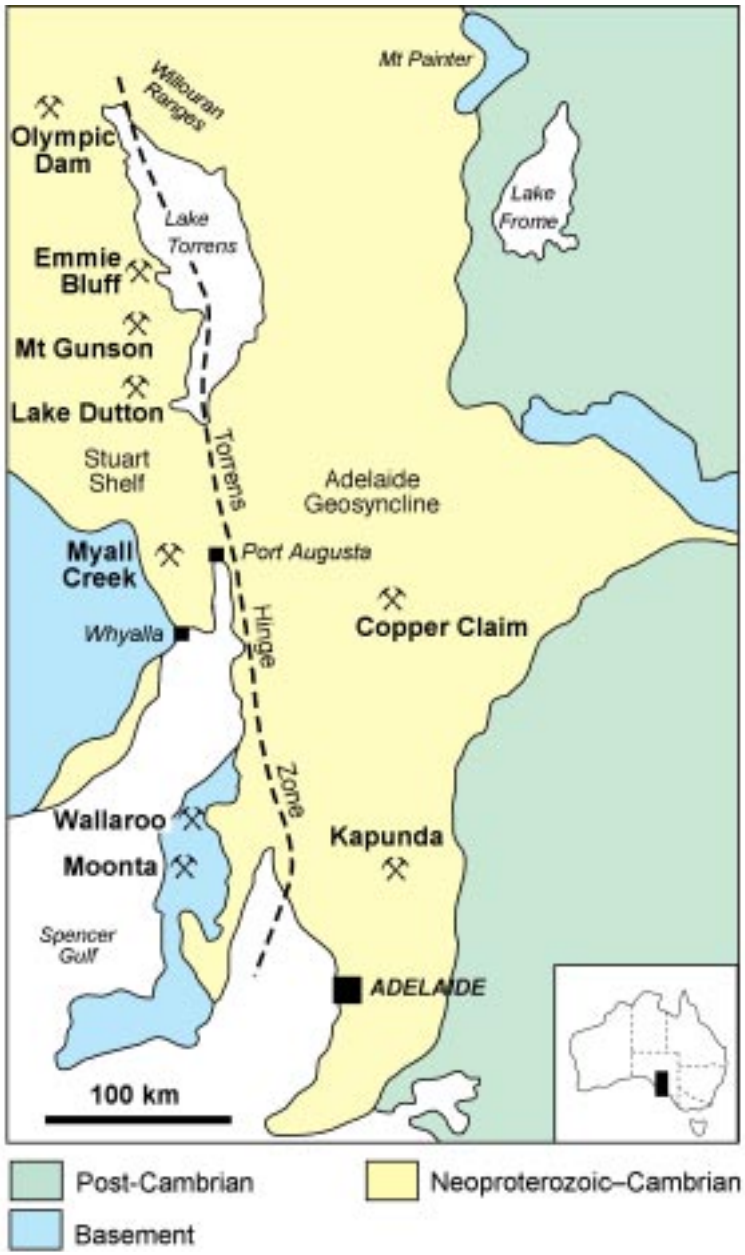

Cu Distribution

- **Cu coincides partly with margins of sub-basins and platformal shoulders**

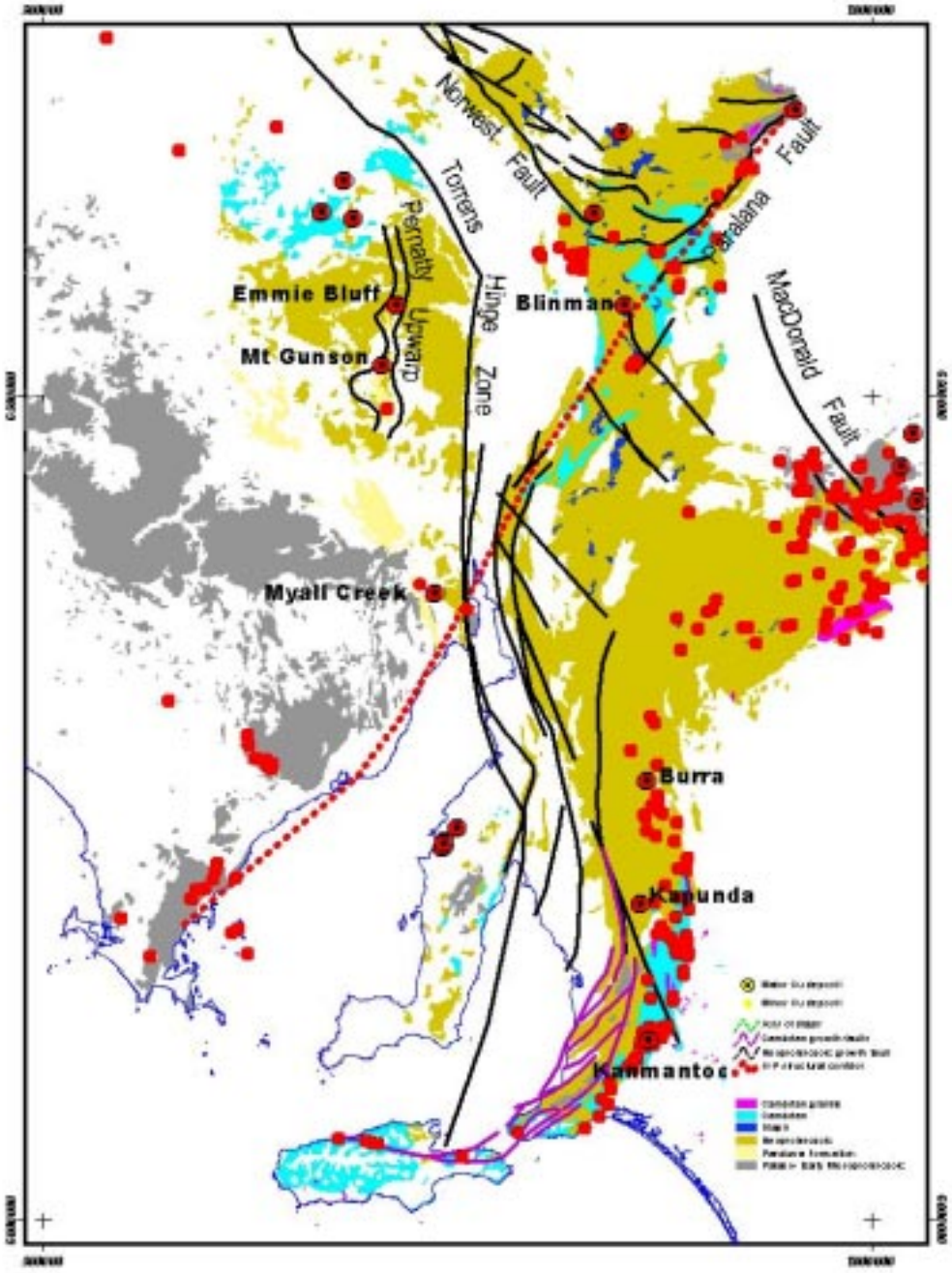

Size and Grade

- Mt Gunson: 5.6 Mt @ 2.1% Cu
- Emmie Bluff: 24 Mt @ 1.3% Cu
- Myall Creek: up to 1.5% Cu

Stratigraphic controls on Cu

- Unconformable contact of the Pandurra Sandstone and Whyalla sandstone
- permeable horizons within the Tapley Hill Formation
  - main mineralised zone at the unconformable base
  - minor mineralisation at the top

Mineralisation

Sandstone-hosted deposits

- Cu sulphides occupy secondary porosity in brecciated upper surface of Pandurra
- Ore mineral paragenesis:
  - Fe-oxides → pyrite → Cu sulphides
- sphalerite and galena represent final mineral products in the ore paragenesis
- no evidence of hydrothermal alteration

Mineralisation (con)

Tapley Hill Formation Cu

- permeable sandstone/silt beds or lamellae
- vein hosted mineralisation in less permeable strata
- Fe and Ti are depleted in mineralised zones
- strong correlation of Corganic, Fe and S
- base metal sulphide introduced late

South Australian Research Framework

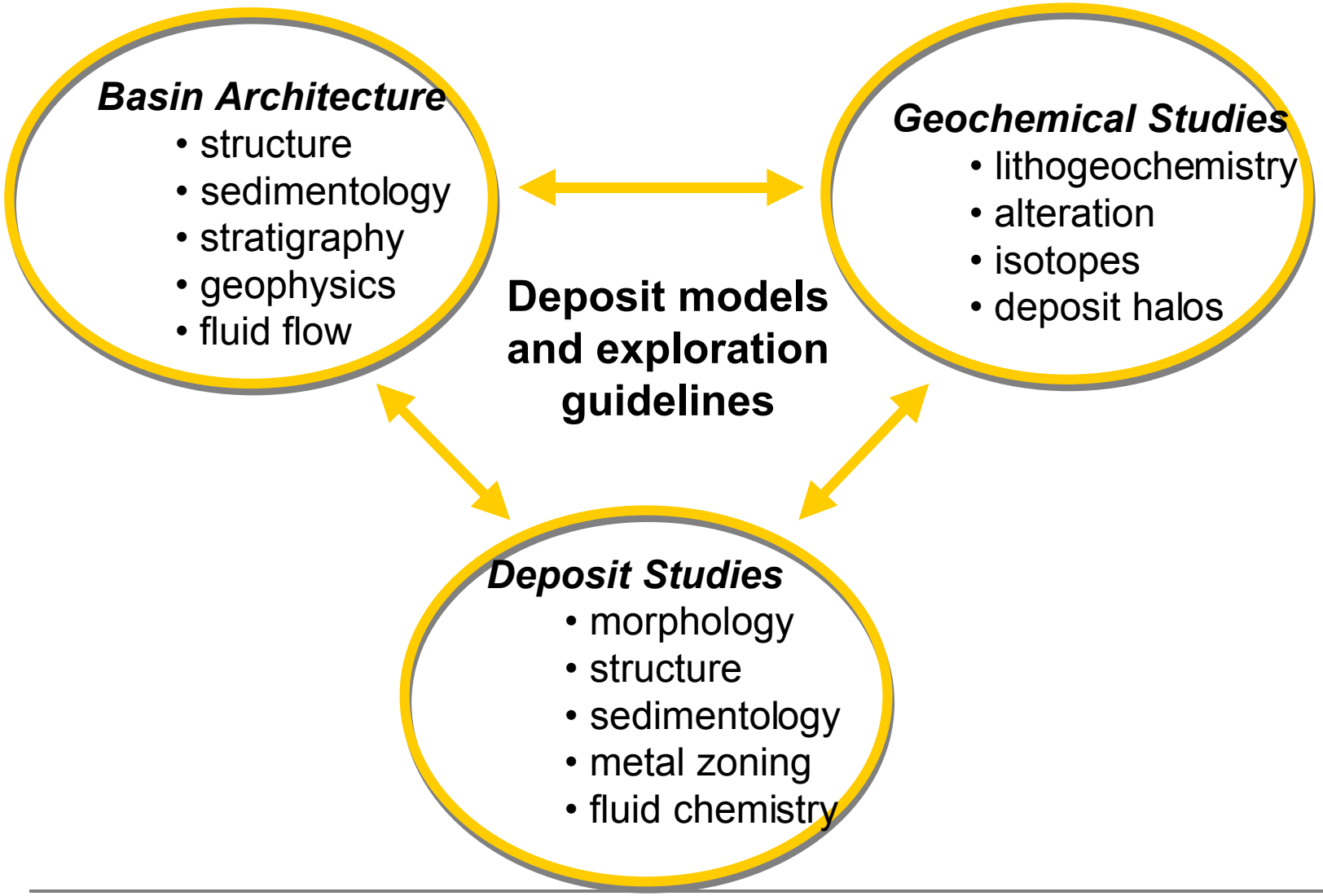

- ‘basin analysis’ builds on existing high quality geological and geophysical databases
  - focus on key areas or stratigraphic levels
  - structural transects
- lithogeochemical and Pb isotope studies of Stuart Shelf Cu deposits
- fluid flow and fluid chemical modelling

Deposit Studies Module

- Review of the Stuart Shelf Cu deposits
- Investigate the relationship between siltstone- and ironstone-hosted Cu at Emmie Bluff

Basin Architecture Module

- Tectono-sedimentary setting of Neoprot sed-hosted Cu deposits
- Sedimentology and structure of the Callanna Group
- Sedimentological and structural studies of basin re-organisation during the interglacial to Marinoan interval (~600Ma)

Geochemical Studies Module

- Chalcophile element chemistry of Tapley Hill Formation siltstones at Emmie Bluff
- Mineralising fluids for Stuart Shelf Cu deposits (chemical modelling)

Progress to date

- Data review and compilation (incl. space-time chart) completed - Selley, 2000 (December Meeting CD)
- Wallace Mackay (Callanna Group PhD) commenced field work in April (draught PhD proposal included here)
- SB & WM commenced transect of the Torrens Hinge Zone - Northwest Fault area, NW Flinders Ranges
- PMcG re-sampled four mineralised Emmie Bluff drill cores for geochemistry and Pb isotopes in April (134 samples)

Table 2 Saline minerals characteristic of evaporites precipitated from the three major brine types

Brine composition and its source or sources	Principal characteristic saline minerals[a]	Key indicator minerals
I. Na-K-CO_3-Cl-SO_4 *Nonmarine waters* (mainly meteoric)	Alkaline earth carbonates, mirabilite, thenardite, trona, natron, thermonatrite,	Na_2CO_3 minerals
	polyhalite, bloedite, kainite, halite, sylvite, carnallite, bischofite	
III. Na-K-Mg-Ca-Cl *Hydrothermal and basinal brines*	Alkaline earth carbonates, gypsum, anhydrite, halite, sylvite,	$KCl \pm CaCl_2$ minerals in the absence of Na_2SO_4 and $MgSO_4$ minerals

Abundant trona/shortite and little or no gypsum/anhydrite in the Callanna Groupwould imply a non-marine setting, and the potential for unusual basin waters compositions

Abundant gypsum/anhydrite pseudomorphs in the Callana Group would imply normal marine conditions

from Hardie, 1991, Ann Revs Earth & Planet Sciences

Paterson Orogen

- Late Proterozoic
  Tarcunyah Group
- Neoproterozoic
  Yeneena Supergroup
  - Throssell Group
  - Lamil Group
- Palaeoproterozoic
  Rudall Complex

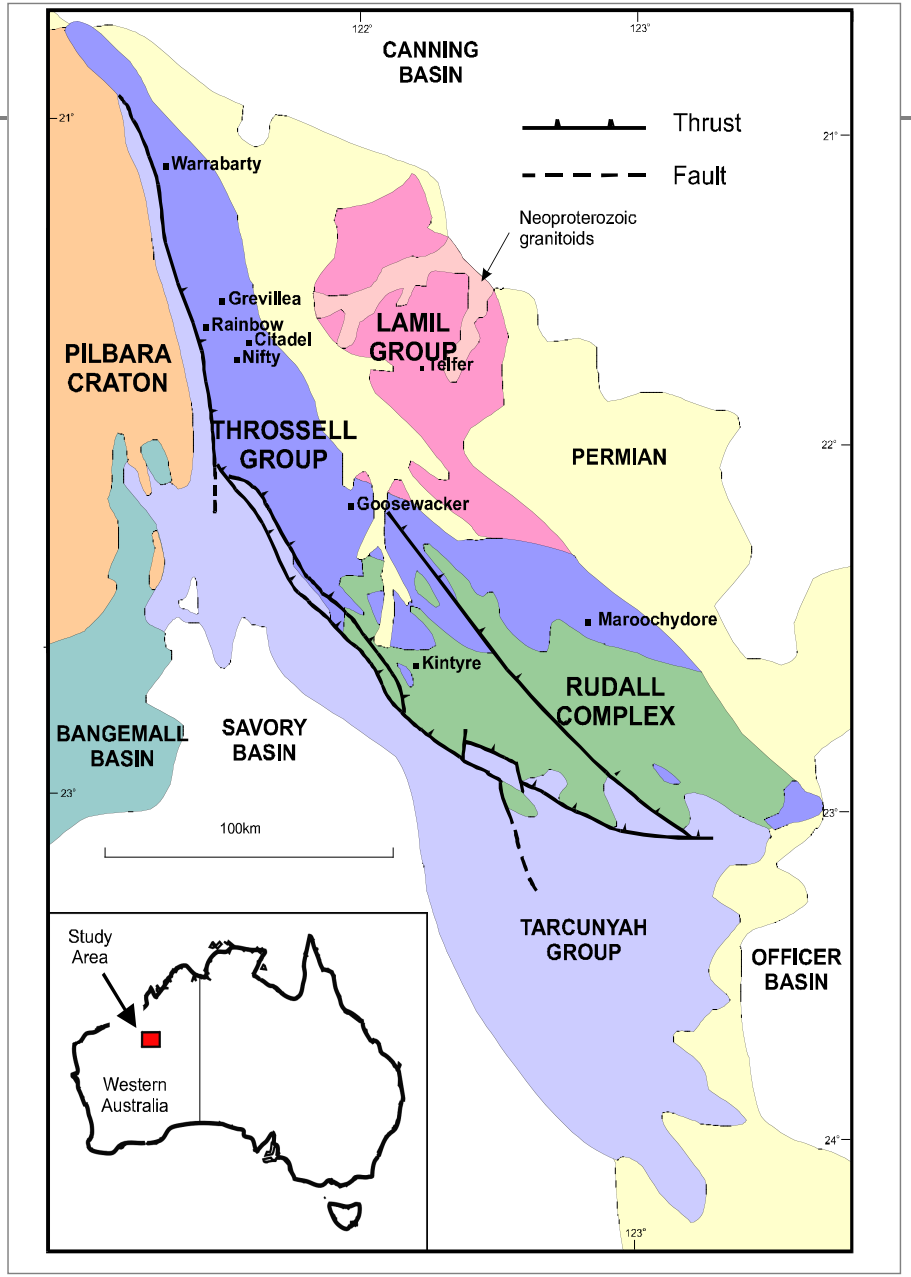

Paterson Orogen

- Tarcunyah Group
- Lamil Group
  - Wilki Quartzite
  - Puntapunta Formation
  - Telfer Formation
  - Malu Quartzite
  - Isdell Formation
- Throssell Group
  - Broadhurst Formation
  - Coolbro sandstone
- Rudall Complex

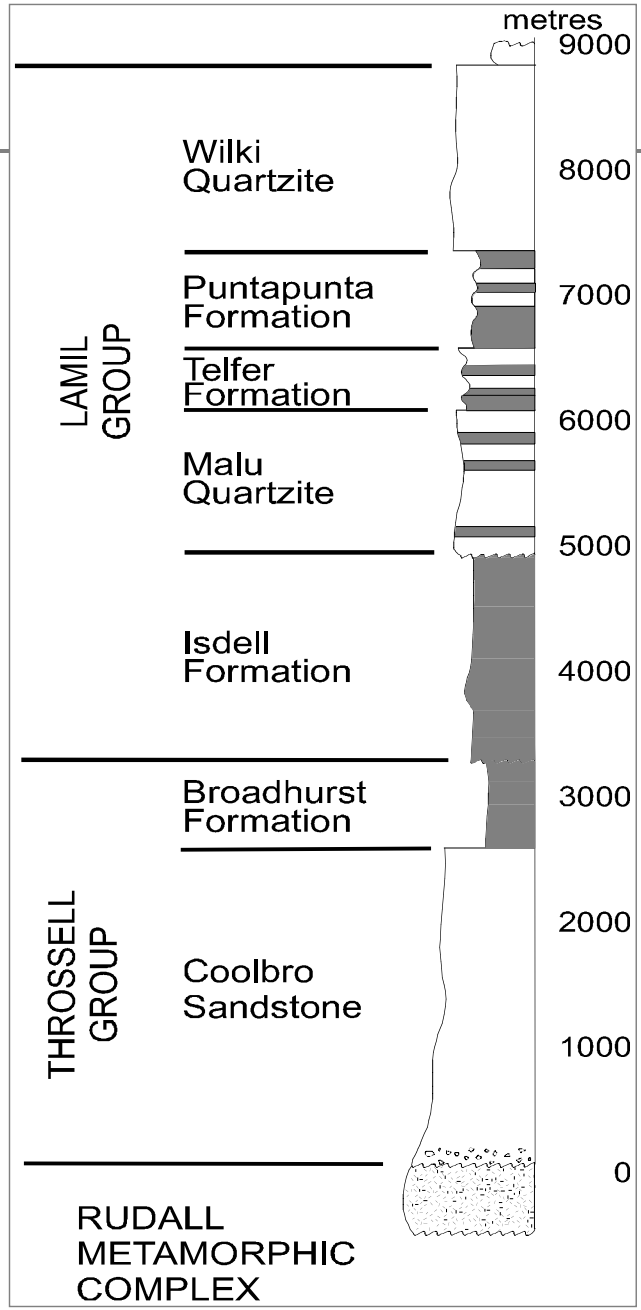

Throssell Group

- **Broadhurst Formation**
  - **1000-2000 m carbonaceous shale, siltstone, dolomite, and dolomitic shale**
- **Coolbro Sandstone**
  - **1000-4000 m cross bedded sst with interbedded shale and siltstone**

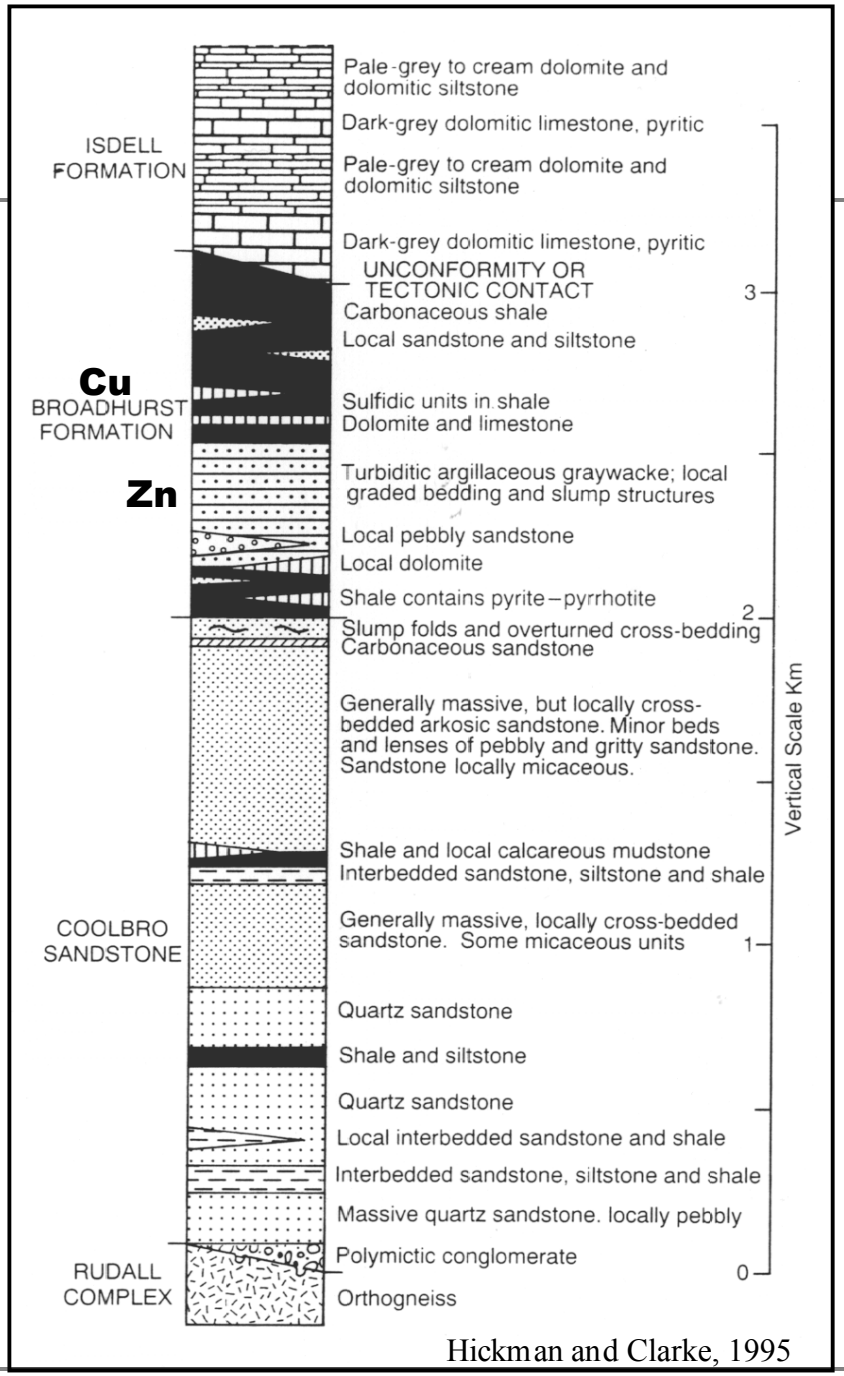

Hickman and Clarke, 1995

Structural data from drill core

Robert Scott and Ron Berry

CODES/School of Earth Sciences
University of Tasmania

UNIVERSITY
OF TASMANIA

Structural data from drill core

The usefulness of structures observed in drill core is often limited by uncertainties regarding their true orientation.

Unless drill core is oriented prior to being broken from the bottom of the drill hole, rotation about the core axis during extraction generally prevents unique determination of the orientations of any structural elements contained within it.

Core rotation

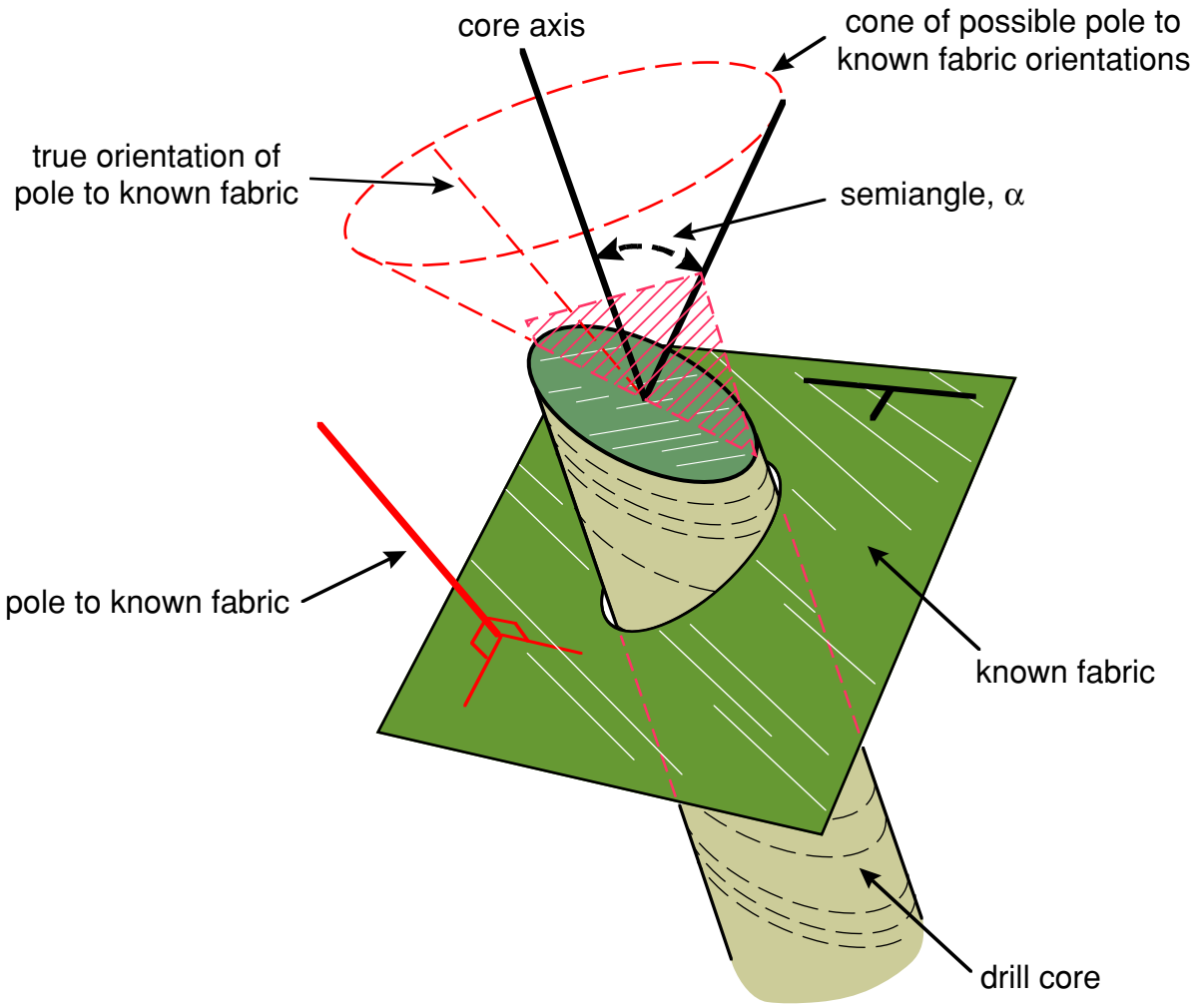

Alignment of orientation marks

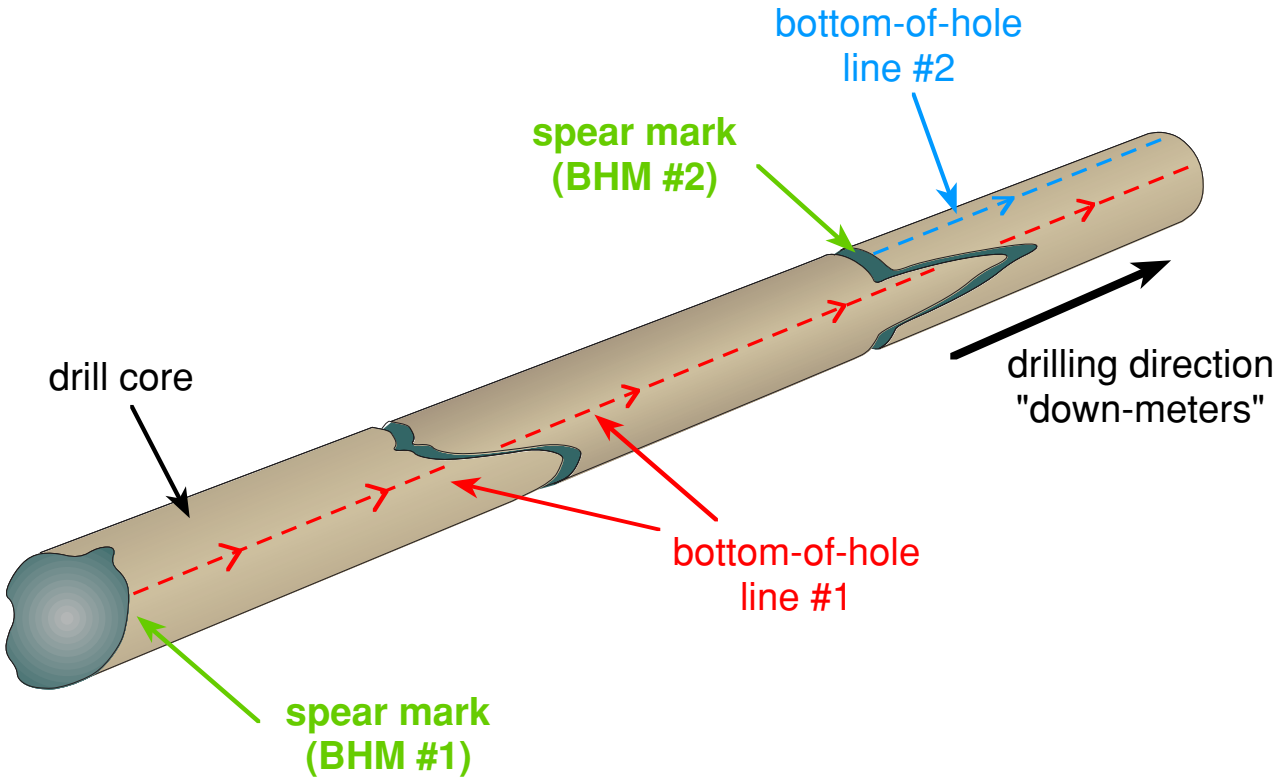

mismatches between bottom-of-hole lines from successive spear tests indicate the technique is unreliable in some situations

Methods of core orientation

- Reorientation based on the known orientation of one (or more) fabrics within the core
  - If a fabric (plane or lineation) in core is consistently oriented, and its attitude is approximately known from external constraints, it can be used to re-orient the core so that the orientation of other fabric elements can be determined

Re-orienting axially-oriented core

- The “best fit” position of the core can be determined in one of two ways:
  - Using the assumed strike of a “known” plane (or trend of a lineation)
  - Minimising the angular discordance (ε) between the known fabric in core and its reference orientation, during rotation of the core about its axis.

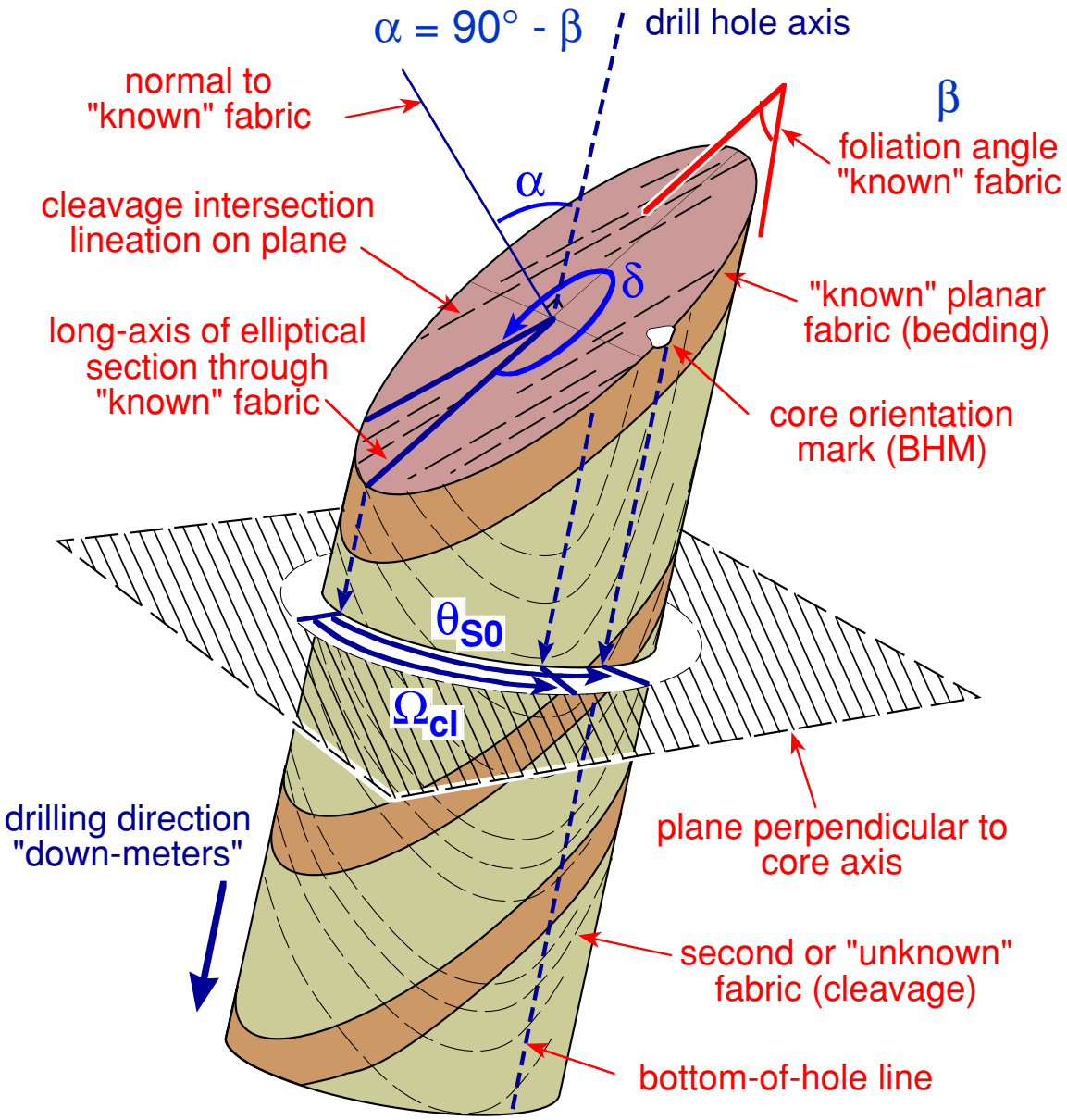

Conventions for measuring fabric angles in core

Measurement of angles in core:

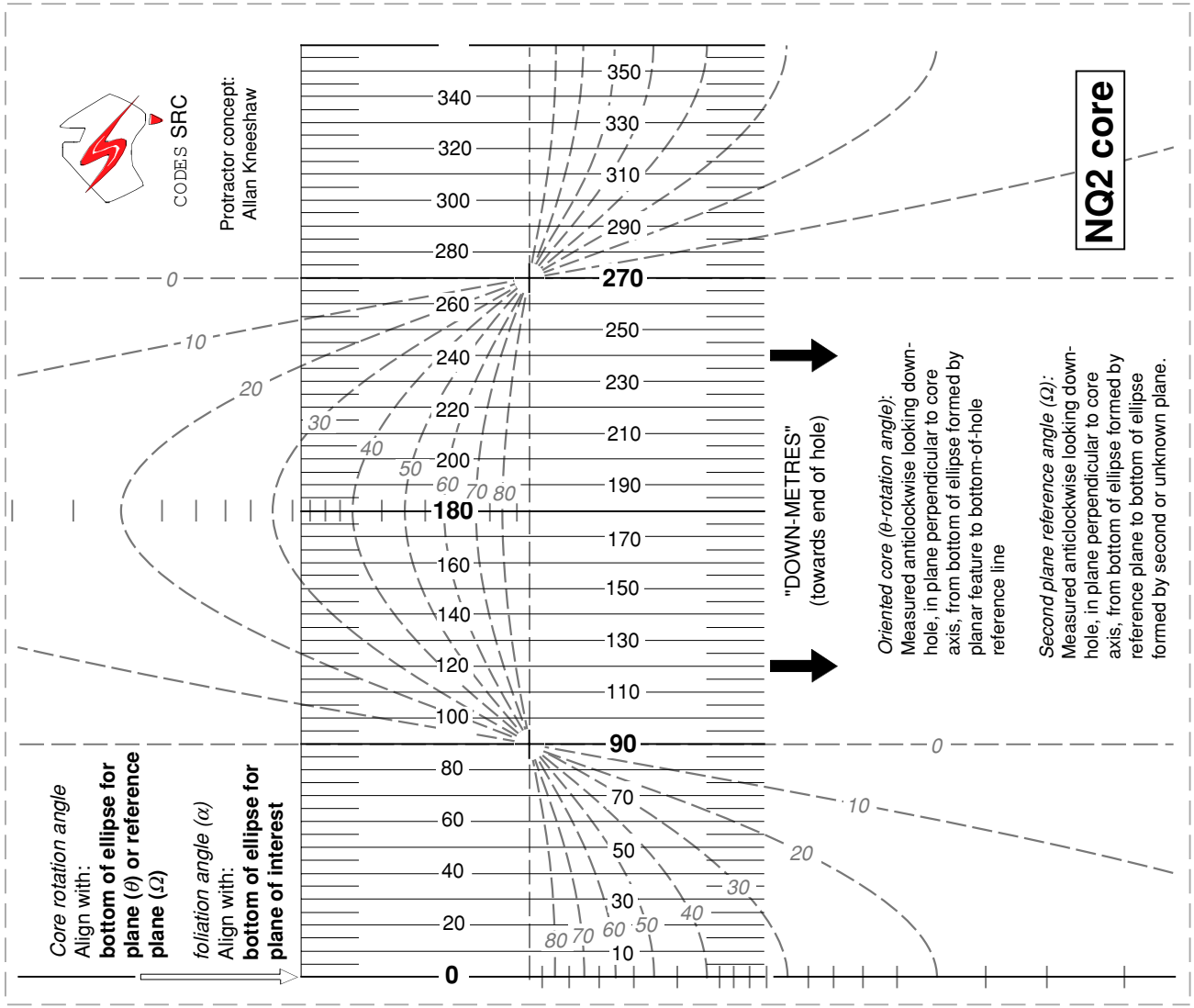

Differences between orientation methods

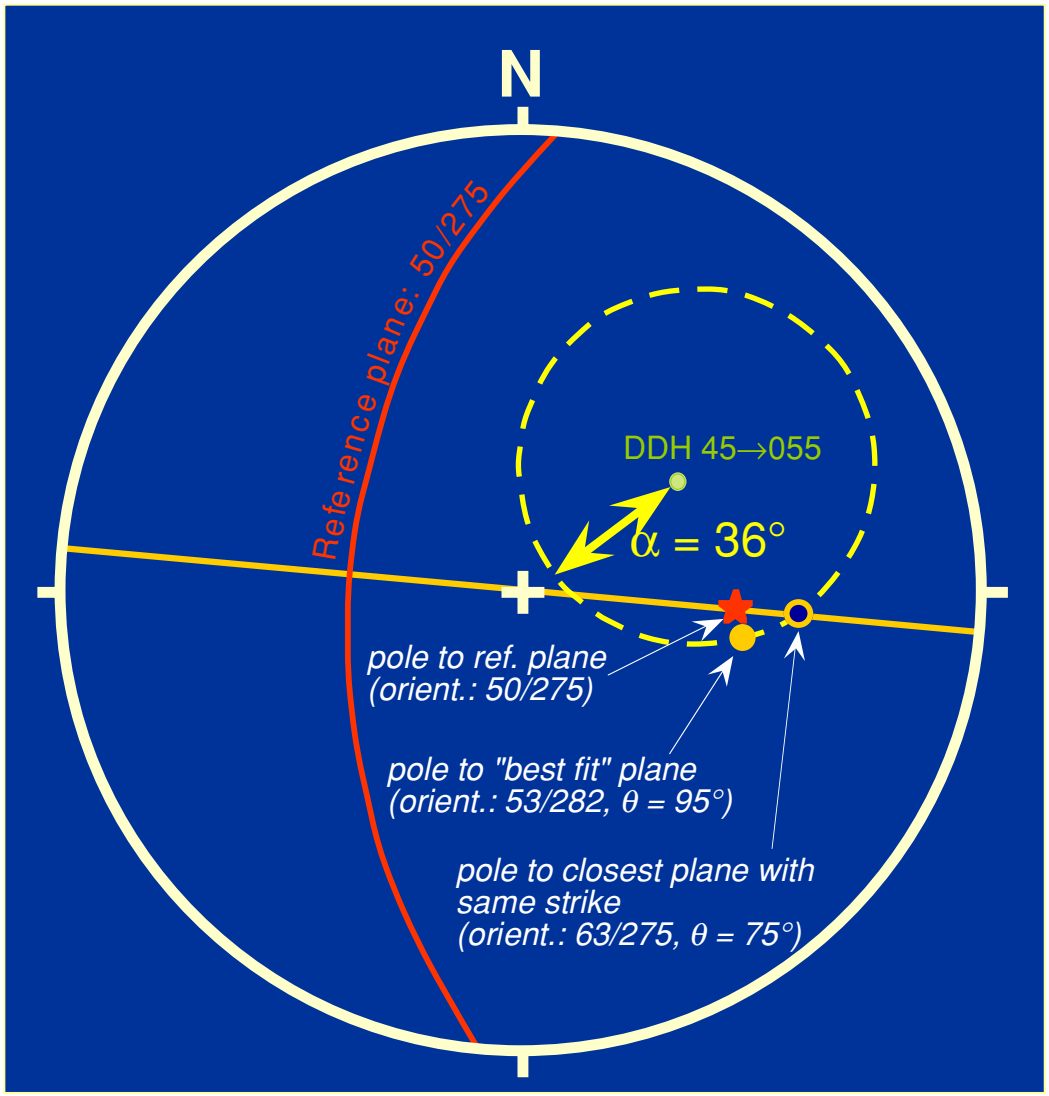

For the situation depicted, the “best fit” positions of core differ by 20° (rotation about core axis) depending on whether the fixed strike or min-ε method is used to re-orient the core.

The calculated orientation of any other fabrics would differ by an amount corresponding to a 20° rotation about the core axis.

Method matching the reference orientation (1)

- Fixed strike (or dip direction)
  - (on stereonet) “best fit” solutions for the known fabric lie along a radial line perpendicular to reference strike
  - “best fit” position of core (i.e. rotation about its axis, measured by θ) depends on the foliation angle for the known fabric in core
  - unique solution only if small circle of possible orientations (radius α_c) is tangent to the plane perpendicular to strike
  - generally two solutions (radius $\alpha > \alpha_c$), but no solution if (radius $\alpha < \alpha_c$)

“Best fit” orientation of core based on the attitude of a known fabric

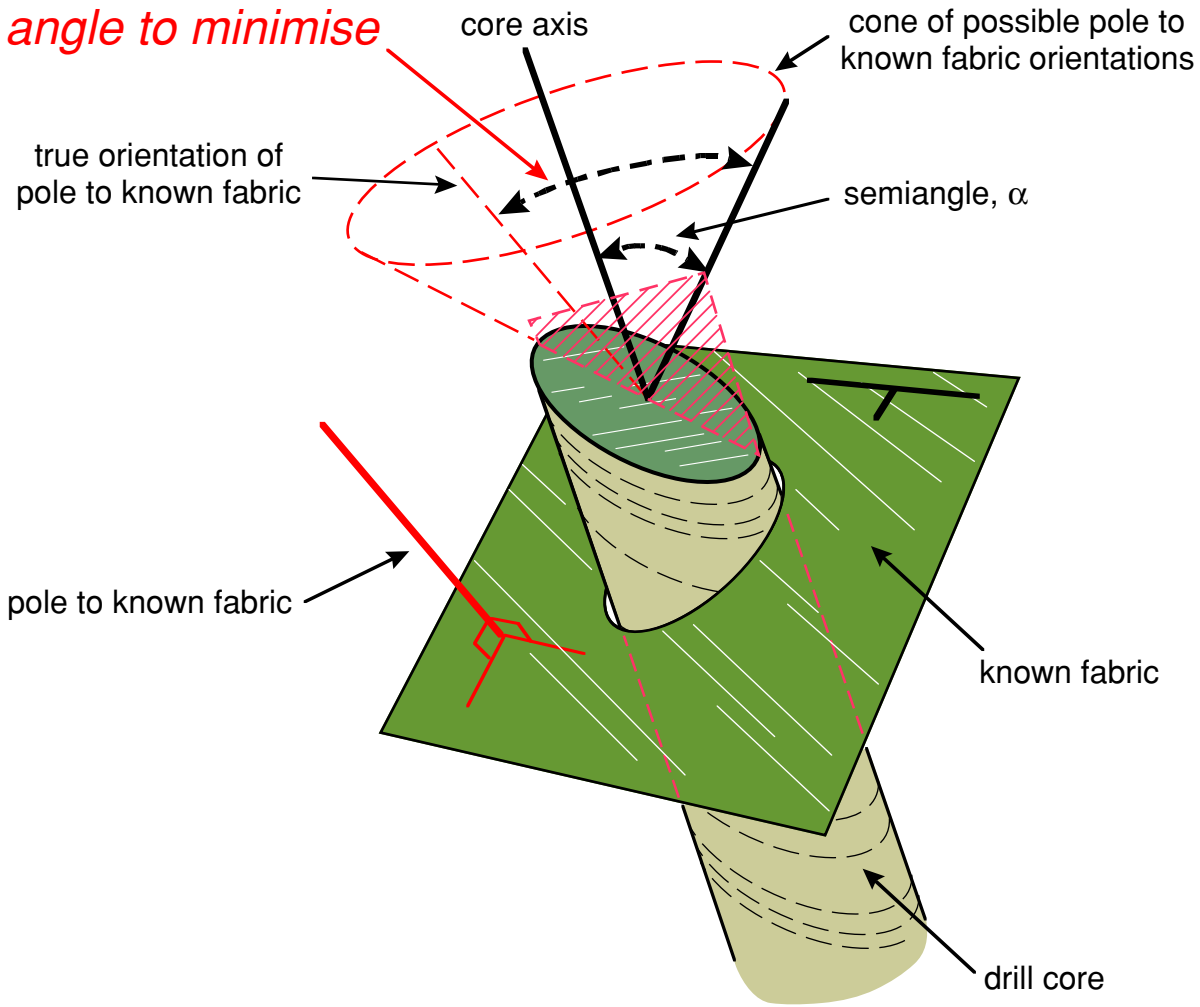

Method of matching the reference orientation (2)

- Minimum discordance (ε) between "known" fabric and reference orientation
  - (on stereonet) "best fit" solutions for the known fabric lie along a plane passing through the drill hole and the reference orientation
  - "best fit" position of core (i.e. rotation about its axis, measured by θ) independent of the foliation angle for the known fabric in core
  - generally unique solution, but two solutions as $\beta \rightarrow 0°$, no solution if $\beta = 90°$

Structural calculator: core orientation program

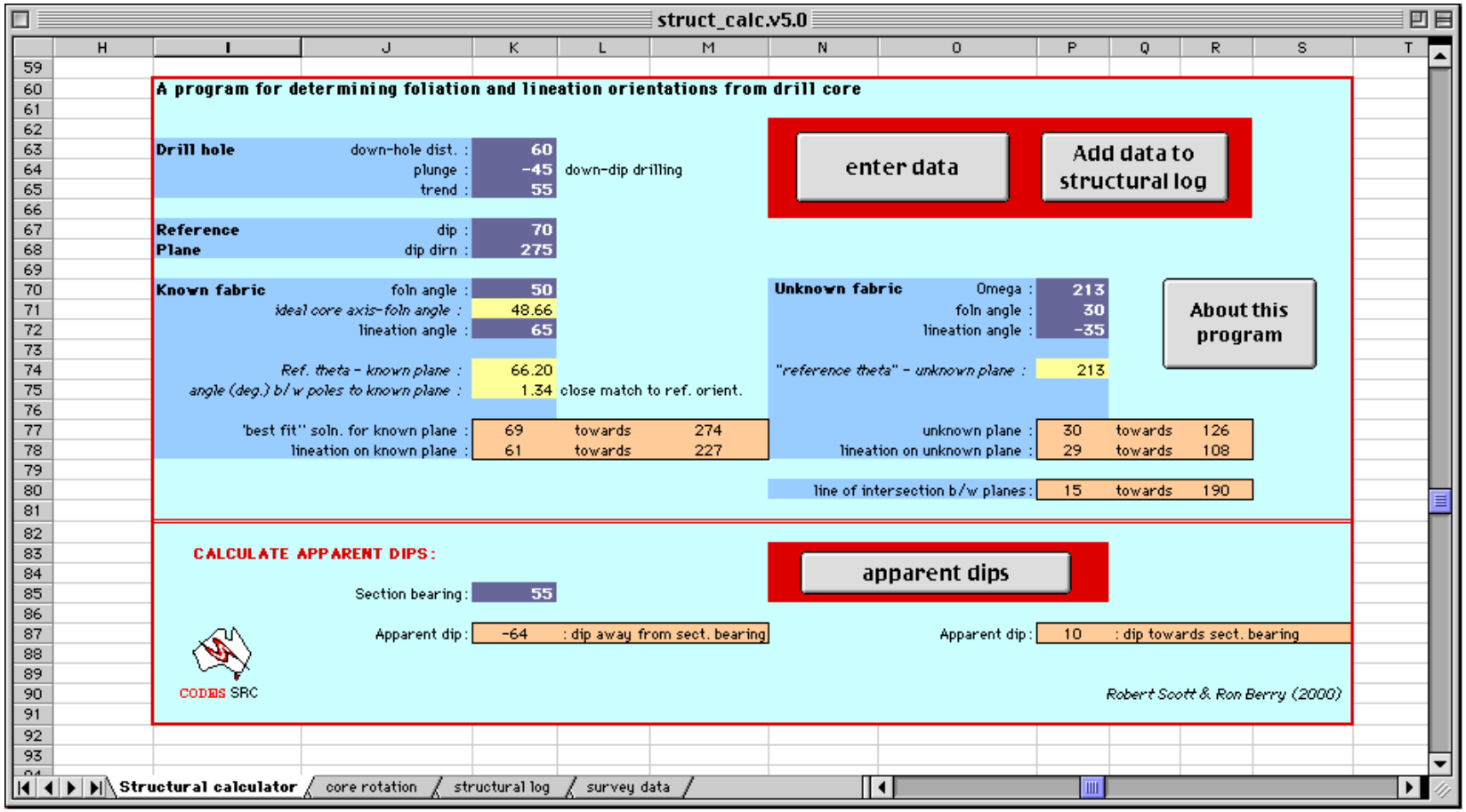

Stores down-hole survey data used to calculate plunge and trend of the drill hole

Stores structural data from the sheet "Structural calculator", entered using the "Add data to structural log" button

Illustrates angular discordance between a fabric in core and its reference orientation, during rotation of core about its axis

User interface of program

Reliability of re-orientation techniques

- Re-orientation methods rely on knowledge of an entity (orientation of a reference fabric) that can never be exactly known at every point down hole
  - accordingly we need to know how much variability in the orientation of the reference fabric is allowable, before the methods yield unreliable (meaningless) results
- How do other factors effect reliability?
  - uncertainties in measurements from core
  - orientation of fabrics with respect to the drill core, etc
- How do the two methods compare?

Scatter in reference fabric orientation

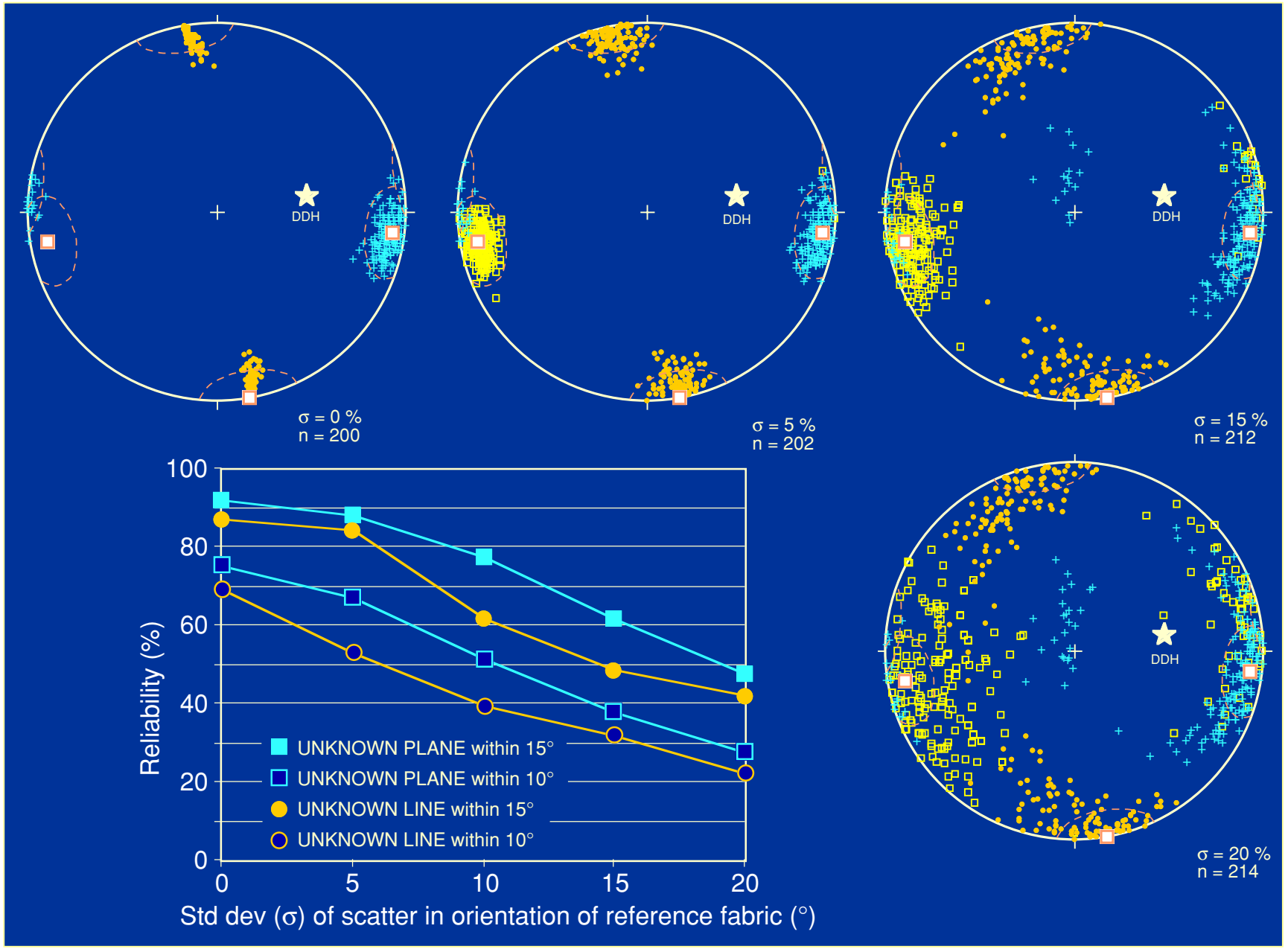

Variation in foliation angle for reference fabric

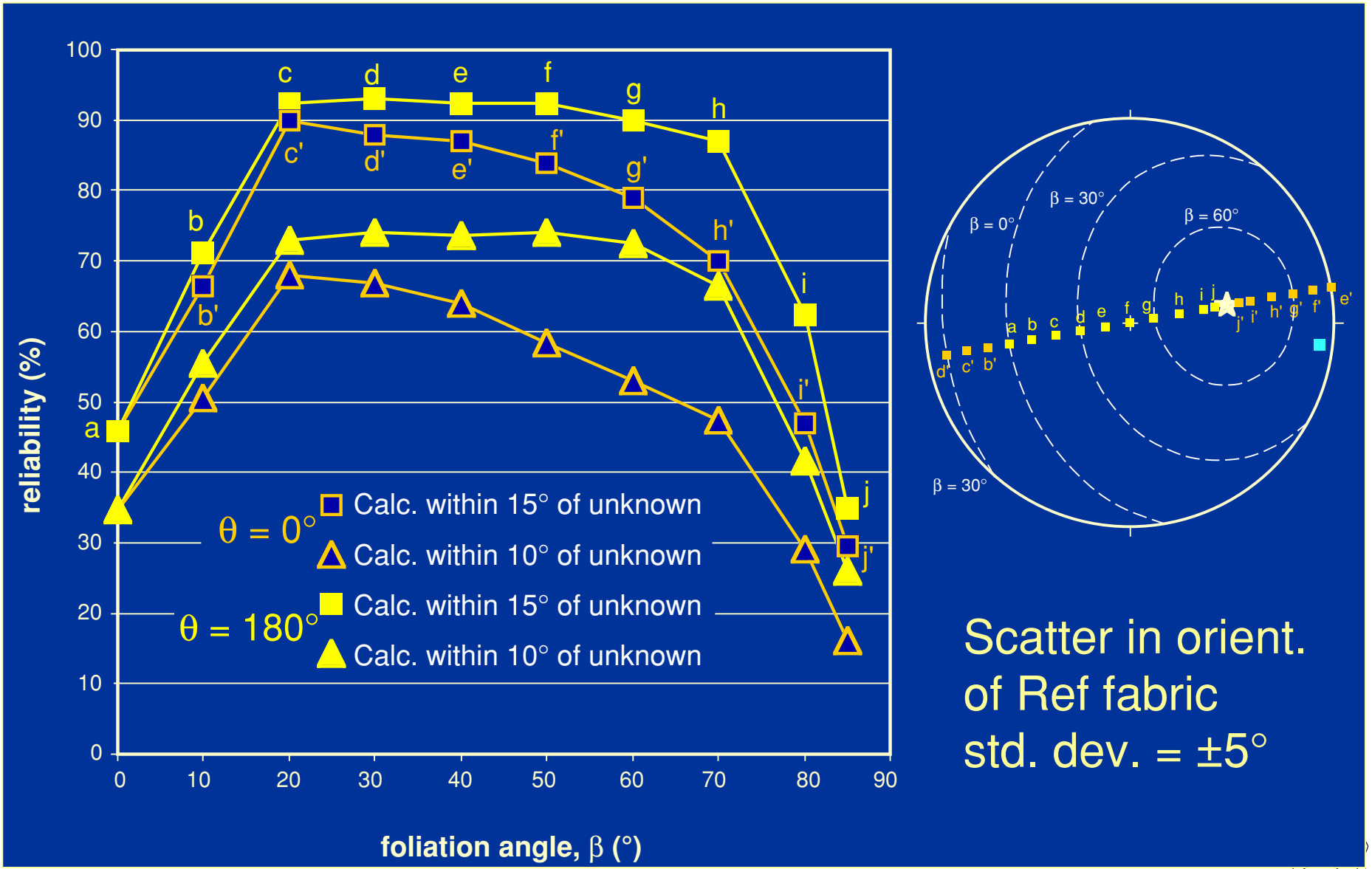

Influence of reference fabric foliation angle on solution

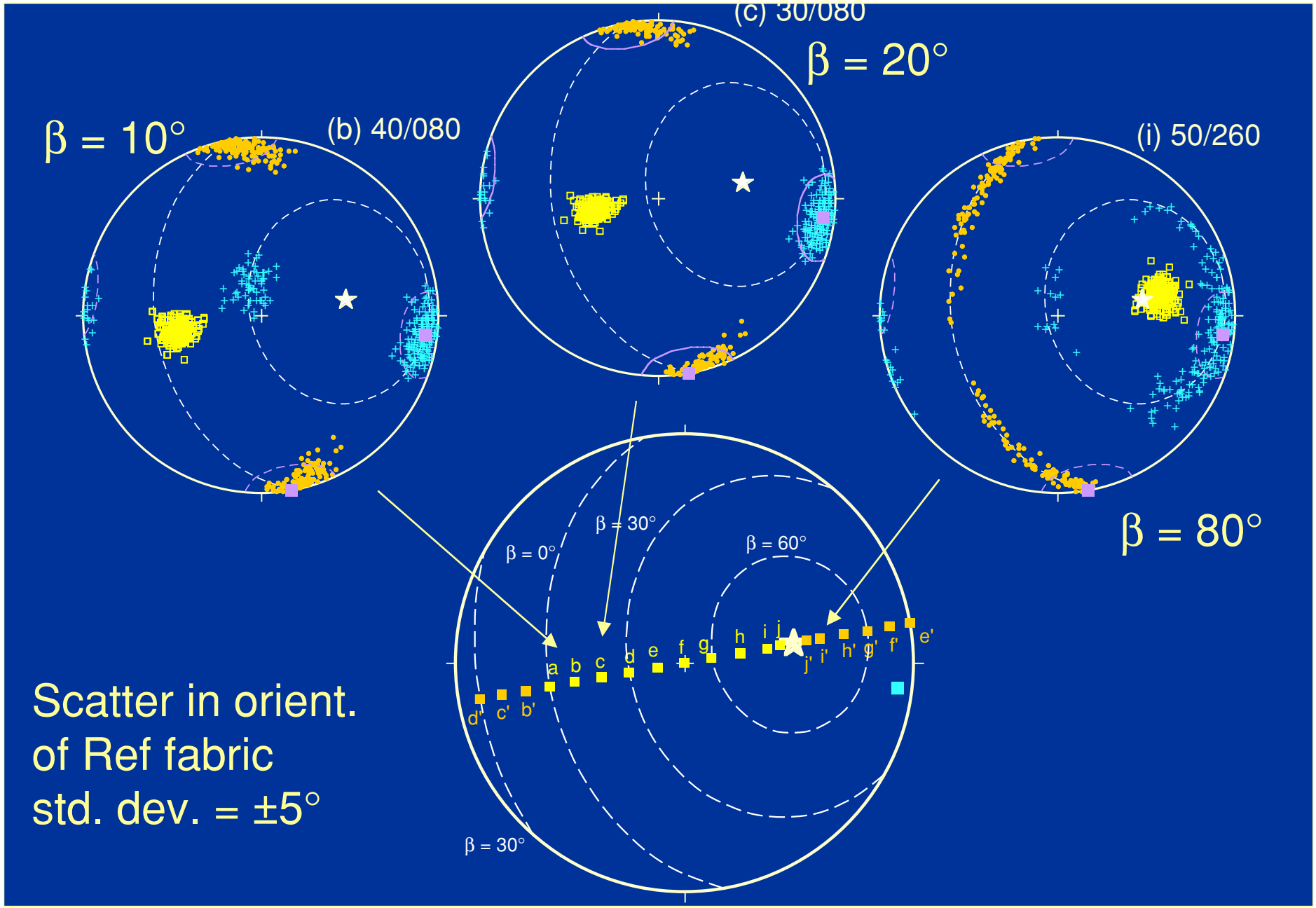

Variation in orientation of reference fabric

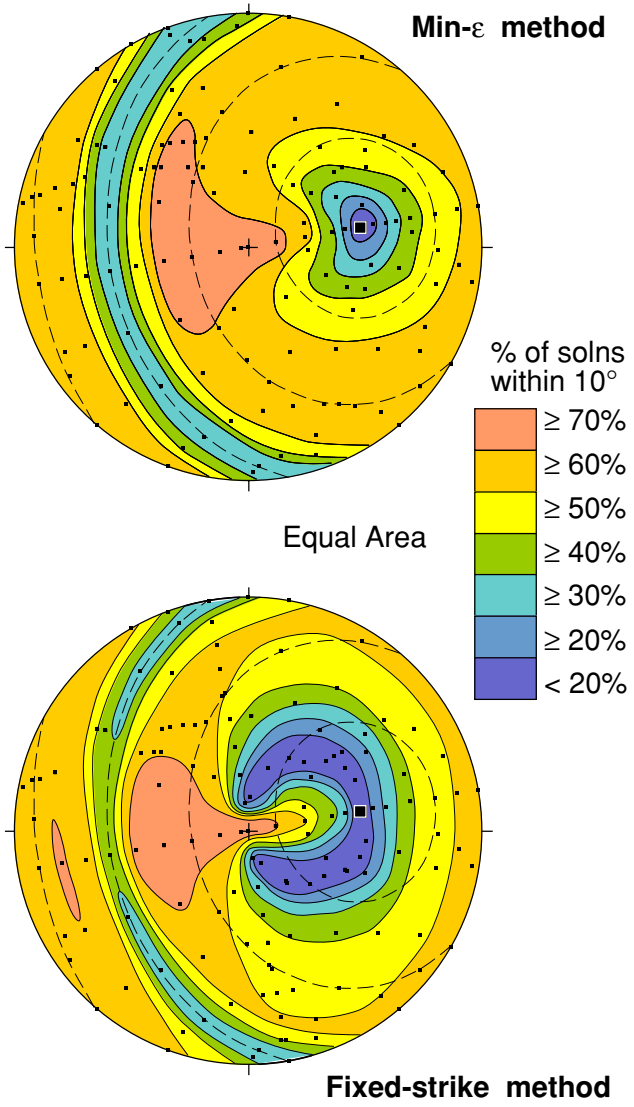

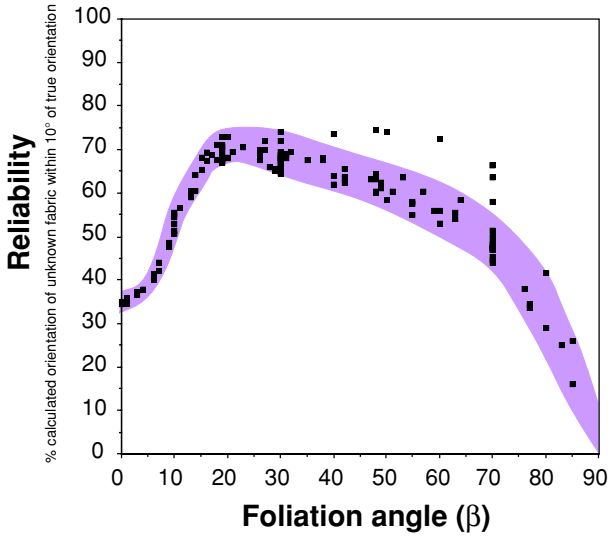

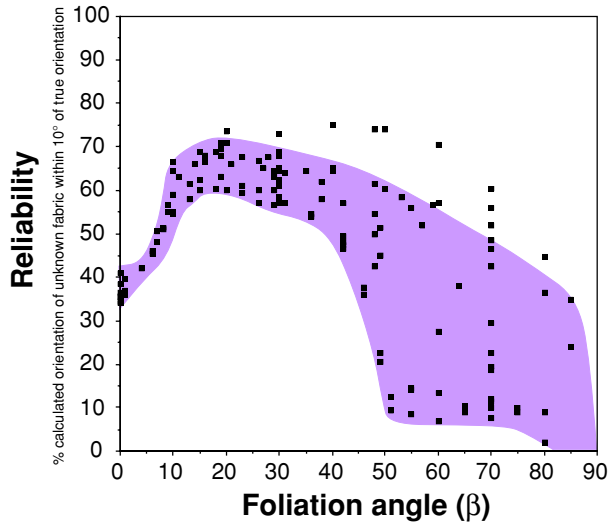

Variation in foliation angle of unknown

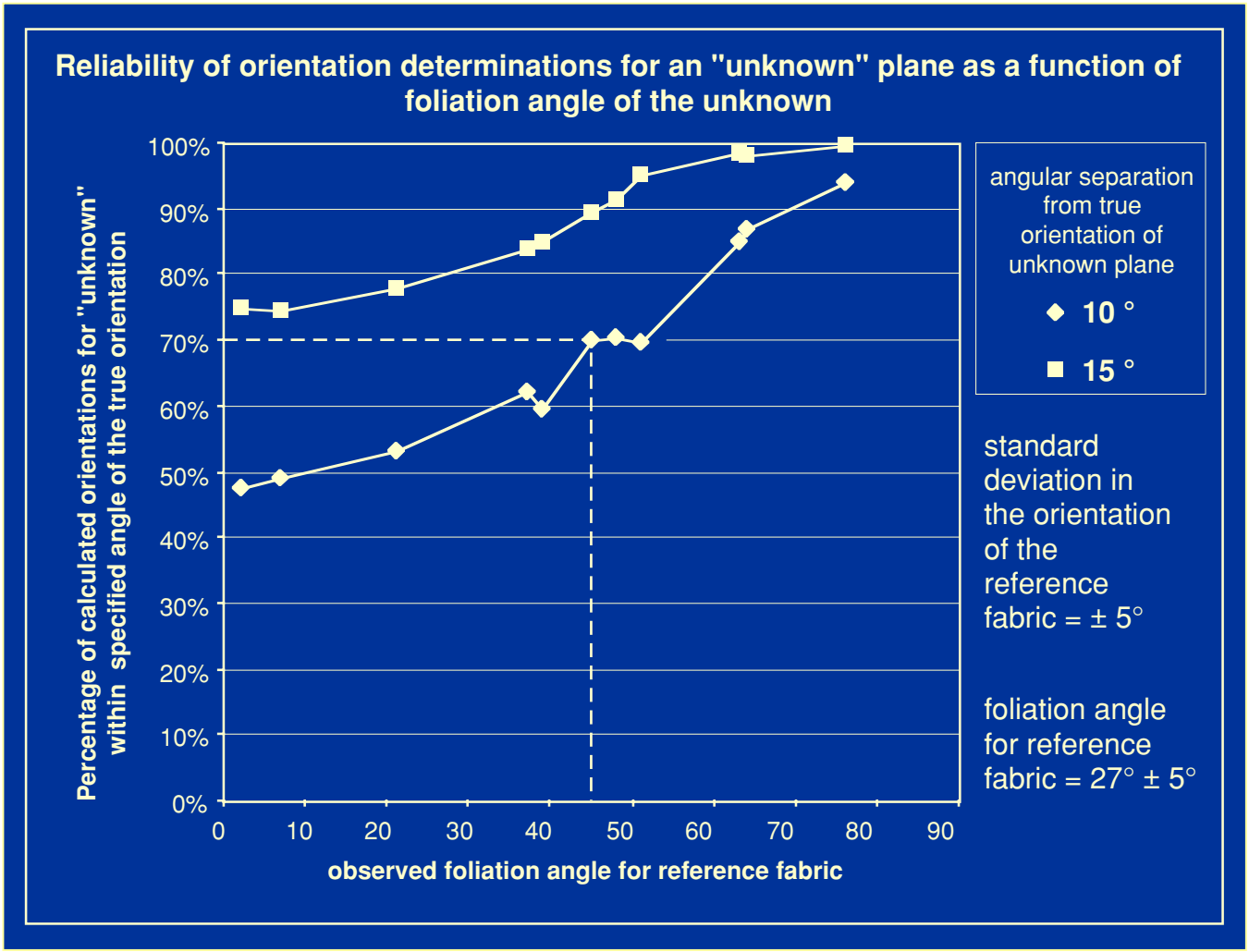

Conclusions

- Axially-oriented drill core may be reliably re-oriented if it contains a recognisable fabric of relatively consistent orientation
- Min-ε method is more robust
- Best results if:
  - foliation angle of “known” fabric in core is 20–60° (ideally 20–30°)
  - foliation angle of “unknown” fabric in core is >45°
  - scatter in the orientation of the reference fabric has std. dev. <10°